Electrochemical Energy Reviews (2023) 6:36
https://doi.org/10.1007/s41918-023-00198-2

REVIEW ARTICLE

# Exploring More Functions in Binders for Lithium Batteries

**Lan Zhang[1] · Xiangkun Wu[1] · Weiwei Qian[1] · Kecheng Pan[2] · Xiaoyan Zhang[1] · Liyuan Li[2] · Mengmin Jia[1] · Suojiang Zhang[1,3]**

Received: 18 August 2022 / Revised: 30 January 2023 / Accepted: 1 August 2023 / Published online: 1 December 2023


**Abstract**
As an indispensable part of the lithium-ion battery (LIB), a binder takes a small share of less than 3% (by weight) in the cell; however, it plays multiple roles. The binder is decisive in the slurry rheology, thus influencing the coating process and the resultant porous structures of electrodes. Usually, binders are considered to be inert in conventional LIBs. In the pursuit of higher energy density, many new binders are being developed for specific targets, such as the high-voltage (typically, ⩾4.5 V) cathodes, conversion/alloy-type cathodes/anodes with large volume effect, and solid-state batteries (SSBs), in which these binders demonstrate their various functions. They may influence the solid electrolyte interface component, ensure the electrode/electrolyte interfacial stability, transport ions/electrons in the electrodes, provide adhesion and flexibility to solid-state electrolyte (SSE) films, etc. Here in this review, we try to summarize the advances on binders, among which the ones for high-voltage cathode materials, thick electrodes, micro-sized silicon particles, SSEs and SSBs are highlighted. We believe that the advanced functional binders would play decisive roles in the future development of high-energy–density LIBs and SSBs.

**Keywords** Lithium battery · Binder · Interphase · Adhesive

## 1 Introduction

The ever-developing society and economics call for advanced energy storage devices with higher energy/power density, better safety, longer service life, low $CO_2$ emission, environmental benignity, and lower cost. As the leading electrochemical energy storage technology, lithium-ion batteries (LIBs) are currently widely adopted in consumer electronics, transportation, aviation, and large-scale energy storage. State-of-the-art (SOA) LIBs are composed of active materials (AMs) and conductive agents (CAs) jointed by binders that are coated on current collectors to form electrodes. The electrodes are separated by polyolefin membranes and enclosed in package materials. Electrolytes are injected so that ions can be transported across the whole cell [1]. Generally, we believe that the percolated ion and electron passages in the cell/electrodes are formed by the electrolytes, CAs and current collectors, respectively. While going to the details, the tiny interfaces such as the solid electrolyte interface (SEI), $Li^+$ solvation sheath, and even the binder, may play indispensable roles. Intensive efforts have been devoted on SEI and electrolyte studies in the past decade to make full use of the advanced AMs including silicon (Si)- and tin (Sn)-based alloy-type anodes [2–8], metal lithium [9–16], nickel-rich cathodes [17–21], sulfur (S) [22–26], etc. On contrast, insufficient attention was put on the binders until people realized that the electrode integrity of Si anodes cannot be guaranteed by traditional ones [27–42]. Therefore, functional binders with higher mechanical strength, self-healing ability, and electronic/ionic conductivity were started to be developed. However, the dominant binders in current LIB industry are still the ones from the very beginning, i.e., polyvinylidene fluoride (PVDF) for cathodes, styrene-butadiene rubber (SBR) and carboxymethyl cellulose sodium (CMC) for anodes.

✉ Suojiang Zhang
sjzhang@ipe.ac.cn

1 CAS Key Laboratory of Green Process and Engineering, Beijing Key Laboratory of Ionic Liquids Clean Process, State Key Laboratory of Multiphase Complex Systems, Institute of Process Engineering, Chinese Academy of Sciences, Beijing 100190, China

2 School of Chemical Engineering, Zhengzhou University, Zhengzhou 450001, Henan, China

3 Longzihu New Energy Laboratory, Zhengzhou Institute of Emerging Industrial Technology, Zhengzhou 450000, Henan, China

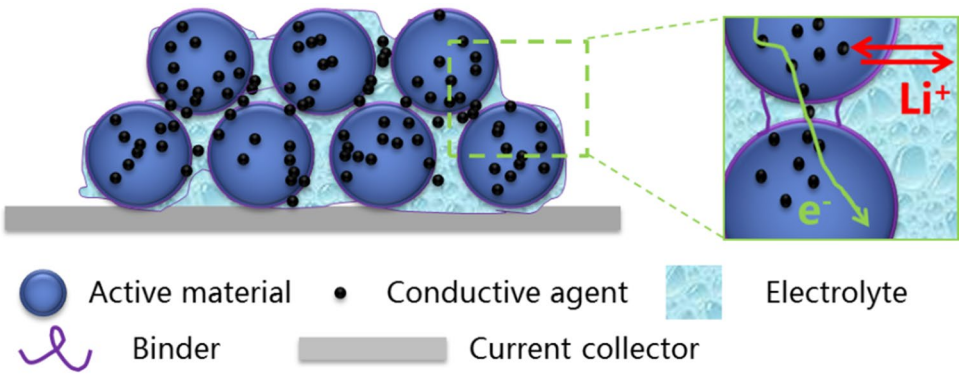


**Fig. 1** Scheme illustrating the ideal connection state between the binders, AM and CA particles in a porous electrode, where the AM should be either encapsulated by lamellar binders or linked by fibrous binders, and the electrolytes (liquid or solid) should fill the pores

Most binders realize the cohesion by physical interlocking [e.g., PVDF, SBR, and polytetrafluoroethylene (PTFE)] or chemical bonding [e.g., CMC and alginate (Alg)] [43]. Adhesion is a complicated process that is influenced by the bulk composition, surface chemistry (e.g., functional groups such as –OH), and the morphology (e.g., the size, aspect ratio, and surface roughness) of both binders and the materials to be cohered. Moreover, the environmental temperature and humidity also affect the adhesion forces and even the mechanisms, which makes the process more intricate. One most typical example is dopamine (dopa) and its derivatives, which are the most widely studied binder family. The catechol group is believed to be capable of interacting with almost all surfaces including metals, oxides and polymers via different mechanisms. Using chemically modified $Si_3N_4$ atomic force microscopy (AFM) cantilevers, Messersmith's group studied the interactions between dopa and various surfaces [44]. They found that dopa is capable of forming high-strength yet reversible bonds with both organic and inorganic surfaces via the adjustment of its own oxidation states. Latterly, they developed a facile surface modification approach, in which a self-polymerization of dopa produced an adherent coating on a wide variety of surfaces [45], where the wettability, processibility and many other characteristics of the materials could be highly changed. Later, inspired by mussels and geckos, the same group realized a highly reversible nanostructured adhesive, which could be even applied under water [46]. Their work highlights the combination of physics and chemistry, which has inspired many later works [31, 47, 48]. Another example commonly used in LIBs is CMC. CMC is believed to act as a surfactant to enhance the dispersity of the hydrophobic graphite. SBR contributes most of the adhesion forces in electrodes by physical interlocking [49]. In Si-based electrodes, it is the carboxyl groups in CMC that form dynamic H-bonds and covalent bonds with the hydroxyl groups on the Si surfaces [50]. That is to say, the same binder may work in different ways when used in different systems. Therefore, it is necessary to understand the properties of AMs in batteries to develop binders with better performance.

In a typical electrode, the AM particles and CAs are closely packed and adhesive to the current collector by the binder. As the most inert material within the cell, the binder should not only keep the electrode integrity and be electrochemically stable but also be easy to be processed, environmentally friendly and cost effective. Because of the low percentage, small size and radio sensitive nature, the binder is usually mixed with the CAs and forms the so-called carbon binder domain (CBD) that is difficult to be distinguished or located in the electrode. As illustrated in Fig. 1, it is widely accepted that the binder either covers the AM particles to form an amorphous coating layer with a thickness of 2–35 nm or becomes fibrous to connect the particles due to the capillary forces [51]. The electrolyte diffuses into the pores of the electrode when being injected, and the binder becomes the first to contact with it in the electrode. Therefore, the binder must keep a low swelling ratio and strong adhesion to the electrolyte so that the electrode integrity can be ensured.

PVDF, CMC and SBR fulfill most of the requirements until some novel AMs with large volume expansion during the lithiation process were developed, such as the alloy-type Si and Sn, the conversion-type sulfur, and their derivatives. Typically, the volume changes of the alloy- and conversion-type AMs during lithiation are higher than that of graphite (about 10%), sometimes accompanied with particle fracture. Therefore, these electrodes usually surfer from larger mechanical stress during the charge/discharge process [52], where binders with more functions are required. Besides, the pursuit of higher energy density also raises new requirements to the binders, e.g., the high-voltage cathodes such as the Li-rich layered oxides (LLOs) need better electrochemical stability as they work at high potential up to 4.8 V. Increasing the thickness of the electrode is a universal way to enhance the battery energy density. However, routine binders usually limit the coating layer to a certain thickness due to the surface tension in the drying process. Therefore, new binders and processing techniques (e.g., the drying method

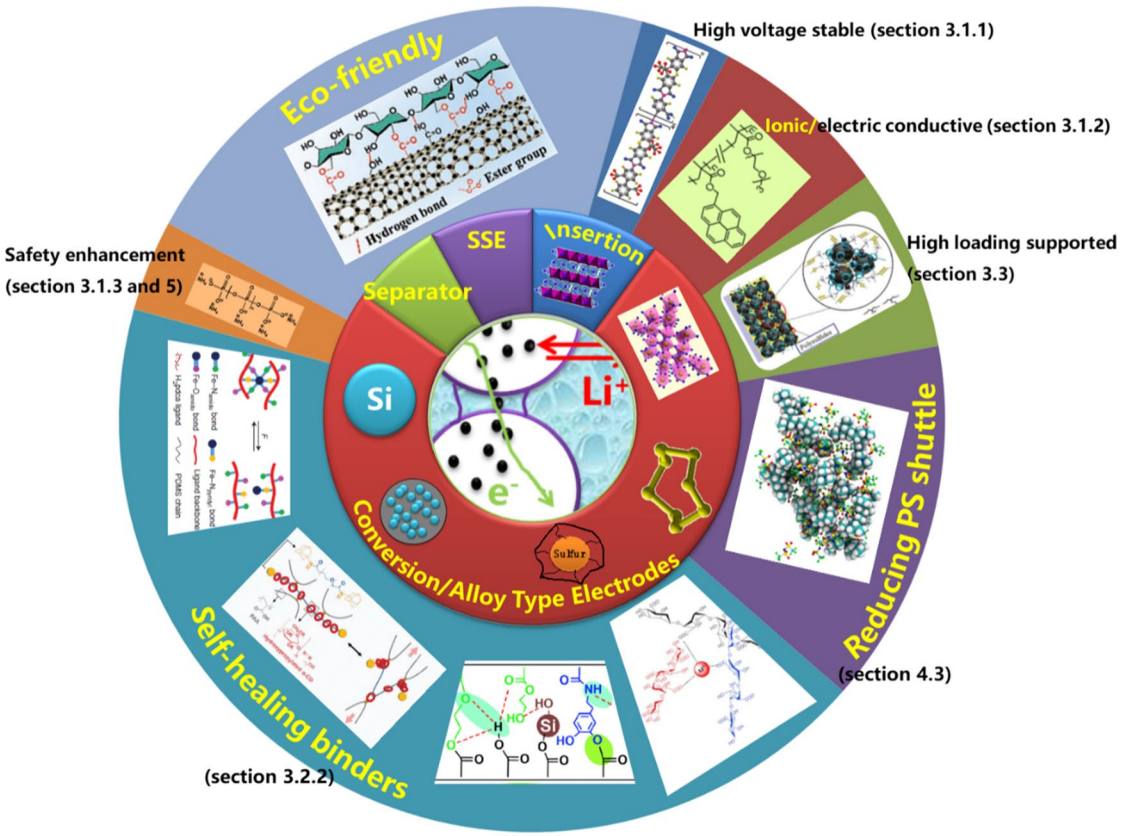


**Fig. 2** Typical binders and their functions toward specific applications. Relevant reports were discussed in the corresponding sections as labeled, and the subfigure for the eco-friendly binder, the carbon nanotube-modified net-like cellulose, was reprinted with permission from Ref. [62]. Copyright © 2021, Wiley. "SSE" is for solid-state electrolyte and "PS" is for polysulfide

[53]) are requisite. Solid-state electrolytes (SSEs) are also drawing more and more attention as they play indispensable roles in solid-state batteries (SSBs), where binders are also necessary for the fabrication of thin SSE films. With these considerations, many natural/artificial polymers and their complex and even inorganic binders with more functions have been developed, as shown in Fig. 2. Considering multiple high-quality review papers focusing on Si [49, 54–59] and S [60, 61] have been published in the past several years, we focus on the state-of-the-art development of binders from the whole cell level. Binders for specific applications, e.g., high-voltage cathodes, thick electrodes and SSBs, are highlighted. We hope to shed some light on the future exploration of new binders in new chemistries.

## 2 Binders for State-of-the-Art LIB Industry

Currently, the industrial production process of LIB electrodes is mainly slurry-coating including four steps: (1) slurry preparation; (2) coating on metal films; (3) drying; and (4) calendering. Typical electrode slurries are non-Newtonian complex mixtures which consist of AMs, CAs, binders and solvents. Herein, the binder is the decisive factor for the slurry's rheological properties (RPs) and processability. The solvent, which is usually ignored as it is removed during the drying process, may also influence the battery performance. Madec's group [63] prepared NbSnSd alloy electrodes with polyacrylic acid (PAA) as the binders dissolved in $H_2O$ and *n*-methyl-2-pyrrolidone (NMP), respectively. They found that the electrode with PAA/$H_2O$ showed higher reversible capacity and lower resistance during the charge/discharge cycles. X-ray photoelectron spectroscopy (XPS) results demonstrated that a thin and continuing SEI was formed in the PAA/$H_2O$ system. Gas chromatography coupled with electron impact mass spectrometry (GC/MS) test further proved that less additives [vinylene carbonate (VC) and fluoroethylene carbonate (FEC)] were consumed in this electrode. Their work also demonstrated the possibility of PAA working as an artificial SEI on the electrode, which is well worth of further study.

Electrodes can be considered as a kind of composite material, in which AMs are connected and wrapped around binders and CAs. It is not only that the binder needs to be

electrochemically stable within the cell working potential range [64], and maintains the integrity and mechanical stability of the coating to ensure that the final electrode composition is evenly distributed, but also that the dissolution, migration and rearrangement of the binder always exist in the electrode manufacturing process to affect the stability and processability of the slurry. Considering the significant influence of the electrode microstructure on cell performance, tracking the evolution of binders is of significance in guiding the LIB production.

### 2.1 Working Mechanisms of Binders in Electrode Processing

The coating process in SOA battery industry requires slurry with certain RPs so that AMs and CAs can be distributed uniformly on the current collector (CC), wherein the binder is the main component to adjust the RPs [65, 66]. It is mainly PVDF for cathodes in oil-based and CMC/SBR for anodes in water-based slurries in SOA LIB production, because they show different influences on the slurry RPs. Multiple forces, e.g., the steric hindrance, chemical bonding and bridging, exist in the slurry owing to the interactions between AMs, CAs and binders, because of which different microstructures can be formed. Li et al. [67] studied the dispersion mechanisms of SBR and CMC in $LiFePO_4$ (LFP) aqueous slurry. They found that SBR just provides steric hindrance to the mixture because of its nonpolar property, while CMC simultaneously exhibits steric and electrostatic repulsions, which are effective for the dispersion of LFP. Notably, it was found that SBR shows a higher priority than CMC to LFP; however, the CAs preferentially interact with CMC. Lee's group [68] also confirmed the priority of CMC to graphite. They systematically analyzed the RPs and concentration of CMC/SBR in graphite anode slurry. It was concluded that CMC plays a leading role in forming microstructures of the slurry. Despite the outstanding dispersion and thickening functions, CMC demonstrates an obvious disadvantage of being relatively brittle. If CMC is used as a sole binder, the graphite electrode will easily collapse during the pressing process and suffer from severe powder loss.

The influence of PVDF on RPs is relatively complicated and still controversial. One theory is that PVDF can hardly adhere to the particle surfaces because of its poor affinity to $LiNi_xCo_yMn_{1-x-y}$ (NCM) and CAs; its function in the slurry is mainly to increase the viscosity without affecting the microstructures formed by CAs and NCM [69]. Another theory is that PVDF tends to chemically bond or physically adsorb to form a coating layer on the AM and CA particles' surfaces. Liu et al. [30] proved that PVDF could form fixed layers on $LiNi_{0.8}Co_{0.15}Al_{0.05}O_2$ (NCA) and acetylene black (AB) with thicknesses of 32 and 9.5 nm, respectively. Absolutely, these thick binder layers on the AM and CA surfaces increase the electrical resistance as the binder is usually ionic and electric insulated [70]. Therefore, it is important to form electron percolate passages in the electrode before the binders cover. Kim et al. [71] studied the slurry viscosity and electrode characteristics by varying the mixing sequence. The lowest viscosity of the slurry was obtained by adding the pre-mixed solid ingredients of $LiCoO_2$ (LCO) and CA into the binder solution. The best electrochemical performance was also observed with this mixing sequence. However, a different conclusion was drawn by Meyer's group [72]. By varying the NMP content, the casting gap and speed, and the mixing sequence, they studied the NCM111 slurry preparation method in details. It was found that although mixing the CA and AM dry powders could enhance the adhesion forces, a dense CB/PVDF layer could form on the NMC surfaces and block the ion transport, thus decreasing the electronic connection and reducing the C-rate capability. Therefore, the electrochemical performance of the cells could be influenced by multiple factors in different time and space scales. There might be some trade-offs among them, which must be carefully considered.

### 2.2 Binder Migration in Drying Process

Electrode drying is an intricate top-down process which includes the diffusion of binders and the sedimentation of particles controlled by the solvent evaporation rate. These parameters are hard to directly measure, therefore, researchers take in-situ analysis of electrode morphology [73, 74] including Raman spectroscopy [73] and real-time fluorescence microscopy [74], and perform model validation analysis [75] to examine them.

Schabel et al. [76] described various component migration processes, as shown in Fig. 3a. In the initial state, all components are distributed evenly on the CC. As the volatile solvent evaporates, the distances between particles decrease with the film shrinking and the menisci forming. The capillary force and gravity enrich the polymer binders and the conductive agents in the upper part of the coating. When solvent is depleted, the film shrinkage stops and a porous electrode is left. The concentration gradient from the electrode substrate to the surface was found to increase for CMC and PVDF binders, while that for AM particles is contrary. This phenomenon highly relies on the drying temperature and the solid content [77]. A fast drying rate can accelerate the migration of the inactive components (the binder and CA). As binder is enriched on the surface of the electrode, the adhesion between the coatings and CC becomes worse, and the electrode may be susceptible to exfoliation and sticky roll. Wang et al. [78] also came to a similar conclusion that the organic material-based LCO electrode film has much higher non-uniformity, weaker adhesion and electrical resistance than the water-based one due to the binder distribution,

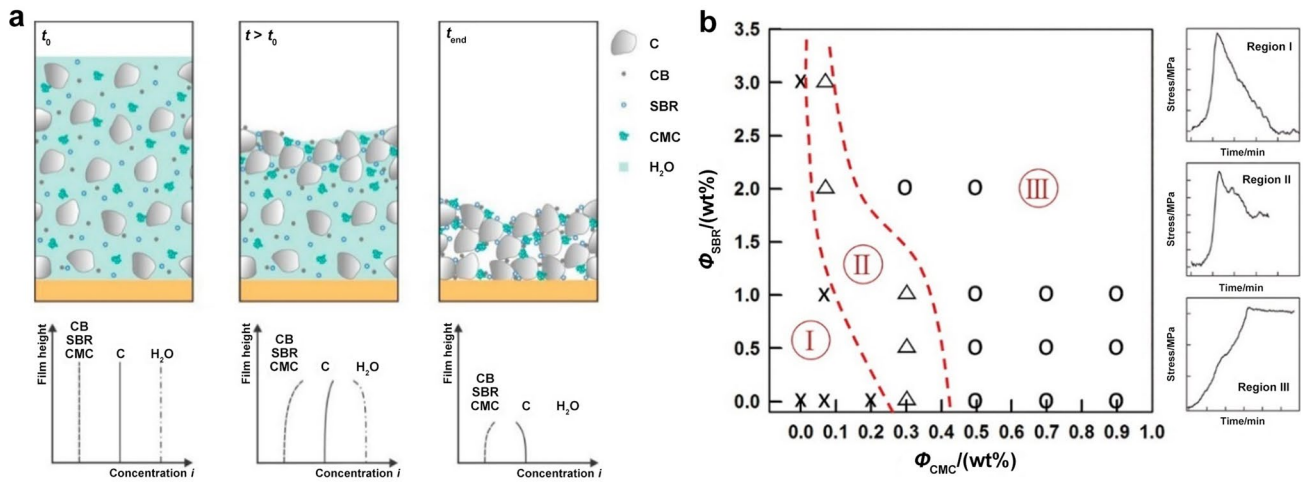


**Fig. 3** **a** Scheme of an electrode film at different drying states. In the initial state ($t = t_0$), C, CB, SBR, CMC and the solvent ($H_2O$) are equally distributed in the film. During drying ($t > t_0$), a consolidated layer forms and the concentration gradients of the components develop, which remains in the dried film until $t = t_{end}$. Reprinted with permission from Ref. [76]. Copyright © 2016, Taylor & Francis. **b** Processing window map for the dried film of CMC/SBR/graphite slurry, in which "X" indicates poor mechanical strength, "△" indicates less mechanical strength, and "○" indicates good mechanical strength of the film. Reprinted with permission from Ref. [79]. Copyright © 2015, American Chemical Society

which can be attributed to the lower evaporation rate of NMP and the longer migration time of PVDF. To ensure the performance of electrodes, the drying temperature should not be too high. However, a low drying temperature can reduce the production efficiency and increase the cost. Therefore, a multi-temperature gradient drying method has been adopted in the actual production process to get a trade-off.

Stress is usually generated due to the shrinkage of the coating layer during the drying process, which causes defects in the films such as cracks, curls and delamination. Ahn's group [79] investigated the stress development in graphite (the diameter of which is ~ 8.11 μm) slurry. The processing window map is shown in Fig. 3b. They found that SBR in a graphite/SBR slurry filled the voids among the graphite particles, while CMC was inclined to be adsorbed onto the graphite particle surfaces. The mechanical strength of the film enhances as the concentration of CMC or SBR increases. It provides a guidance that with a proper concentration of CMC or SBR, a film with superior mechanical strength can be obtained.

## 2.3 CBD Analysis and Influence on Battery Performance

Electrodes require elaborate structural design to ensure LIBs with high electrochemical performance. Although the binder content is quite low in SOA battery industry, it plays a vital role in electrodes [80]. As shown in Fig. 4, binders and nanosized CAs are often mixed with each other to form a so-called CBD in the electrodes, which is filled among the AM particles [81, 82]. The distribution and microstructure of CBD have vital influences on battery performance as they not only maintain the integrity of the electrode structure but also form the electron passages between AM and CC. More importantly, the micropores in the CBD in fact accommodate most of the electrolytes where $Li^+$ ions pass through. As testified in Mehdi's work, a decreased capacity was found in blocking CBDs as the $Li^+$ transport was hindered [83]. However, a fully open CBD may be harmful to long-term stability as the side reactions between the electrode and electrolyte accumulate.

Generally, the distribution of the carbon-binder is ignored in the electrochemical simulation and the mesoscopic structure model of electrodes. The macroscopic conductivity is used to describe the electrode electronic conductivity. However, many researches show that the content and morphology of CBD greatly change the transport properties of ions and electrons. Thus, the CBD cannot be ignored. Miranda et al. [84] further simulated and optimized the proportions of binders and CAs considering the conductivity and mechanical stability of the electrodes. They found that for both nanosized LFP and micro-sized $LiMn_2O_4$ (LMO), the optimal slurry formulation depends on the ratio between the binders and CAs, which should be less than 4. Thiele et al. [85] firstly used a 3D reconstruction of synchrotron X-ray tomography to realize virtual design of electrodes with AM particles, CBD and pores filled with electrolytes. They found that the structure of CBD has a significant influence on both ionic and electric conductivity, especially when the electrode is under a discharged state. A fibrous CBD, i.e., with low tortuosity, is in favor of higher conductivity. Vogel's work [86] came to a similar conclusion after they studied

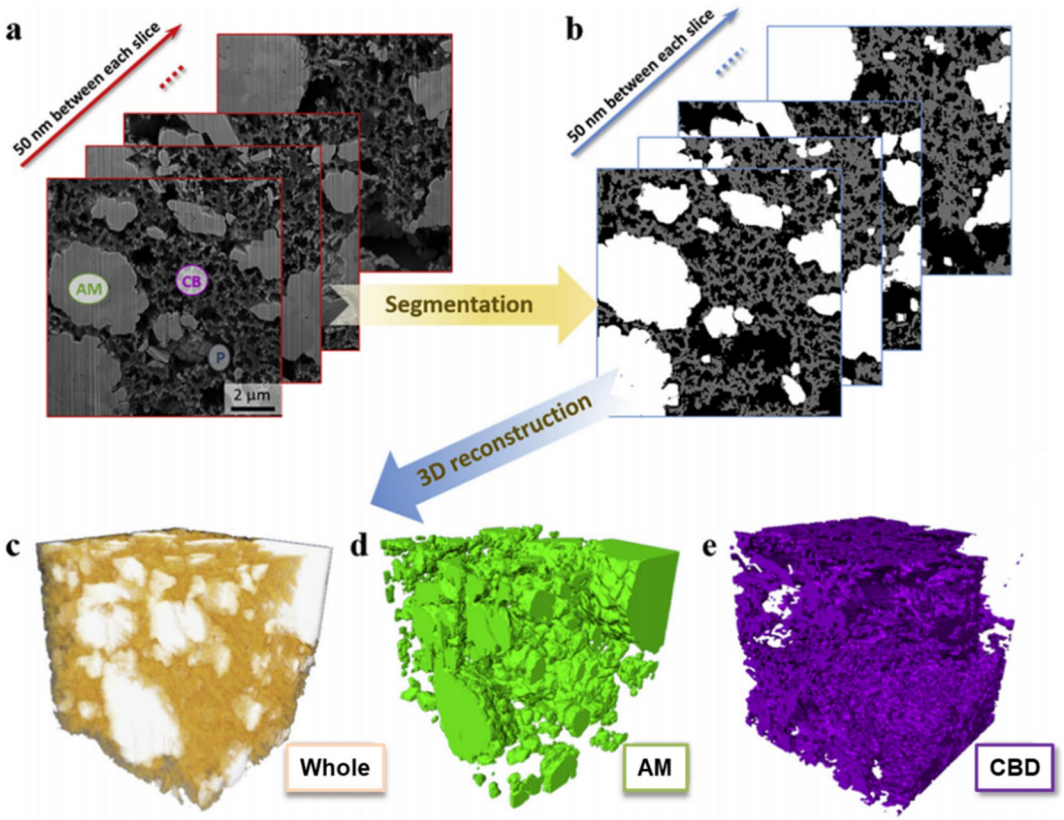


**Fig. 4** Schematic diagram of a 3D reconstruction process: **a** taking a series of cross-sectional FIB-SEM images; **b** image segmentation; **c** an overview of the reconstructed 3D cathode structure; **d**, **e** 3D structures of active material (AM) and CBD, respectively. Reprinted with permission from Ref. [82]. Copyright © 2016, Elsevier

the local conductivity of a commercial NCM electrode using nano-scale four-line probes. They correlated the result with the microstructure characteristics of the electrode, and highlighted that the heterogeneity of the electrode structure may lead to different ion/electron transport efficiency, and thus local SOC differences.

The distribution of CBD in the electrode depends on the raw material properties and the processing conditions. Meanwhile, it also affects the battery performance [87, 88]. In Lee's work [88], the binder (PVDF) was dissolved in a lithium bis(trifluoromethanesulfonyl)imide (LiTFSI)/ethylene carbonate (EC) + propylene carbonate (PC) electrolyte at 150 °C other than NMP at room temperature. The thermal induced phase separation leads to a bicontinuous network of ion and electron in the electrode, with which the areal capacities of both LTO and LFP electrodes are as high as 10 mAh $cm^{-2}$. Therefore, high-performance LIBs need more detailed electrode microstructure designs. The optimization of electrode and CBD microstructures is an effective way to improve battery performance.

## 3 Novel Binders for LIBs

PVDF and CMC + SBR are the most commonly used binders in SOA battery industry for cathodes and anodes, respectively. The crosstalk between cathode and anode draws plenty of interest as the transition metal (TM) ions may dissolve into the electrolytes, shuttle to the anode, and poison the SEI. However, the influence of binders has been long underestimated. Rago et al. prepared 1.5 Ah NCM523||graphite full cells with different binders and studied the overcharge process in details [89, 90]. In one case, 5% and 6% (both by weight ratio) PVDF were used as the binders for the cathode and anode, respectively [89], which was sorted as the NMP system. As a comparison, 4% PVDF + 1% CMC and 4.8% SBR + 1.2% CMC were used [90] and sorted as the aqueous one. They found that the TM ions shuttle to the anodes when the cells were overcharged in both cases; however, the ion loss in the NMP system is more serious especially when the state of charge (SOC) is higher than 160%. Moreover, the dendrite on the anode is prominent in the NMP system. They believed that the better stability of the aqueous system is attributed to the higher adhesion force, which leads to a uniform electric

field, thus the material failure is reduced. Although the influence of the cathode binders was not discussed, their work still highlights the importance of binders, not only for the cycle performance but also for the safety in use. Therefore, we briefly summarize the recent advances on the binders for LIBs, then go to other fields such as solid-state and lithium metal batteries.

## 3.1 Binders for Cathode Materials

PVDF is the most widely used binder for cathodes owing to its excellent chemical and thermal stability and the acceptable mechanical strength to encapsulate AM particles. However, it has many drawbacks as summarized in Zhang's work [91], such as the weak interaction with AM particles, the loss of mechanical strength due to the swollen of liquid electrolytes at elevated temperatures, low electronic and ion conductivity, the inconvenience of recycle, and the environmental issues for the use of NMP as the solvent for processing. Moreover, the development of novel high-energy–density cathodes, such as the high-voltage ones [e.g., LLO, spinel $LiNi_{0.5}Mn_{1.5}O_4$ (LNMO)] and the conversion-type metal fluorides ($MF_x$), and new requirements including better electrochemical stability, volume adaptability, eco-friendliness [92] and ionic/electronic conductivity are also issues for advanced binders.

### 3.1.1 High-Voltage Binders

High-voltage cathode materials such as Ni-rich NCM, spinel LNMO, and LLO [representing $xLi_2MnO_3{\cdot}(1-x)LiMO_2$, M = Mn, Ni, Co] are critically important for LIBs to achieve higher energy density. However, for high-voltage operations, the unstable cathode-electrolyte interfaces (CEIs), oxidative decomposition of electrolytes and the dissolution of transition metals (TMs) can lead to sharp capacity declines. Utilizing novel binders is an effective way to enhance the cycle stability as they can either form a stable CEI or scavenge the free radicals generated by the cathode materials under high SOC, thus suppressing the parasitic reactions. Recent binders focusing on high-voltage cathode materials are briefly summarized in Table 1. The semi-crystalline structured PVDF was classified as a linear binder in Duh's [93] and Liao's [94] work, and it shows limited contact area with AMs. They believed that the amorphous polymers such as CMC and sodium alginate (SA) have better contact with AMs and can be classified as steric binders. Latterly, many other polymers including the guar gum (GG) [95], fluorinated polyimide (FPI) [96], PAA [97], etc., were found to be effective toward LNMO and LLO. These polymer binders can not only form protective coating layers on the AM particles thus interrupting the direct contact of AMs and electrolytes, but also sometimes interact with the AMs to keep their structures stable in long-term cycles. Cao's group proved that PAA could form a uniform coating layer with a thickness of ~ 10 nm on LLO; moreover, as depicted in Fig. 5a, a H-Li exchange reaction took place between the binder and LLO and the proton increased the TM ion migration energy barrier, which finally led to better structural stability [97]. Chen et al. found that the $Na^+$ in CMC and SA can partially penetrate into the LLO lattice and work as a pillar to enhance the structural stability, thus endowing the battery with better cycle performance and reduced voltage decay [98].

Other than LLO, the LNMO suffers from less structural change but has a higher working potential. The serious electrolyte oxidation and TM ion loss caused by Jahn–Teller effect restrict it from commercial applications. Duh's group found that CMC/SA could form a thin but effective protecting layer on LNMO particle surfaces, thus hindering the dissolution of TM and improving its high-temperature cycle stability [93]. Natural fibers are no doubt a great treasure for binder applications due to their natural abundance, rich functional groups, and easy processibility [99, 100]. Sericin was applied by Chen's group in LNMO electrodes [99]. It can not only well interlock the AM particles and form a thin CEI, but also have good affinity to electrolytes via the –NH and –C=O groups, as shown in Fig. 5b, thus enhancing the rate capability. The cell still works even under a high current density of 20 C. The full cell also shows a high capacity retention of more than 80% after 1 000 cycles. Cui's group found that the phenol group on lignin can scavenge the free radicals generated on the electrode/electrolyte interfaces thus restricting the electrolyte oxidation [100].

### 3.1.2 Conductive Binders

The percolated ion transportation within the cell and the electron passages among the electrodes are the essential prerequisites for batteries to work. Generally, the ion passages are constructed by the electrolytes permeating in both electrodes and separator, and the electron conductive network by CA, AM and CC. The binders, usually the first layer coating on AMs and being insulate, may reduce the overall conductivity especially when used with large quantities [30]. As mentioned in Chen's work [99], the binders form a resistant layer and energy barrier for the $Li^+$ before the intercalation/conversion reactions take place. A space charge layer and a small voltage hysteresis may exist on the AM/binder interfaces, which could further influence the self-discharge rate due to their insulating nature. A conductive binder (either electronic or ionic) may alter this phenomenon. On the one hand, the conductive binder could work as a buffer layer between the AMs and electrolytes, altering the structure of the inner Helmholtz layer [106], thus influencing the component of SEI/CEI. On the other hand, the conductive binder

**Table 1** Binders for high-voltage cathode materials in recent literature

| Binder | Electrode/voltage range | Function mechanism | Rate/retention | Ref. |
|---|---|---|---|---|
| PAALi | LNMO/3.00–4.95 V | Coating, wetting, and extra Li source | More than 110 mAh $g^{-1}$ under 20 C | [101] |
| CMC and SA | LNMO | Serve as a protective film to inhibit the serious Ni and Mn dissolution at elevated temperatures | 1 C/CMC: 94.1%; SA: 98.1% after 100 cycles, 55 °C | [93] |
| PVDF and P(BMA-AN-St) | LNMO/3.5–4.9 V | Possess better adhesion force, build the conductive network structure, the nitrile group has better electrochemical compatibility | 1 C/92%@300 cycles | [94] |
| Sericin | LNMO | Stabilize the CEI layer and suppress the self-discharge | 80% retention after 1 000 cycles, full cell | [99] |
| Lignin | LNMO/3.5–5.0 V | Scavenge the free radicals thus preventing the electrolyte from being oxidized | 1 C/94.1%@1 000 cycles | [21] |
| P(MVE-LMA) | LNMO/3.5–5.0 V | Form CEI, suppress the oxidative decomposition of electrolytes and stabilize the lattice structure of LNMO | 1 C/92%@400 cycles | [102] |
| GG | LLO/2.0–4.7 V | GG could coat tightly on the surface of AM particles, hindering the side reactions and corrosion of the electrode | 100 mA $g^{-1}$/95.2%@250 cycles | [95] |
| FPI | LLO/2.5–4.7 V | Form an amorphous robust surface layer, suppress metal dissolution and cathode degradation with the CEI | LMNC//graphite full cells 0.2 C, 89%@100 cycles, 55 °C | [96] |
| PAA | LLO/2.0–4.8 V | React with oxygen species to form a uniform and tightly coated film | 200 mA $g^{-1}$/88.5%@500 cycles | [97] |
| CMC and SA | LLO/2.0–4.8 V | $Na^+$ ions in CMC and SA can occupy lithium vacancies during cycling and act as a pillar to stabilize the crystal structure | 0.1 C, 80 cycles, no capacity decay | [98] |
| XG | LLO/2.0–4.8 V | The double helix structure and abundant carboxyl groups reduce the TM ion loss | 0.1 C, 200 cycles, 98.4% | [103] |
| PAA | NCM811/2.7–4.3 V | React with the residual Li to form an ion conductive protection layer | 1 C, 300 cycles, 66.6% | [104] |
| SPDX | NCM811/3.0–4.3 V | Form a strong but flexible protecting layer on AM particles and reduce the TM loss | Full cell, 250 cycles, 96.9% | [105] |

Note: The data in Table 1 are extracted from different references, thus exhibiting different significant digits

is meaningful for thick electrodes (especially for those with AMs with large volume variations during the lithiation process such as Si and S, which will be discussed later) in which the electrons have longer ways to travel during the charge/discharge process. The extra $Li^+$ and ion passages may reduce the local concentration polarization, thus enhancing the battery kinetics. Therefore, there are lots of publications in the past few years focusing on this area.

Ionic conductive binders have long time been ignored until the recent intensive study on SSBs. This is mainly due to that the liquid electrolytes form the ionic percolation in LIBs. Hence, it calls for new passages in SSBs. For SSBs, polyethylene oxide (PEO) [107] and its derivatives/composites [108–110] are the most commonly used binders. It has been widely accepted that the EO group can both dissociate and transport $Li^+$ by the chain motions. The performance of the PEO family is largely influenced by the salt content (or the ratio between Li and EO), liquid electrolyte (PEO reacts with $LiPF_6$, especially under high temperatures [111]), and the working potential of the cathode (PEO

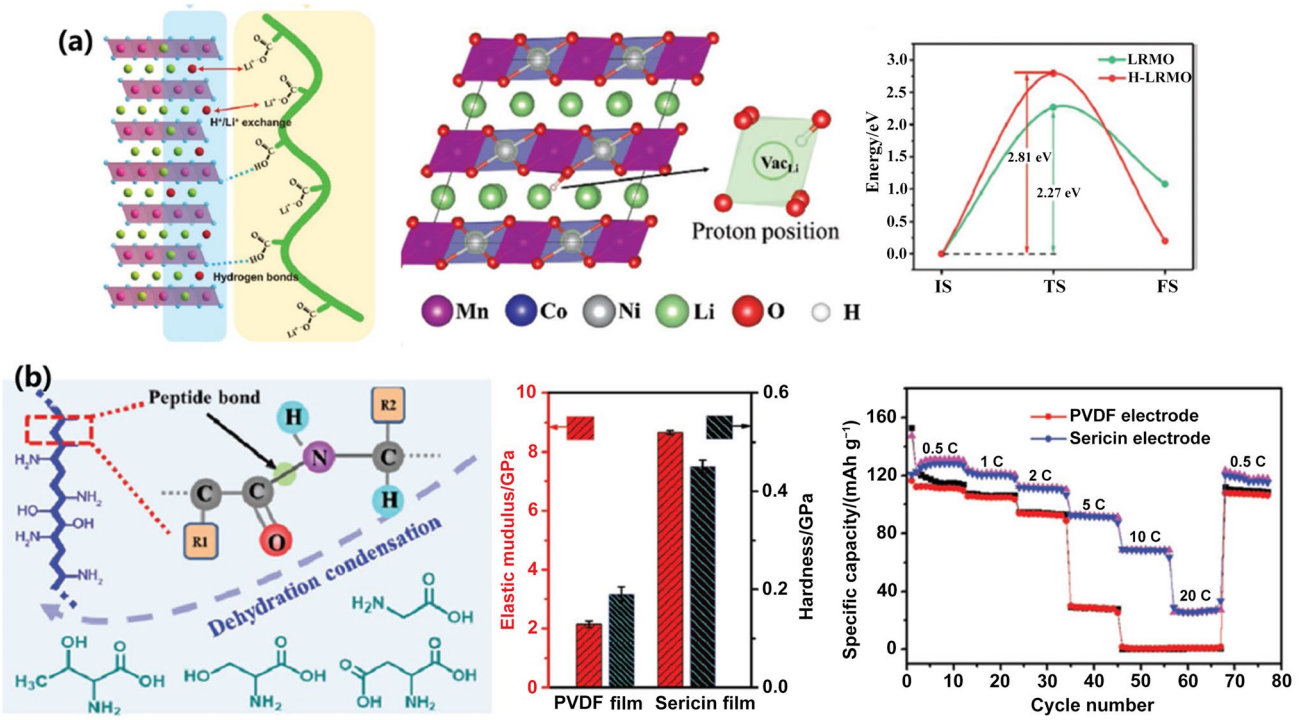


**Fig. 5** **a** Schematic diagram of the function between PAA and LLO, a $H^+/Li^+$ exchange process takes place between them, and the proton increases the energy barrier for the TM ions to migrate to the Li position. Reproduced with permission from Ref. [97]. Copyright © 2020, Wiley-VCH. **b** The rich functional groups on sericin not only endow it with strong elasticity and hardness but also enhance its rate capability when it is applied as a binder for LNMO. Reproduced with permission from Ref. [99]. Copyright © 2017, Wiley-VCH. All rights are reserved

usually suffers from oxidation beyond 4.0 V). Otherwise, intrinsic ionic conductive polymers and single-ion conductors (SICs) may solve the above issues as they contain $Li^+$ in their molecular structures [112] and are less sensitive to the additional electrolytes. Figure 6 shows the molecular structures of typical $Li^+$ ion conductive polymer binders. Generally, the main chains encapsulate the AM particles, and the side chains not only provide stronger interactions with the AM particles via the polar functional groups but also transport the $Li^+$ by its motion under the electric field. Bouchet and coworkers reported the first single-ion BAB triblock copolymer, in which the block B is poly(styrene trifluoromethanesulfonylimide of lithium) P(STFSILi) and A is PEO [112], shorted as P(STFSILi)-*b*-PEO-*b*-P(STFSILi) as shown in Fig. 6a. The block B enables it with ionic conductivity and high electrochemical stability, and A endows it with water solubility and good flexibility; thus, the polymer can work as not only the electrolyte but also the binder for LFP electrodes. The SSB works stably under 80 °C. In fact, some other SIC binders have already been studied in previous works. Creager's group [113] used a short-side-chain analog of lithiated Nafion (having a PTFE-like backbone and simpler $–OCF_2CF_2SO_3Li$ pendant side chains, as shown in Fig. 6e) as the binder for an LFP electrode and tested it in LFP||LTO full cells. As a result, the cell with SIC binder showed similar reversible capacity to that with PVDF under lower C rates (0.2 C and 1 C). When the current density further increases, the SIC one demonstrated its advantages. It is worth noting that the authors also tested the cells with a low concentration electrolyte with merely 0.1 M (1 M = 1 mol $L^{-1}$) $LiPF_6$, in which the SIC further illustrated its superiority.

Latterly, researchers continued the structure optimization work of SIC binders. He et al. [114] adopted lithium polyacrylate (PAALi, Fig. 6b) with terpene resin as a tackifier for LFP cathodes, which guaranteed rapid $Li^+$ transportation channels among the LFP particles. Yuan et al. [115] used a waterborne lithiated ionomer binder (PSBA-Li, Fig. 6d) in LFP electrodes. They found that with a low dosage of merely 1.5%, the cell showed satisfying performance, which is much better than the counterpart with the same quantity of PVDF. They attributed the enhanced rate capability to the functionality of the $Li^+$ attached to the molecule chains. Considering the weak adhesion forces of most SICs, Ji et al. [116] designed a 3D hierarchical walnut kernel shaped conducting polymer binder (CPB, Fig. 6c). The nitrile and ether groups of the CPB endow superior bonding strength and the $–SO_3^-$ provides efficient $Li^+$

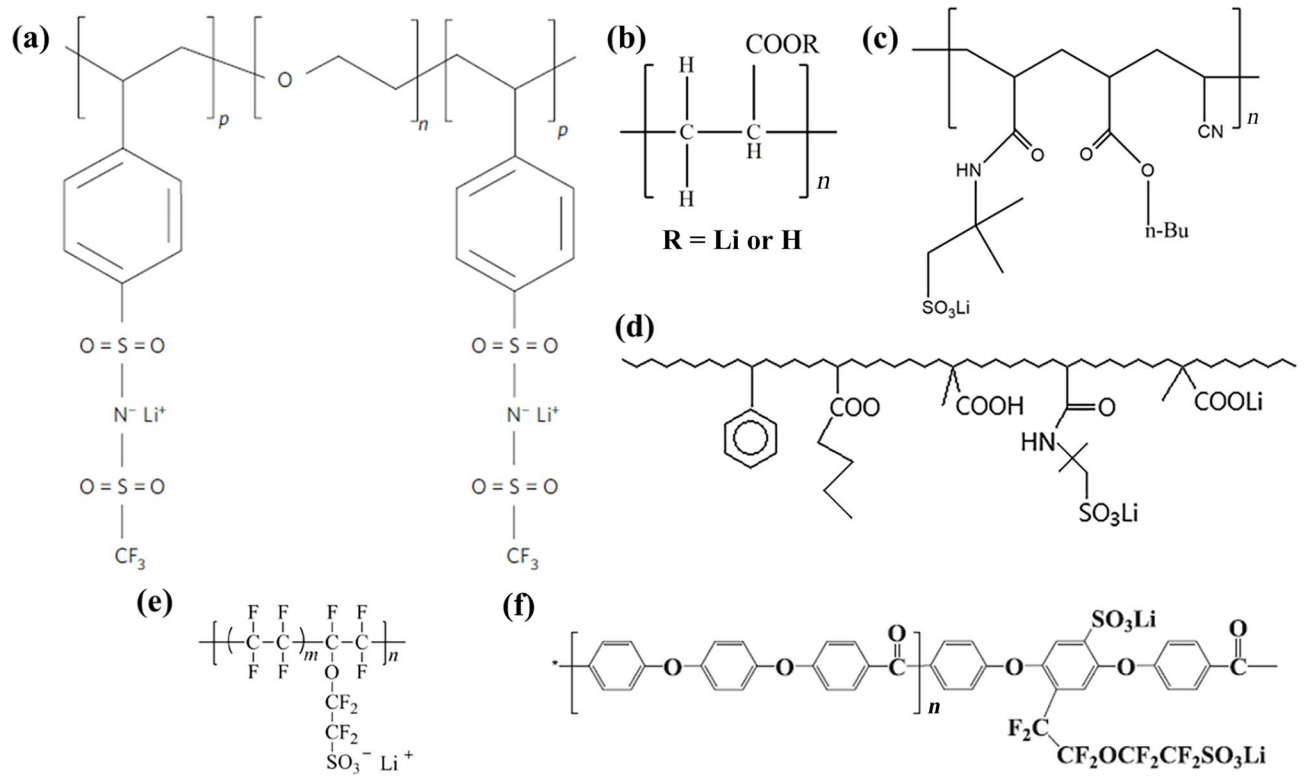


**Fig. 6** Molecular structures of typical $Li^+$ ion conductive polymer binders. **a** P(STFSILi)-*b*-PEO-*b*-P(STFSILi). Reproduced with permission from Ref. [112]. Copyright © 2013, The Author(s), under exclusive license to Springer Nature. **b** PAALi. Reproduced with permission from Ref. [114]. Copyright © 2017, Wiley-VCH. **c** 3D hierarchical walnut kernel shaped conducting polymer binder. Reproduced with permission from Ref. [116]. Copyright © 2018, Elsevier B.V. **d** Waterborne lithiated ionomer binder (PSBA-Li). Reproduced with permission from Ref. [115]. Copyright © 2018, American Chemical Society. **e** A (PTFE)-like backbone and simpler $–OCF_2CF_2SO_3Li$ pendant side chains. Reproduced with permission from Ref. [113]. Copyright © 2010, IOP Publishing Ltd. **f** Lithiated fluorinated sulfonic groups (SPEEK-FSI-Li). Reproduced with permission from Ref. [119]. Copyright © 2014, Elsevier Ltd. All rights are reserved

pathways. With these features, the CPB-based LFP electrode revealed excellent electrochemical performance compared to the PVDF-based system. Xue et al. [117] synthesized lithiated poly(perfluoroalkylsulfonyl)imide (PFSILi) and mixed it with PVDF as the binder for an LFP cathode and achieved satisfactory performance at high rates. The PFSILi added interconnected ion channels to the electrode owing to the charge delocalization over sulfonimide backbone. Besides, massive $Li^+$ were held owing to the high cation exchange capacity. At the same time, PVDF was introduced to hinder the polymer crystallinity and enhance the adhesion strength of the composite binder. As a result, the LFP electrode demonstrated a high and stable reversible capacity > 100 mAh $g^{-1}$ under a 5 C rate and 60 °C, while the PVDF counterpart showed a sharp decline.

Anion-type ionic conductive binder was also developed recently. Chen and coworkers prepared a copolymer binder with acrylic acid (AA), 2-hydroxyethyl acrylate (HA) and 1-vinyl-3-ethylimidazolium hexafluorophosphate (VEH) [118]. The authors believed that the AA-HA-VEH binder could prevent the diffusion concentration gradient during lithiation and promote the $Li^+$ transportation from the electrolyte to the LFP particle centers. Meanwhile, it also showed high adhesive ability, low resistance and polarization, and long-term cycle stability (with 3% AA-HA-VEH, it kept 97.01% of its capacity after 400 cycles at 0.5 C) when applied in LFP electrodes.

Another important direction for conductive binders is electronic or mixed (both ionic and electronic) conductors. Conducting polymers (CPs), such as polyaniline (PANI) and polypyrrole (PPy), usually possess conjugated π electron structures, which endow them with strong backbones, substantial conductivity, low solubility (difficult in handling) and high melting points. Therefore, although they have early been developed, they were only recently be trailed when alloy-type anodes, such as Si and Sn that need binders with higher stress to ensure the percolated electron passages even on volume variation, were studied [120–124]. CPs are also meaningful for the cathodes with limited volume effects especially for those with low conductivity such as LFP [125,

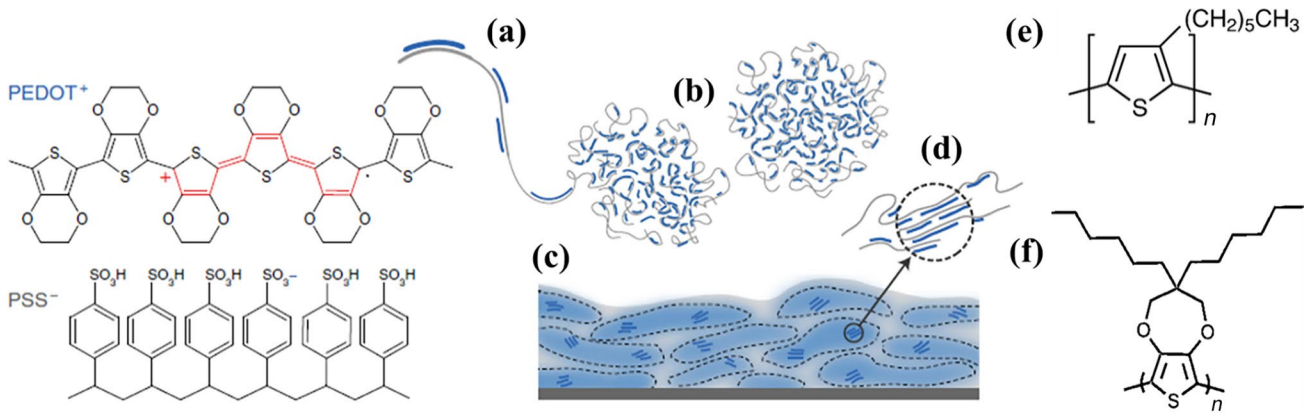


**Fig. 7** Chemical structures of the polythiophene binder family. The PEDOT:PSS and the commonly described microstructure of CP system **a** synthesis onto PSS template, **b** formation of colloidal gel particles in dispersion and **c** resulting film with PEDOT:PSS-rich (blue) and PSS-rich (gray) phases. **d** Aggregates/crystallites support enhanced electronic transport [130]. Structures of **e** P3HT and **f** PProDOT-$Hx_2$. (**e**) Reprinted (adapted) with permission from Ref. [132]. Copyright © 2018, American Chemical Society. (**f**) Reprinted (adapted) with permission from Ref. [133]. Copyright © 2020. American Chemical Society

126], $LiFe_xMn_{1-x}PO_4$ (LFMP) [127] and $LiMn_2O_4$ (LMO) [128, 129], as they can enhance the electron transport by working as a conductive coating layer. The biggest hurdle in applying CPs as binders lies on their solubility and processability. Polythiophene family is the most widely studied CPs working as binders due to their adjustable solubility by substitution. As a typical solvable CP, poly-3,4-ethylenedioxythiophene/polystyrene sulfonate (PEDOT:PSS, Fig. 7a [130]) was successfully used as a binder for LFP and LFMP in Vorobeva's work [126, 127] due to its mechanical robustness, good electrochemical stability and impressive electrical conductivity. The same group further extended the work to LMO materials [129] by using PEDOT:PSS and CMC, resulting in a 5 times higher electronic conductivity (0.50 vs. 0.11 S $cm^{-1}$) than that of PVDF. Benefiting from the CP binder, LMO particles kept good electrical connections with the CC, thus revealing a significant decrease of interfacial resistance, good rate capability (75 mAh $g^{-1}$ at 10 C discharge) and excellent cycling stability at 1 C (less than 5% decay after 200 cycles). Zhang and coworkers used it together with carboxymethyl chitosan (CTS)/SBR and compared the pouch cells' performance, which is much closer to the application level [131]. They optimized the ratio between PEDOT:PSS and AB (1:1, in weight ratio) in coin cells by measuring electric conductivity, peeling strength and compaction density of the electrode sheets. They reduced the dosage of each to 1% in the pouch cells and the LFP ratio was improved to 94%. Additionally, 4% CTS/SBR was used as a stronger adhesive. The resultant 10 Ah pouch cell showed similar cycle stability to that with PVDF [89.7% vs. 90% retention after 1 000 cycles at 1 C/2 C (charge/discharge)], and enhanced rate performance at a 7 C rate (98% vs. 95.4% to that of 1 C) owning to the conductive nature of PEDOT:PSS. Moreover, this binder system is water soluble, where NMP is not needed. Furthermore, PEDOT:PSS is a mixed conductor rather than being just electronic conductive [130]. Not only can the PSS chain enhance the dispersity of PEDOT and realize its doping, where electrons can be swiftly transported by the π–π stacking electron cloud, but also the $–SO_3H$ group could interact with the ions in the electrolytes thus enhancing the ion transport, as shown in Fig. 7b–d. Therefore, there might be more spaces to explore the function mechanisms of PEDOT:PSS binders.

Other mixed conductors were also reported. Bruce et al. [132, 133] examined poly(3-hexylthiophene-2,5-diyl) (P3HT) (Fig. 7e) and dihexyl-substituted poly(3,4-propylenedioxythiophene) (PProDOT-$Hx_2$) (Fig. 7f) in their work. They found that P3HT can be electrochemically doped in the potential range where NCA is electrochemically active, thus providing high electronic and ionic conductivity. The resultant NCA electrode demonstrated not only high rate performance (110 mAh $g^{-1}$@16 C) but also long-term cycle stability (80%@1 000th cycle, 16 C). However, the use of a high polar solvent (1,2-dichlorobenzene) in this work as the processibility of P3HT is yet to be enhanced. Therefore, the same group further developed PProDOT-$Hx_2$ and tested it in a high-loading NCA electrode. With a low weight ratio of 4%, the NCA electrode with 11 mg $cm^{-2}$ demonstrated a high discharge capacity of ~ 110 mAh $g^{-1}$ under a 2 C rate, while that of PVDF is only ~ 74 mAh $g^{-1}$, which highlighted the importance of bicontinuous electron and ion passages.

To summarize, SIC and CP binders could reduce the polarity and enhance the rate performance by supplying additional ion and electron passages in the electrode. Some of them are water soluble, which may reduce the electrode preparation cost. For SIC binders, similar to SIC electrolytes, their ionic conductivity is still quite limited ($10^{-7}$–$10^{-5}$ S $cm^{-1}$ under room temperature). Although this

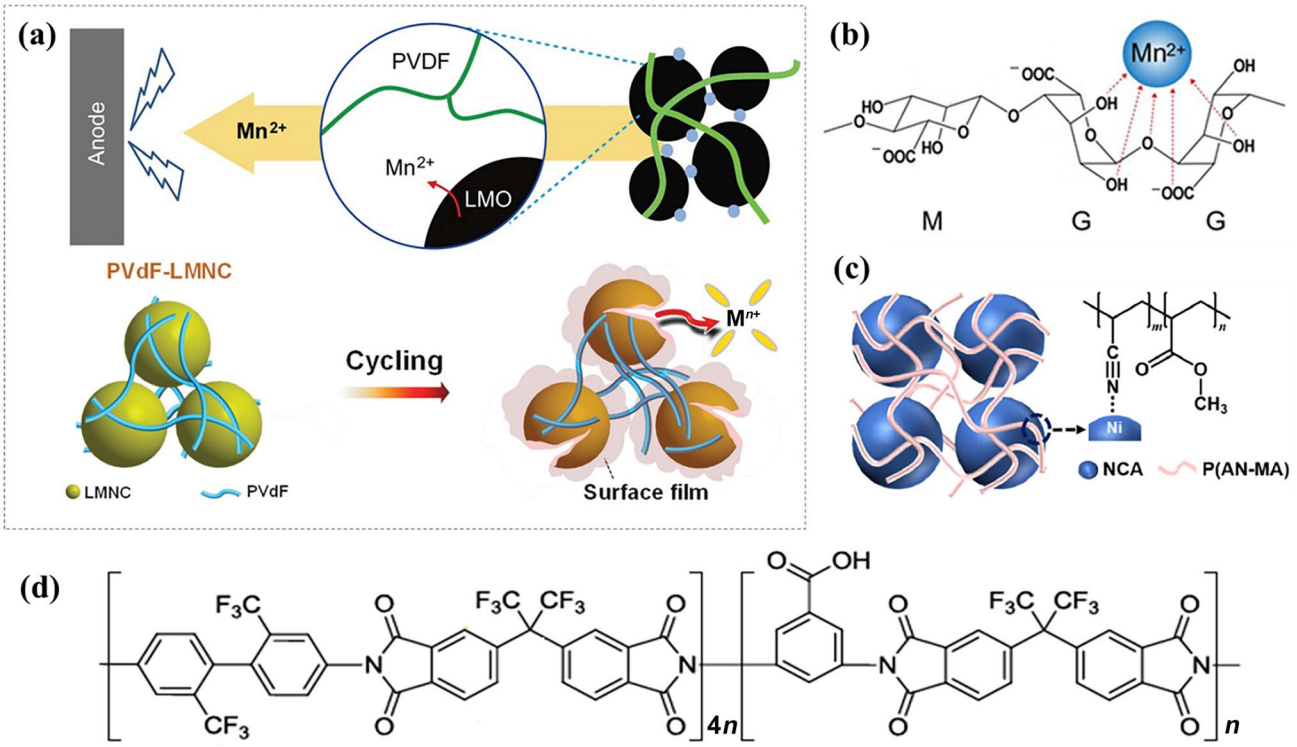


**Fig. 8** Performance degrade mechanism at high temperatures and typical binder solutions. **a** Two major capacity loss reasons: TM loss and particle/electrode clasp. Reprinted with permission from Ref. [134]. Copyright © 2013, The Royal Society of Chemistry. Reprinted with permission from Ref. [96]. Copyright © 2017, Wiley-VCH. **b** The "egg box" effect of SA. Reprinted with permission from Ref. [134]. Copyright © 2013, The Royal Society of Chemistry. **c** The interaction between P(AN-MA) and NCA particles. Reprinted with permission from Ref. [139]. Copyright © 2021, Science Press and Dalian Institute of Chemical Physics, Chinese Academy of Sciences. Published by Elsevier B.V. and Science Press. All rights are reserved. **d** Chemical structure of FPI [96]. Copyright © 2017, Wiley-VCH

limited ionic conductivity is enough for binders as nanometer-scale thin coating layers are formed and the areal resistance is low enough for batteries to work, higher conductivity definitely further increases the performance. As to the CP ones, because the conductivity of most CPs highly relies on the doping state (which is susceptible to SOC of the electrode), a proper CP selection is of vital importance. Besides, the working mechanisms of these binders are still yet to be explored. Therefore, the key to use these polymers as binders lies on several aspects: (1) to enhance the processibility and reduce the film thickness; (2) to increase the conductivity and electrochemical stability; and (3) high adhesive force is indispensable for binders.

### 3.1.3 Thermal Resistant Binders

High-temperature (⩾ 55 °C) working stability is a challenge for LIBs, not only due to that the accelerated parasitic reactions between electrolytes and electrodes lead to transition metal ion loss and SEI destruction [134, 135], but also because that the adhesion forces of conventional binders decrease remarkably in high-temperature environments [96, 136, 137], where the electrode integrity cannot be assured, and as a consequence, LIBs show declined CE and cycle life [138] (Fig. 8a). Binders are unquestionably one of the most convenient methods to elevate the hurdles. On the one hand, the thin layer formed by binders can be an artificial CEI/SEI to capture the dissolved TM ions [134] or HF; on the other hand, stronger adhesion can also be achieved by binder optimization [137]. SA is currently famous for working as binders for Si, as reported by Yushin's group [28]. SA can also be used in cathodes such as LMO to decrease the Mn ion loss due to its "egg box" effect [134]. Choi's group found that SA has a strong $Mn^{2+}$ trapping ability, thus easing the poison risk of the SEI by the TM ions, as shown in Fig. 8b. Therefore, the batteries with SA binders showed enhanced cycle stability under both room temperature and 55 °C. Song et al. used fluorinated polyimide (FPI, Fig. 8d) as a multifunctional binder for $Li_{1.2}Ni_{0.132}Mn_{0.54}Co_{0.13}O_2$ (LNMC) even though the cut-off voltage is 4.8 V. They found that the LNMC interacts with FPI via the carboxyl group, on which the TM ion loss and phase change are greatly suppressed. They attributed the enhanced thermal stability of FPI to the imide benzene rings. As a result, the LNMC electrode

demonstrated an enhanced capacity retention of 89% after 100 cycles under 0.2 C and 55 °C.

Polyacrylonitrile (PAN) is well acknowledged with its excellent thermal stability due to the presence of –C≡N groups, which also exhibits a wide electrochemical window and high melting point [140]. Song et al. [139] reported a multifunctional binder through a typical free radical copolymerization of acrylonitrile (AN) and methyl acrylate (MA) for an NCA cathode operating at 55 °C. The PAN endows the binder with enhanced interfacial stability via –C≡N···$Ni^{3+}$ coordination, and the polymethyl acrylate (PMA) improves the processability of the binder (Fig. 8c). The two segments work together and provide superior thermal stability and adhesive ability to the electrode, thus the electrode delivered 81.5% capacity retention after 100 cycles at 55 °C.

The above section has summarized functional binders contrapose to different cathode materials. Each cathode material has its own characteristics, with which different requirements for binder properties are issued. For high-voltage materials, such as LNMO, LCO, LLO and Ni-rich NCM cathodes, more attention should be put on the cathode/electrolyte interfacial stability, including the yield of free radicals, and the voltage and capacity decays which result in poor cycle stability. MIC binders should be considered for poor conductive cathode materials, e.g., LFP, $LiMnPO_4$ and LMO. To enhance the cycle stability under elevated temperatures, thermal stable binders can make a potential contribution.

## 3.2 Binders for Anode Materials

### 3.2.1 Advanced Binders for Insertion-Type Anode Materials

Most SOA commercial anode materials, such as graphite and LTO, are insertion type with limited volume effect on lithiation (10% and 0, respectively). Moreover, they are more conductive and less oxidative than cathodes, hence, there are more candidates for anode binders. CMC is a 2D linear polymeric derivative of cellulose, and is made up of β-1,4-linked glucopyranose residues with varying levels of carboxymethyl group (–$OCH_2COOH$) substitution. Drofenik et al. reported CMC as the earliest water-soluble binder in 2003 [141]. They found the electrochemical performance of CMC is at least as good as that of PVDF for graphite anodes. However, it is very stiff and has a small elongation at break [142]. Afterward, Lee et al. reported an emulsified mixed binder (CMC/SBR) [143], with which the graphite slurry exhibited improved dispersion stability and homogeneity when compared to that with only CMC. Moreover, CMC/SBR is helpful to forming denser but less brittle coatings, with which the electrode exhibited high initial discharge capacity and stable cycle performance. In fact, CMC/SBR is almost the only choice of binders in battery industry for graphite anodes in the past decade. Its dosage in SOA jelly rolls is usually less than 4% and well fits the water treatment process, which makes it quite challenging to develop other new binders. Although researchers have carried out some studies on new binders such as PAAX (X = Li, Na and K) [144], bio-derived Alg, chitosan, xanthan gum (XG) [145], and poly(hydroxybutyrate-co-hydroxyvalerate) (PHBV) [146]; however, it seems that CMC/SBR will still dominate this area.

Spinel LTO was popular for its zero strain on lithiation, outstanding low-temperature and long-term cycle performance, and SEI free property. Moreover, LTO is compatible with both Cu and Al current collectors. However, it has a theoretical capacity of 175 mAh $g^{-1}$ and a high lithiation potential of 1.55 V (vs. $Li/Li^+$), which limits its energy density and thus wide applications. Binh et al. introduced a high molecular binder by a copolymerization of poly(ethylene glycol) methyl ether methacrylate (PEGMA), methyl methacrylate (MMA), isobutyl vinyl ether (IBVE), and poly(PEG-*co*-MMA-*co*-IBVE). It possesses high adhesion and elastomeric properties and good $Li^+$ conductivity. The electrode exhibited a high active mass loading of 28 mg $cm^{-2}$ and an areal capacity of 4.2 mAh $cm^{-2}$ at 0.5 C [147]. Other polymer binders, such as CMC [148], galactomannan gum [149] and XG [150], have also been investigated. However, similar to the case as in graphite, the challenge for LTO binders is also limited but for those thick electrodes.

### 3.2.2 Binders for Alloying-Type Anode Materials

Alloying-type anode materials (e.g., Si and Sn) are recognized as promising anodes for LIBs, due to their much higher specific capacity than graphite, moderate operating voltage, and abundant natural resources [151, 152]. However, the severe capacity fading, ascribing to the dramatic volume changes (such as for Si, up to 300%) during the alloying/dealloying process, limits their practical applications [153]. Silicon has a high theoretical capacity of 3 580 mAh $g^{-1}$ on lithiation ($Li_{15}Si_4$); however, the large stress in the alloying process may pulverize the particles, break down the conductive networks, destroy the SEI and finally lead to active material loss [80, 154]. Although these issues can be relieved by preparing nanostructured or composite materials such as Si/graphite (Si/C), local volume changes still hinder their development. The typical commercial Si/C anode contains only 5%–15% (by weight) Si. Binders are believed to be the most convenient method to promote the advance of high-capacity Si-based anodes, as they are capable of keeping the electrode integrity, working as the flexible artificial SEI and adjusting the SEI component [155, 156], and even transporting the electrons. Therefore, tremendous efforts have been paid on relevant researches, especially on nano-sized Si particles and their composites. Typical bio-material

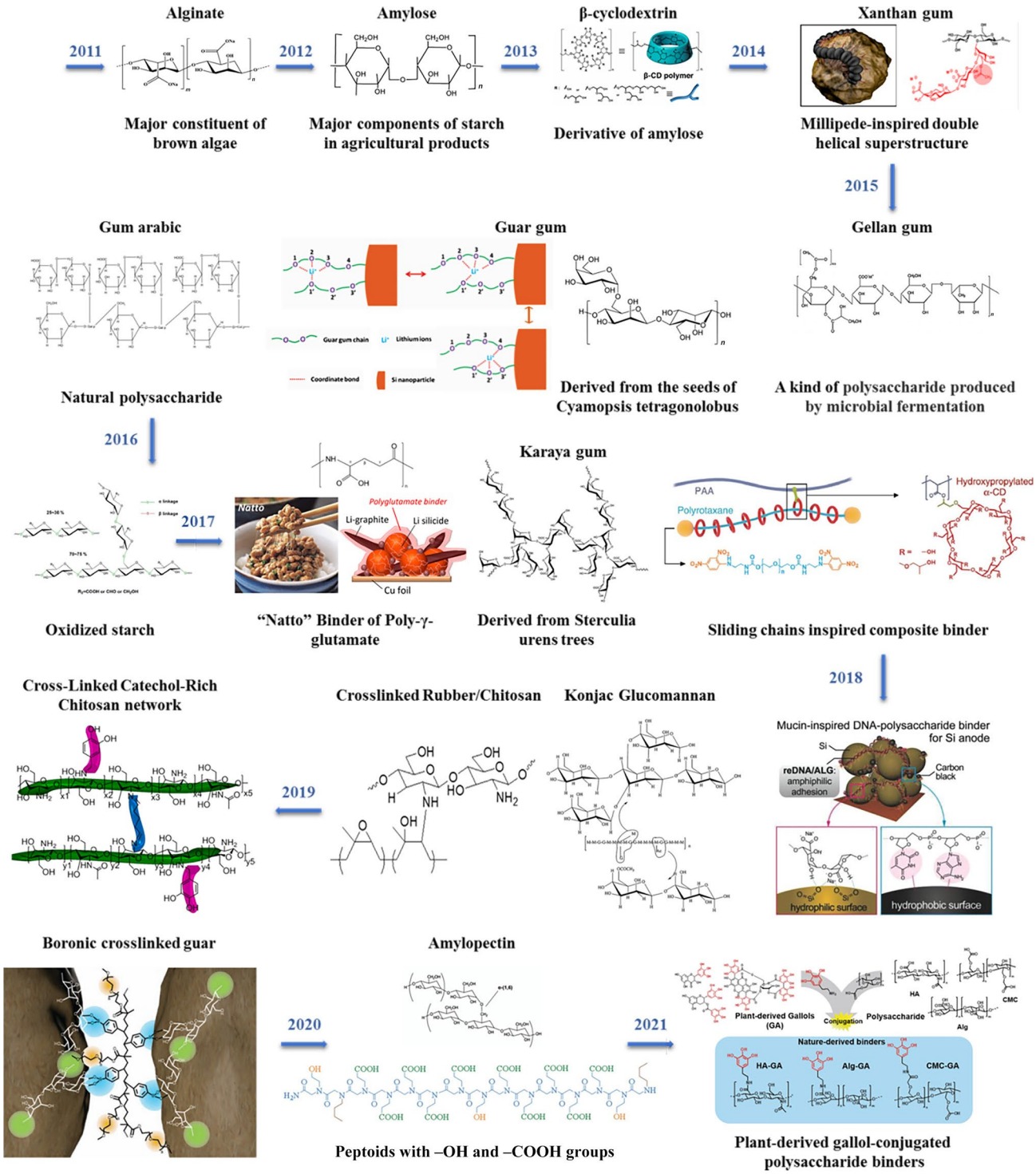


**Fig. 9** Development process of bio-inspired polymer binders for Si electrodes

derived and nature inspired binders are shown in Fig. 9 [7, 28, 29, 31, 32, 34–36, 38–40, 124, 157–168]. Meanwhile, several high-quality review papers have also been published summarizing these advances from different angles [80, 155, 169–172], such as self-healing binders, conductive binders, multifunctional binders, etc. Therefore, we will simply analyze the status of quo and highlight several works on micro-sized Si particles (μ-Si), which may be more suitable for future applications.

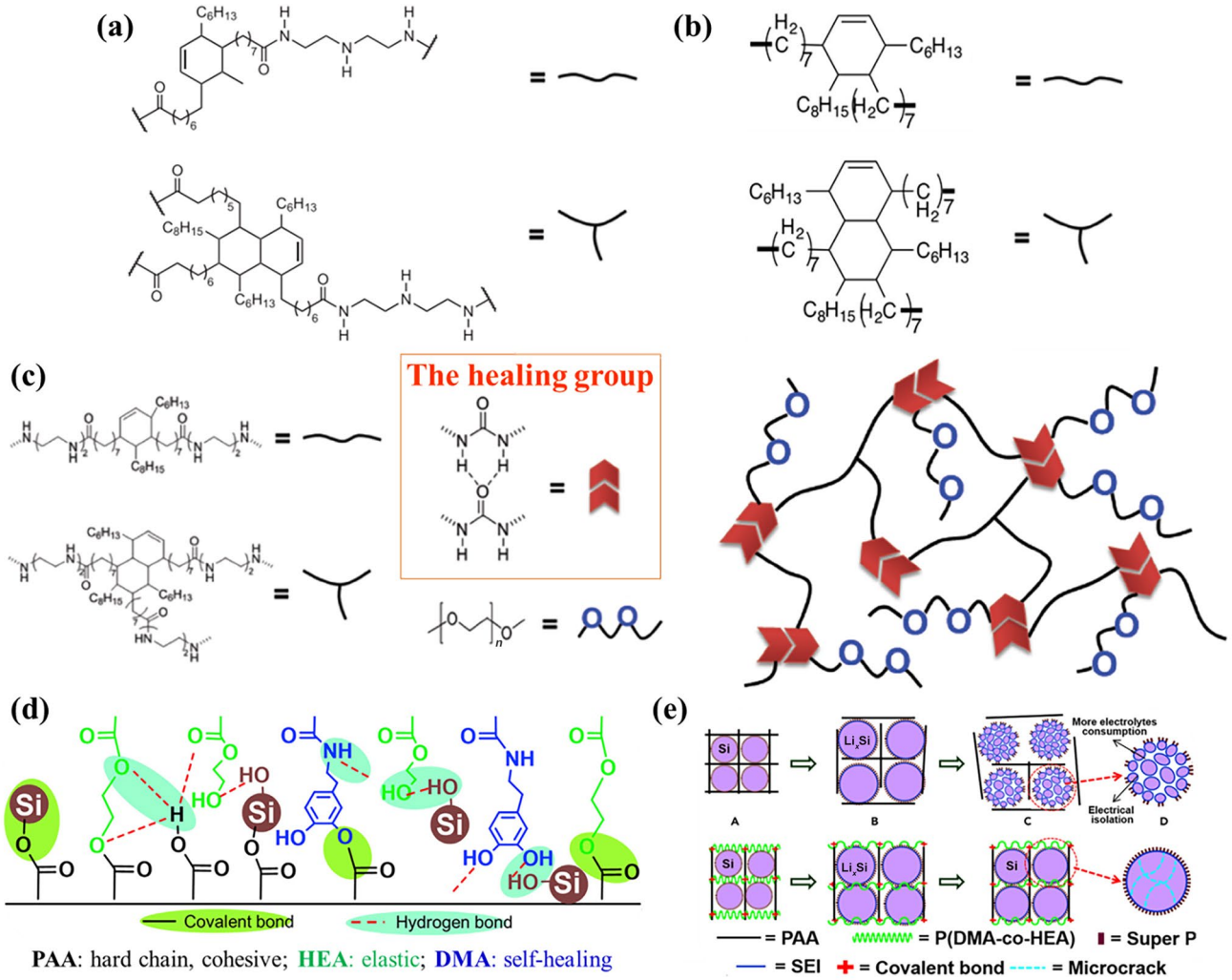


**Fig. 10** Typical self-healing binders and their functional groups. **a** The bidentate and tridentate groups used in the reported works, where the bidentate one links two healing groups, and the tridentate ones realize the crosslink and facilitate the self-healing. Reproduced with permission from Ref. [32]. Copyright © 2013, Nature. Reproduced with permission from Ref. [36]. Copyright © 2015, Wiley-VCH. **b** Groups endow the SHP with fast healing ability with short relaxation time. Reproduced with permission from Ref. [178]. Copyright © 2016, American Chemical Society. **c** Typical structure of an ionic conductive SHP and the healing group. Reproduced with permission from Ref. [180]. Copyright © 2018, Wiley-VCH. **d, e** Functional groups of the PAA-P(HEA-*co*-DMA) binder and their working mechanisms in μ-Si. Reproduced with permission from Ref. [40]. Copyright © 2018, Elsevier

Most efforts on Si-based anodes have been devoted to nanosized materials in the past ten years, since it has been found that there is a critical size for Si to fracture, which is about 150 nm for particles [173] and 240–360 nm for nanopillars [174]. Integrated nanoparticles unquestionably bring about many advantages such as a longer cycle life, impressive rate performance, and even high areal capacity. However, these superiorities are usually at the cost of high binder/CA ratios and high electrolyte usage [3, 175], which may lead to reduced energy density on the cell level. In fact, there are only limited publications including the electrolyte quantity, which has made it difficult to evaluate the performance in practical applications. Most SOA Si/C anodes just get the specific capacity of 450–650 mAh $g^{-1}$ [176, 177], corresponding to a Si content of ~ 10%. Moreover, the nanoparticles need to be encapsulated by graphite to avoid continuous SEI breaking/regeneration, which not only consumes the active Li and electrolytes but also leads to poor battery kinetics. Recently, some groups started to trial μ-Si in their research and some promising results were obtained. Here, we highlight these works.

The μ-Si has been long ignored in the first decade of this century due to its inevitable volume change during the charge/discharge process, even though it is much cheaper than the nanosized counterparts. Besides, although μ-Si has a relatively small surface area, the fracture or pulverization

caused by expansion may lead to fresh Si exposure and further electrolyte consumption [36], where the key issues are still there. Self-healing binders (SHBs) [32, 36, 40, 178–180] and SSBs [181] bring about possible solutions. Cui and Bao's group prepared a series of SHBs with the same H-bind healing sites and main chains with both bidentate and tridentate groups (as shown in Fig. 10) [32, 36, 178, 180], which endow the binders with either fast healing or ionic conductive ability. They reported the first SHB for μ-Si in 2013. This polymer is composed of the healing groups linked by the structures as shown in Fig. 10a. Low-cost metallurgical Si and a composite binder (SHB:CB = 20:3, in weight ratio) were used by a weight ratio of 1:1, then an electrode with an areal capacity of 1.5–2.1 mAh $cm^{-2}$ was prepared. Although the cell only showed 25 cycles (80 cycles in the rate test), it is still impressive since this is the first time for μ-Si to demonstrate its possibility. Latterly, the same group further optimized the electrode composition, including the particle size (~0.8 μm) [36], electrode preparation method (drop casting the AM and polymer composite one by one), binder ratio, and the areal capacity, after which a promising rate and cycle life were achieved. They even reported a binder that has a short relaxation time less than 10 s, which allows it to realize on-site level fast healing [178]. However, the binder ratio is still higher than that in SOA electrode architectures, for SHBs need fully percolated networks and certain thicknesses to realize their healing [182]. Moreover, as discussed in their work, the electrical healing of the electrodes was based on the CB distributed in the SHBs. Upon repeatedly stretching and relaxation, the CB particles may slowly form aggregates in the polymer matrix. As a result, the conductivity decreases and the capacity loses [36]. The ion and electron bicontinuous passage is still the bottle neck for μ-Si electrodes. Binders with stronger adhesive forces and electronic conductivity are needed. Considering the strong cohesive ability and low surface selectivity of the dopa group [46], Xu et al. prepared a water-soluble SHB (the functional groups are shown in Fig. 10d), the poly(acrylic acid)-poly(2-hydroxyethyl acrylate-*co*-dopamine methacrylate) [PAA-P(HEA-*co*-DMA)]. The binder is so strong that it could well encapsulate the Si particles even on its expansion or cracking states. With a low dosage of 10%, the electrode can achieve an areal capacity of 4.2 mAh $cm^{-2}$ under a current density of 0.5 A $g^{-1}$. They also tested the binder in full cells with an NCM111 counter electrode and the cells demonstrated a life more than 120 cycles. There are several other reports on SHBs using μ-Si [179, 183, 184]. However, hurdles still remain to settle, such as reducing the binder ratio and enhancing the rate capability.

Inspired by the sliding chains where the stress can be effectively dissipated, Choi's group developed a composite binder composed of polyrotaxane (PR) comprising polyethylene glycol (PEG) threads and α-cyclodextrin (α-CD) rings functionalized with 2-hydroxypropyl moieties covalently integrated with PAA, namely, PR-PAA (as shown in Figs. 9 and 18c) [38, 185]. PR-PAA showed less stress but higher strain (390%, larger than the theoretical expansion ratio of Si which is 300%) than PAA. Meanwhile, it kept its original shape after 10 stretch-recovery cycles even the strain is up to 200%, which allowed it well adaptive to μ-Si electrodes. The resultant Si anode (~3 mAh $cm^{-2}$) with 10% PR-PAA could work for more than 400 cycles with a Li counter electrode. Full cells with NCA cathodes also demonstrated satisfying performance.

In general, those efforts on μ-Si have attained great success in the past decade. The binder ratio has been reduced to about 10%; the areal capacity has been approaching the commercial level; and the cycle life has also been enhanced to hundreds of times. However, we can also note that there is still a big issue to be addressed: the volume expansion inevitably brings about cracks/fractures, and an SEI can still be generated on the fresh electrode surface and consumes the liquid electrolyte and the active $Li^+$ (as shown in Fig. 11a) [38]. Prelithiation [186–189] can largely compensate the active $Li^+$ loss, however, only in the initial cycles. SSBs might be a solution. Meng's group believed that the SEI in SSBs only forms on the Si/electrolyte interface without propagation in the long-term cycles (Fig. 11b). Moreover, considering the semi-conductor nature of Si and Si–Li alloy, they believed that both $Li^+$ and electrons can be transported in the electrode, thus the least binder or conductive agent is needed. In fact, only 0.1% PVDF was used in their work. A high areal capacity (~13.3 mAh $cm^{-2}$ in theory) electrode with 3.8 mg $cm^{-2}$ Si was prepared with a thickness of 27.2 μm and approximately 40% porosity. Interestingly, a shrinkage in porosity was observed during the charge/discharge process. As illustrated in Fig. 11b, the lithiation of Si caused the particle expansion and the electrode densification, which makes the ion/electron transport between adjacent particles possible. Figure 11c further shows the cycle performance of the as-prepared Si||NCM811 full cell under a 1 C rate and room temperature. Clearly, it exhibited good stability and a little bit low reversible capacity (~40% of its theoretical value). Although the binder made little contribution in this work, when considering the cell was tested under certain pressure where the electrode integrity was guaranteed, and when it goes without these physical barriers, strong binders are still needed. Huang et al. adopted SA as the binder for a micro-Si@$Li_3PO_4$@C electrode, and used it as the counter electrode of NCM111 in SSBs with CPEs based on PVDF, PVDF-HFP, LiTFSI, $Li_7La_3Zr_2O_{12}$ (LLZO), and PC (3D-PPLLP-CPEs) [190]. The cell showed good cycle stability and satisfying rate capability, with no capacity decay after 100 cycles (0.2 C). At the same time, the Si@$Li_3PO_4$@C anode also kept a high reversible capacity more than 1 000 mAh $g^{-1}$ after 200 cycles under a current density

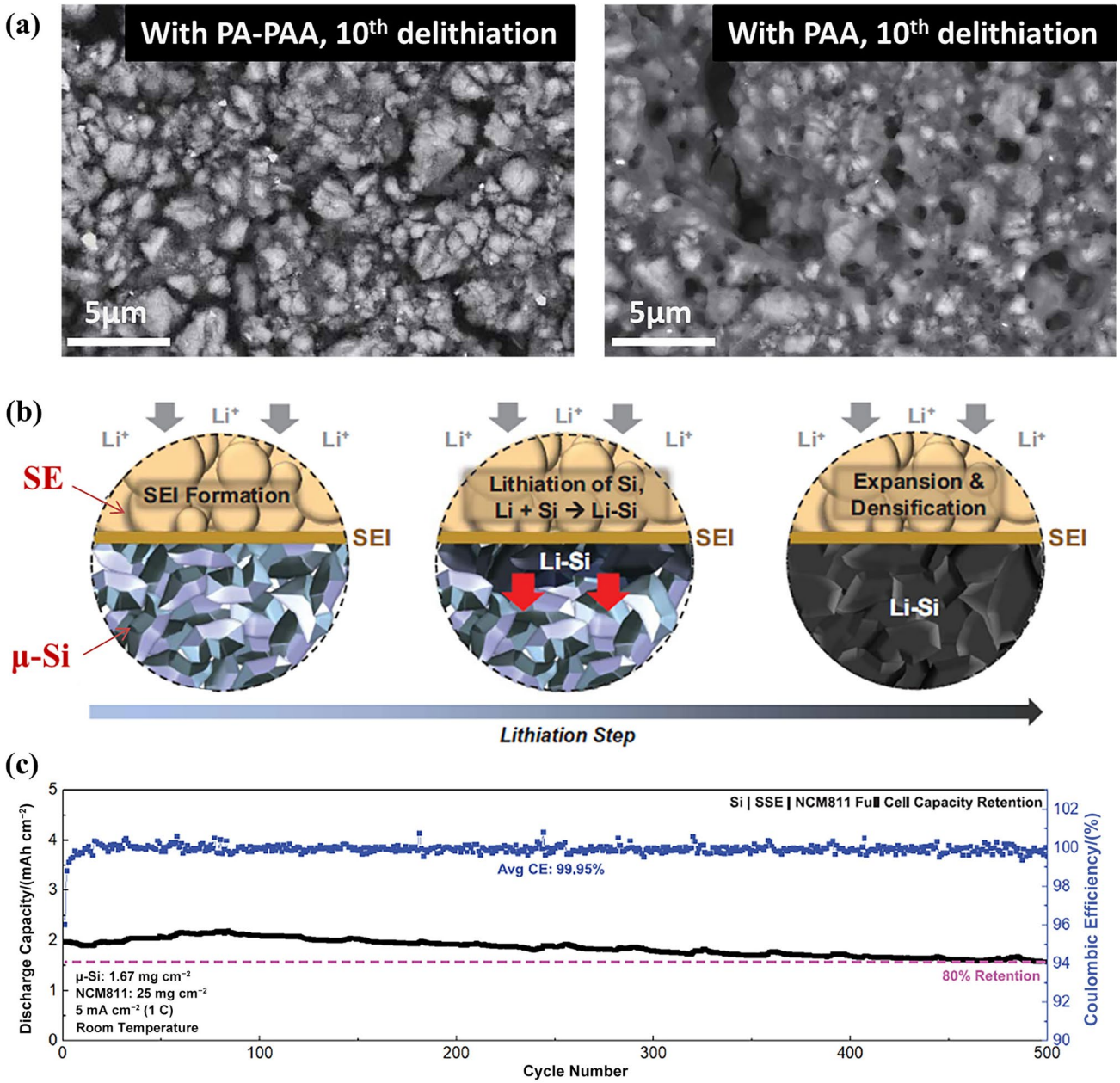


**Fig. 11** **a** Although PR-PAA can largely prevent the μ-Si from fracture compared to PAA, the particle size still shrinks and new surfaces are exposed. Reproduced with permission from Ref. [38]. Copyright © 2017, The American Association for the Advancement of Science. **b** SSBs might be a solution to the continuous propagation of SEI on μ-Si. **c** Solid-state full cells showed a long cycle life about 500 cycles, with about 40% capacity delivered. Reproduced with permission from Ref. [181]. Copyright © 2021, The American Association for the Advancement of Science

of 0.6 A $g^{-1}$ when the test was conducted within liquid electrolytes. In general, there is a large space for the exploration of μ-Si to be utilized in solid-state batteries.

Nanostructured Si is no doubt one of the most popular anode materials in the past decade. Meanwhile, the raise of μ-Si also provides a new approach to realizing higher energy density and longer cycle life. However, there are still some challenges to be settled, such as the SEI accumulation and active material loss, electrolyte and active $Li^+$ consumption, and thickness change on the cell level. Therefore, it may still have a long way for μ-Si to be commercially used.

### 3.3 Binders in Thick Electrodes

Increasing the coating thickness or areal capacity of LIB electrodes is one direct and effective approach to enhancing

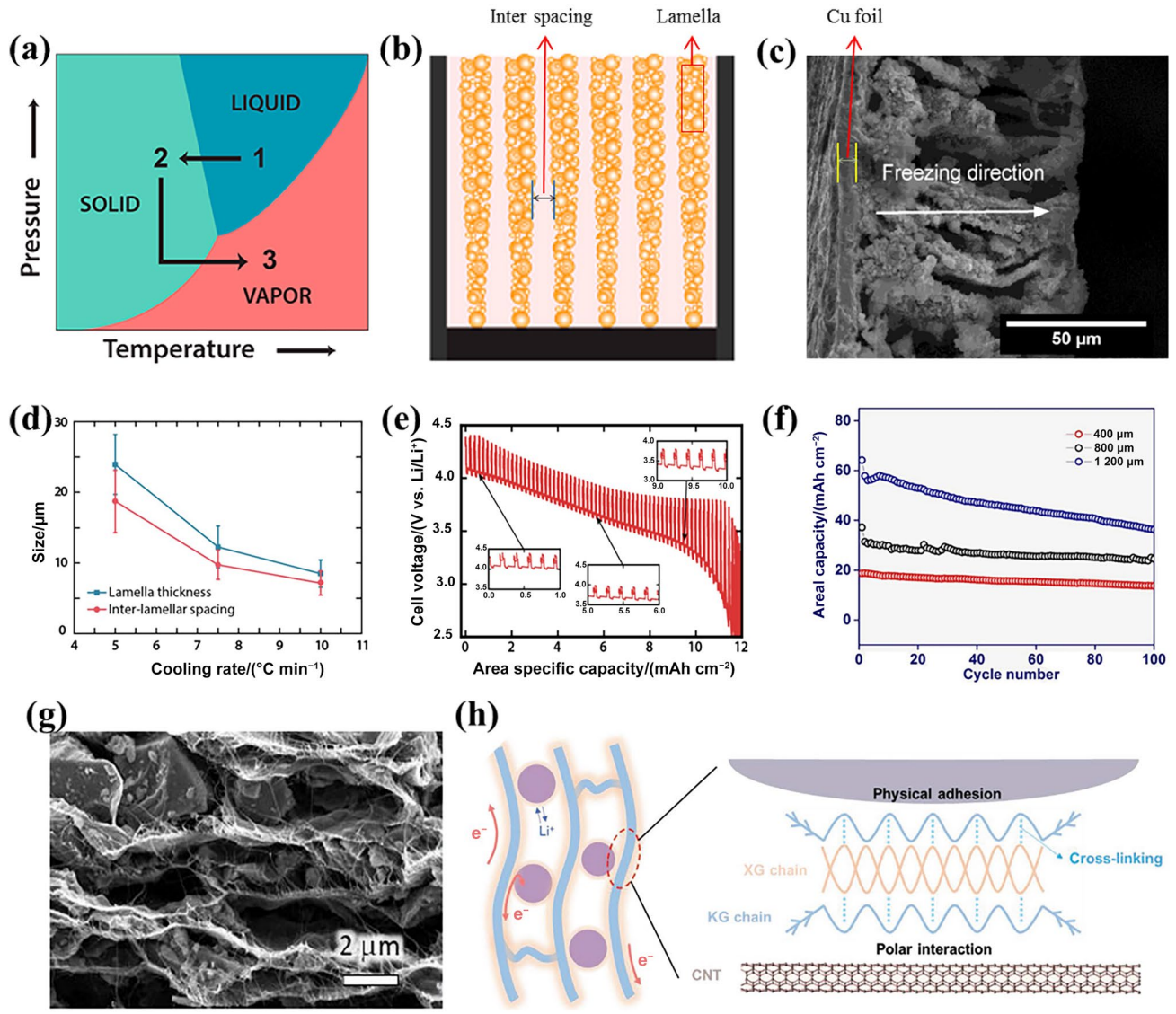


**Fig. 12** **a, b** Schematic diagram of ice templating. Both lamella and inter-spacing are illustrated in (**b**). Reproduced with permission from Ref. [198]. Copyright © 2018, American Chemical Society. **c** Typical cross-sectional morphology of the freeze casting LTO electrode [199]. Copyright © 2017, The Author(s). **d** The influence of cooling rate on the sizes of lamella and inter-spacing of NCA electrodes [191]. Copyright © 2018, The Author(s). **e** Hybrid pulse power characterization (HPPC) result of a thick NCA electrode obtained by freeze casting, the areal capacity of which is more than 12 mAh $cm^{-2}$ [191]. Copyright © 2018, The Author(s). **f** Freeze casting is also feasible for thick sulfur electrodes, the thickness of which is as much as 1 200 μm and the areal capacity is more than 60 mAh $cm^{-2}$ [201]. Copyright © 2021, The Author(s). **g** Microstructure of a CNT segregated μ-Si electrode. Reproduced with permission from Ref. [203]. Copyright © 2019, Springer Nature. **h** Function mechanisms of CNT, XG and KG in thick electrodes obtained by IT method. Reproduced with permission from Ref. [192]. Copyright © 2021, Wiley

the energy density by minimizing the inactive component ratio at the cell level [88, 191, 192]. However, thick electrode design goes along two major challenges: the coating layer cracking due to the surface tension in the drying process and the degrading rate performance due to the longer ion/electron diffusion pathways. The critical thickness ($h_{max}$, the thickness without cracking) can be calculated by Eq. (1) [193, 194], where $G$ is the shear modulus of the particles, $M$ is the coordination number, $\varnothing_{rcp}$ is the particle volume fraction at random close packing, $R$ is the particle radius, $\gamma$ is the solvent-air interfacial tension, and $P_{max}$ is the maximum attainable capillary pressure. Most of these parameters are highly decided by the shapes and sizes of the AM particles, and the solvent adopted under certain drying temperatures. Therefore, $P_{max}$, which depends on the channel geometry, becomes the key for the preparation of thick electrodes when the binder-aided-coating method is used. Meanwhile, certain channel geometries such as the vertical porous structure

[191, 195–202] can also facilitate the electrolyte infiltration, promote the ion transport, and enhance the electrochemical performance of thick electrodes. Thus, researchers have paid much intention on this area.

$$h_{\max} = 0.64\left[\frac{GM\varnothing_{\mathrm{rcp}}R^3}{2\gamma}\right]^{1/2}\left[\frac{2\gamma}{(-P_{\max})R}\right]^{3/2} \quad (1)$$

Freeze casting or ice templating (IT) is a convenient and versatile method for the preparation of electrodes with vertical pores. It can be used for various AMs such as LTO [199] (as shown in Fig. 12c), NCA [191], LCO [197], LFP [200], graphite [198], and even sulfur [201]. Water sublimation in cold soil is inclined to form the so-called needle ice with particular shapes and sizes (the lamella and inter-spacing, respectively), occurring via capillary action under certain circumstances (as illustrated in Fig. 12a, b). Taking advantage of this property, Chiang's group reported a method to prepare thick NCA electrodes, with 1% PEG-300 as the surfactant and 1% Darvan 7N and Aquazol polymer as the binder. A paralleled porous structure was formed under the freezing rates of 5–10 °C $min^{-1}$ after sintering to remove the extra binder and surfactant. They found that both the lamella thickness and the inter-spacing can be controlled by the freezing rate, and that these parameters further influence the electrochemical performance of the electrodes. With a thickness of ~ 330 μm, the NCA electrode delivered a high discharge capacity of ~ 12 mAh $cm^{-2}$ under the hybrid pulse power characterization mode, which manifested the feasibility of this method for the preparation of thick electrodes (Fig. 12e). Latterly, Huang's work further highlighted the importance of the freezing direction [197]. With 3.7% CMC as the binder, they prepared LCO electrodes with a thickness of 900 μm via both isotropic ice templating (IIT, uniform freezing from all directions) and directional ice templating (DIT). It proved that IIT is incapable of forming the vertical porous structures. Meanwhile, they found that sintering is not necessary, which makes the process more facile. They also believed that the avoidance of sintering could retain the sub-micron pores and promote a relatively high electrode/electrolyte interfacial area thus enhancing the reaction kinetics. As a result, the coral-like LCO electrode demonstrated outstanding rate performance, and the areal capacity was higher than 8 mAh $cm^{-2}$ even under 5 C rate.

Thick electrodes can also be obtained without using traditional polymer binders. Nicolosi and coworkers reported a segregated CNT network (Fig. 12g) strategy to construct thick electrodes with microsized AM particles, where the CNT works as both electron passages and physical binders [203]. With the thicknesses up to 800 μm, the areal capacity of the μ-Si electrode is as high as 45 mAh $cm^{-2}$. Pan's group combined this strategy with the IT method as illustrated in Fig. 12h [192]. Due to the templating effect of ice, much less CNT is needed to form the parallel structure; meanwhile, the XG and KG copolymer binder reinforced the contact between the AM particles and the conductive networks. As a result, with the AM ratio > 95%, the areal loading of the NCM811 electrode is up to 217.6 mg $cm^{-2}$ with a capacity of 30 mAh $cm^{-2}$.

The IT strategy is also feasible for SSBs. Sun's group prepared an LFP electrode using PEO/LiTFSI (EO:Li = 16:1) as both the binder and the $Li^+$ passages by the IT method with AN and water as the solvent (1:9, in volume ratio) [200]. The parallel pores not only decreased the ion transport distances and enhanced the rate performance but also balanced the $Li^+$ flux thus reducing the dendrite risk. As a result, the LFP SSB with an areal loading of 10.5 mg $cm^{-2}$ delivered a high areal capacity of 1.52 mAh $cm^{-2}$.

IT is no doubt an effective method to prepare thick electrodes with high areal capacity and good rate performance. Although the function of binders has not yet been deeply studied, considering their effectiveness on slurry rheology, surface tension and capillary force, we believe that it is well worthy of being explored.

Thick electrodes can also be obtained by a simple binder optimization. Schappacher's group studied the performance of 3 water-soluble binders (CMC, PAA and PEO) in NCM111 electrodes [204]. They found that with octanol added, the assembly of CMC, PAA and PEO (1:1:1) could reduce the slurry viscosity thus increasing the solid content to 65%. Electrodes with an areal loading of 60 mg $cm^{-2}$ were prepared, however, the rate performance is yet to be enhanced. They also found that higher solid contents would lead to smaller pore sizes in the electrodes and inferior battery kinetics. Therefore, it is of vital importance to take the process conditions into account in new binder development, as it is not only the adhesion force but also the functional groups and slurry rheology that decide the final performance.

### 3.4 Binders for Advanced Separators

Separators have significant influences on the cell performance, such as the rate capability, energy density, and even the safety in use [205–208], because the thermal runaway of batteries usually starts from an inner short circuit, i.e., the penetration, shrinking or melting of the separator. Several high-quality reviews [209–211] have already summarized the requirements on separators, such as chemically and electrochemically stable within the working potential of the cells, highly porous, mechanically robust, thermally stable in certain temperature range, etc. Therefore, here we will omit this part and just simply review the binders applied in separator modification that aims to fulfill these requirements.

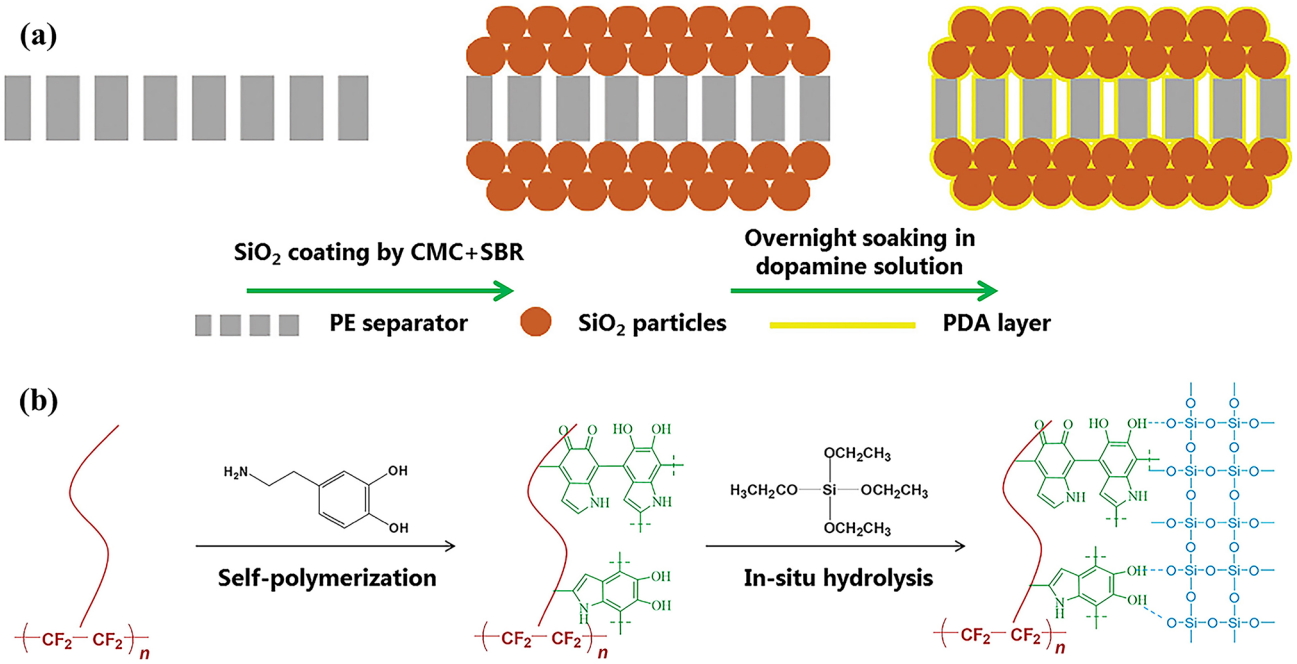


**Fig. 13** Two ways of using PDA as the binder for separators. **a** The coating method [213]. Copyright © 2016, The Author(s). **b** The binding method. Reproduced with permission from Ref. [221]. Copyright © 2020, Elsevier

Coating is unquestionably the most convenient solution that is easy to realize mass production, where binder is indispensable. Currently, most of the power batteries for EVs adopted ceramic powder (mostly $Al_2O_3$) coated polyolefin membranes, where PVDF or PVDF-HFP was used as the binder. With single or both sides coated, although only a thickness of about 1–5 μm, these separators are stabler on thermal shock [212–214], crash or even nail penetration [215]. Generally speaking, the coatings inevitably lead to lower porosity and less electrolyte uptake of the separators [216, 217], as the coating material, especially the fluid binder solution, could fill into some of the pores. Therefore, strong adhesive forces (to reduce the binder dose) and high thermal stability are required on the binders for separator coating applications. In these considerations, some polymers with high melting temperatures such as CMC [212, 215, 217–219], polydopamine (PDA) [213, 220, 221], PAALi [222], and some thermoset polymers like polyethylene terephthalate (PET) [223] and polyimide (PI) [214], are applied. Zhao's group prepared a PE-$SiO_2$@PDA composite membrane [213] as shown in Fig. 13a, where PDA not only worked as a binder but also formed a self-supporting film throughout the PE network and ceramic layer, thus providing an extra backbone for the separator. The membrane could maintain its physical strength up to 200 °C, which is much higher than that of PE or the one simply using CMC-SBR as the binder (the intermediate product in Fig. 13a). Moreover, the pouch cell using this PE-$SiO_2$@PDA membrane did not short circuit even after 170 °C high-temperature standing for 100 h, which demonstrated its enhanced safety. Due to the continuous pursuit of high energy density in LIBs, thinner separators are still urgently needed. Considering the relatively high density of ceramics, traditional coating process may add too much weight to the separators. In-situ polymerization might be a good way to control the binder and ceramic quantity. Xiao's group prepared a silica coated expanded polytetrafluoroethylene (ePTFE) separator with PDA as the binder (ePTFE-PDA-$SiO_2$) [221], as shown in Fig. 13b. By simply immersing the ePTFE matrix into dopamine solution with the pH controlled for 10 h, 3.7% PDA can be polymerized onto the matrix and worked as binders. The composite separator containing 3.3% silica not only is nonflammable but also exhibits good thermal stability, high electrolyte uptake, and thus better rate capability and cycle stability when used in batteries. These two works demonstrated two distinct methods to use PDA, either as a coating layer or as a binder. Both showed great potential to future applications.

Binders are also used in inorganic separators. A 37-μm thick $Al_2O_3$ separator was reported in Xiang's work [224]. With SBR as the binder and PEG as the pore-former, the membrane is flexible and nonflammable. Moreover, it showed better affinity to the electrolyte than PE, where the electrolyte contact angle is 0°. Applied in an NCM111||graphite coin-type full cell, it delivered a high discharge capacity of 128 mAh $g^{-1}$ under an 8 C rate, where that of the cell with PE separator is only 105 mAh $g^{-1}$.

Considering the indispensable role of the separator in LIB industry and its significant influence on cell performance, lighter and more reliable separators are yet to be developed. In view of the rapid development of binders for silicon anodes and high-voltage cathodes, those advanced multifunctional binders may provide new solutions for the separator modification.

## 4 Binders for Lithium Metal and Solid-State Batteries

Considering the high flammability of organic liquid electrolytes and the low energy density of LIBs, solid-state batteries (SSBs) especially the solid-state lithium metal batteries (SSLMBs) with nonflammable SEs and high-capacity electrodes are good choices for energy storage systems [225, 226]. In recent years, relevant researches have mainly focused on binder-free SSBs with quite thick SEs for the ease of manufacture and investigation. However, the electrolyte needs to be thin enough (< 50 μm) to achieve practical energy density [227, 228], where a certain amount of binder is necessary to compensate for the brittleness of inorganic solid electrolytes (ISEs) [229]. Moreover, binder-free SSBs produced by dry methods (e.g., cold or hot pressing) can only be used on the laboratory scale, hence more attention has been focused on wet methods which are applicable to the well-established roll-to-roll processes to produce LIBs on a larger scale [230, 231]. The choices of binders should be carried out with great care to ensure the compatibility with solvents (only in wet methods) and solid electrolytes [232]. Moreover, most polymeric binders are ion- and electron-insulating, which leads to the reduction of ionic conductivity and thus jeopardizes the cell performance [231]. Therefore, suitable binders are still a big challenge in SSBs' preparation. In this part, we summarized the materials and the relevant techniques for the preparation of ISE films and electrodes, and tried to shed some light on the design and development of advanced SSBs.

### 4.1 Binders for Solid-State Electrolytes

Solid polymer electrolytes (SPEs) can form flexible thin films through the interlocked polymer chains, where no extra binders are needed. Therefore, we mainly discuss the binders for inorganic electrolyte films. ISEs, especially the sulfides, have ionic conductivity as high as $10^{-2}$ S $cm^{-1}$ at room temperature, which is comparable to or even higher than that of liquid electrolytes [233, 234]. However, ISEs are brittle and difficult to form intimate contact among particles. Mixing ISEs with polymeric binders is a promising method to obtain homogeneous and highly-processible SE films, for which the wet method (with solvent) is most commonly used. Sulfide ISEs are highly sensitive to common solvents, such as water and some polar solvents, e.g., NMP, DMF (*N*,*N*-dimethylformamide), AN (acetonitrile), DMC (dimethyl carbonate), and so forth [235–237]. According to the hard and soft acids and bases (HSAB) theory, electrophilic species of sulfides can trap lone-pair electrons in highly electronegative elements such as the O and N of high polarity solvents [238]. For example, the glass–ceramic $Li_7P_3S_{11}$, which is well known for its ultra-high room-temperature ionic conductivity, is ready to react with AN and DMC to form insulate $PS_4^{3-}$ and $P_2S_6^{4-}$, resulting in reduced ionic conductivity [236]. Therefore, the compatibility of the binder, electrolyte and solvent has become the primary factor to be considered. Nonpolar or less polar solvents came into the public sight and were screened for the preparation of stable sulfide ISE slurry. A wide range of solvents and polymer binders have been investigated to match with the sulfide electrolyte $75Li_2S$-$25P_2S_5$ in Choi's work [239]. After comparing the physical properties of eight common solvents (with the polarity index *P* ranging within 0.1–6.7), especially the polarity and vapor pressure which are the two most critical parameters to be considered, they found that solvents with high *P* values (> 4.0) would react with the SSE, while heptane ($P = 0.1$), toluene ($P = 2.4$) and *para*-xylene (*p*-xylene, $P = 2.5$) with low *P* values were relatively stable. Then two choicest polymeric binders [polybutadiene and acrylonitrile butadiene rubber (NBR)] were used to prepare slurry with the three selected solvents. After the tests of conductivity and adhesion, *p*-xylene and NBR were considered to be the suitable solvent and binder, respectively. Latterly, Riphaus's group studied the binder influence on $Li_{10}SnP_2S_{12}$ (LSPS) SSE film preparation [240]. Five polymer binders [polyisobutene (PIB), SBR, PMMA, poly(ethylene vinyl acetate) (PEVA) and hydrogenated nitrile butadiene rubber (HNBR)] with the average molecular weight ($M_w$) ranging between $1.9 \times 10^5$ and $3.1 \times 10^6$ were used in their study with toluene as the solvent, and the binder ratio was controlled between 2.5% and 10% (by weight). All binders showed good compatibility toward LSPS; however, freestanding films could be formed when PMMA was used as the binder due to its too rich functional groups. As to the other binders, it was found that all of them influence the $Li^+$ diffusion according to the NMR results. Less binder with appropriate $M_w$ and polar functional groups such as 2.5% HNBR seems to be the optimal binder for this system.

Although less polarity solvents are conducive to meeting the compatibility requirements of sulfide ISEs, the limited grain boundary conductivity still hinders their practical applications. Extra $Li^+$ passways are needed between the ISE particles. Jung's group did a series of work in this respect [238, 241–243]. Taking advantage of the HSAB theory, they found that the solvated ionic liquid (SIL), LiG3 [a complex between LiTFSI and triethylene glycol dimethyl ether (G3),

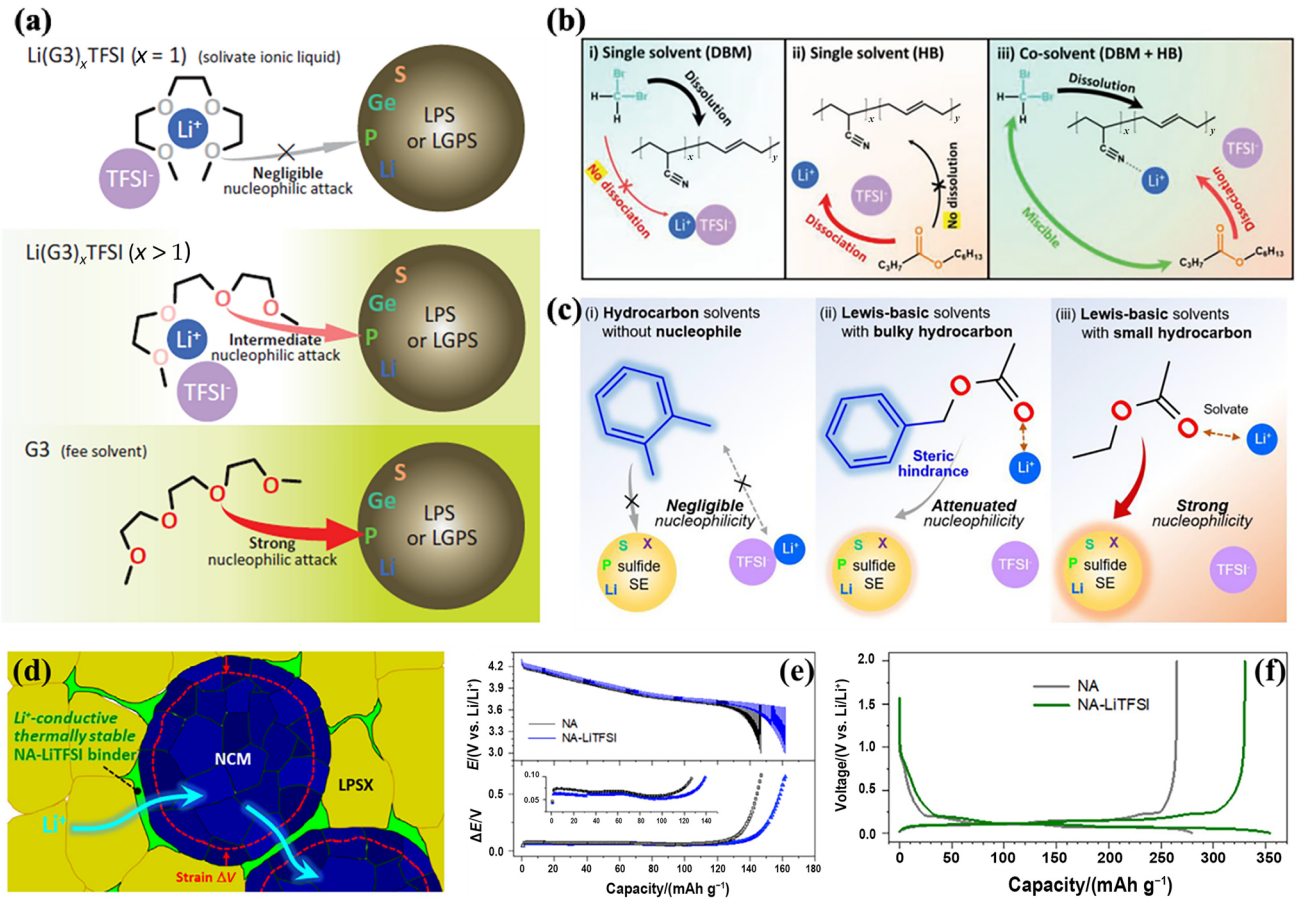


**Fig. 14** Schematic diagrams illustrating the interactions between solvents, salts and ISE in SSBs. **a** Functions between LiTFSI, different amounts of G3, and LGPS. Reproduced with permission from Ref. [238]. Copyright © 2015, Wiley. **b** Co-solvent effect on LiTFSI and NBR binders. Reproduced with permission from Ref. [242]. Copyright © 2021, Wiley. **c** Lewis-acid solvent with bulky hydrocarbon is compatible with the sulfide ISE. **d** The NA-LiTFSI couple could compensate the ion passways between LPSX particles and buffer the stress between NCM and LPSX. **e** GITT profiles of NCM SSBs with different binders. **f** Charge/discharge profiles of graphite SSBs with different binders. Reproduced with permission from Ref. [243]. Copyright © 2021, Elsevier

with a molar ratio of 1:1], is stable toward LGPS, as shown in Fig. 14a [238]. The SIL could not only provide additional ion passages but also largely reduce the SE/electrode porosity. The resultant LFP SSBs could work at 30 °C and deliver a high reversible capacity of 144 mAh $g^{-1}$. As no binder was included in this work, both electrodes and SEs were prepared by the hot process and showed limited flexibility. Therefore, the same group developed wet methods to fabricate SE films and electrodes. They found that a co-solvent composed of less-polar dibromomethane (DBM) and more-polar hexyl butyrate (HB) is compatible with $Li_6PS_5Cl_{0.5}Br_{0.5}$ (LPSX) and able to well dissolve the NBR binder and LiTFSI (the sketch map is shown in Fig. 14b). Slurry-processable solvents with different DBM/HB proportions were prepared to explore the dispersion of NBR and the performance of ASSBs. Excellent cycle performance of NCM/Gr ASSBs was obtained when the ratio of the DBM/HB co-solvent was set to 2:8 (volume ratio) with 1% LiTFSI. A 15 mm × 20 mm pouch-type full cell was prepared based on this concept and tested under 30 °C. A capacity close to the theoretical value was delivered. The nitrile group on NBR could dissociate lithium salts and thus work as a $Li^+$ transport site. Therefore, the NBR-LiTFSI system not only physically binds the AM and SE together but also chemically realizes the ion transport. Recently, they further optimized the binder and solvent system to achieve better thermal stability and less environmental concerns [243]. An NA-LiTFSI composite binder including NBR, poly(1,4-butylene adipate) (PBA) and LiTFSI was used for both NCM electrodes and LPSX SE films with benzyl acetate (BA) as the solvent. Comparing with HB and ethyl acetate, the bulky benzyl group on BA (Fig. 14c) reduces its reactivity toward the sulfide SE by its steric hindrance effect while still keeping the ability to dissociate the lithium salt, where a higher reversible capacity is achieved when LiTFSI is added (Fig. 14e, f). Meanwhile, it also enhances the binder's thermal stability and the

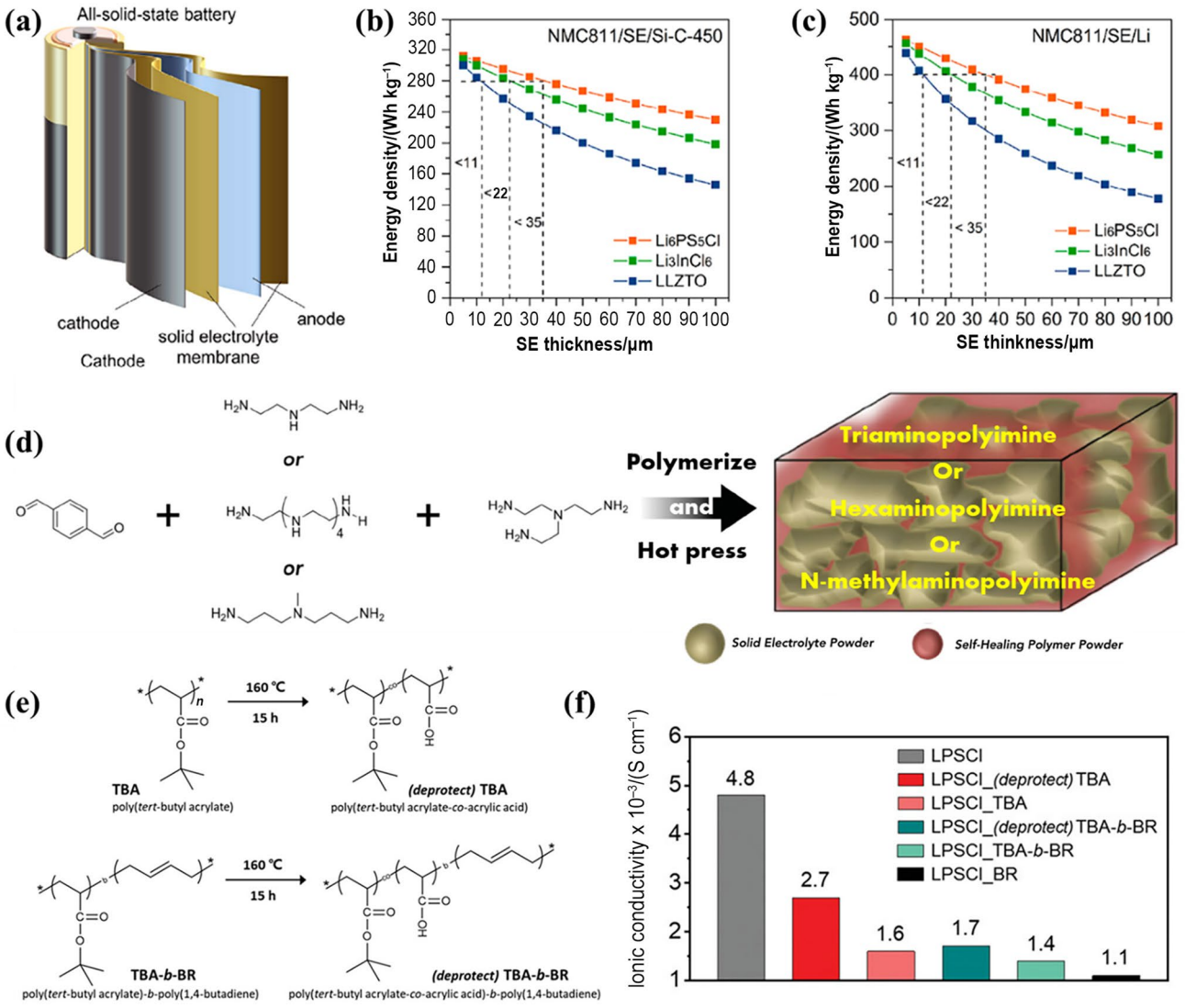


**Fig. 15** **a** Schematic diagram of a cylindrical solid-state battery. **b** Calculated gravimetric energy density of all-solid-state batteries with a configuration of NMC811|SE|Si–C-450 as the function of SE membrane thickness from 5 to 100 μm. **c** Calculated gravimetric energy density of all-solid-state batteries with a configuration of NMC811|SE|Li as the function of SE membrane thickness from 5 to 100 μm. Reproduced with permission from Ref. [246]. Copyright © 2022, American Chemical Society. **d** Molecular structure of the thermoset self-healing polymers and schematic diagram of the SEPM electrolyte. Reproduced with permission from Ref. [248]. Copyright © 2015, Wiley. **e** Structural changes of poly(*tert*-butyl acrylate) (TBA) and poly(*tert*-butyl acrylate)-*b*-poly(1,4-butadiene) (TBA-*b*-BR) after thermal deprotection. **f** Lithium-ion conductivity of the LPSCl solid electrolyte composite films containing (deprotect) TBA, TBA, (deprotect) TBA-*b*-BR, TBA-*b*-BR, and BR binders. LPSCl:binder = 97.5:2.5 by weight. Reproduced with permission from Ref. [251]. Copyright © 2020, Wiley

compatibility with the graphite anodes. Figure 14d shows the overall function mechanism of the composite binder: transporting $Li^+$, buffering the volume change of NCM, and linking AM and SE particles together. It is worth noting that the areal AM loadings of the electrodes in Fig. 14e, f are 14 and 7.5 mg $cm^{-2}$, respectively, quite close to the SOA LIB level. However, the SE contents in the electrodes are still a little bit high (24.5%–47.5%, in weight percentage), where more research efforts are deserved.

Leaving aside the compatibility between binder, electrolyte and solvent, the insulated polymeric binders can reduce the conductivity and lead to poor cell performance, which is also a major challenge. Inada et al. investigated the ionic conductivity and morphology of composite SSEs including ISEs and organic polymers used as binders prepared by both dry and wet methods [244, 245]. The ISEs adopted in their work are $0.01Li_3PO_4$-$0.63Li_2S$-$0.36SiS_2$ and $Li_{3.25}Ge_{0.25}P_{0.75}S_4$. SBR and silicone rubber were used as the binders. The electrolytes prepared by the dry process showed

good contact between SBR granular domains and ISEs, which resulted in high ionic conduction. However, when the wet process was adopted, the insulated SBR covers on the surfaces of ISEs and reduces the conductivity dramatically. For this reason, they developed a liquid silicone as a binder. The ionic conductivity of the composite can stay in the order of $10^{-4}$ S $cm^{-1}$, even if the silicone content is as high as 10% (volumetric percentage).

Reducing the SE membrane thickness can effectively enhance the energy density of the cells, as depicted in Fig. 15a–c [246]. Although the density of the ISEs is different, it is hard for the SSBs with similar electrode configurations to get comparable energy density (280 Wh $kg^{-1}$) with SOA LIBs unless the ISE thickness could be reduced to 11, 22 and 35 μm for LLZO, $Li_3InCl_6$ and $Li_6PS_5Cl$ (LPSCl), respectively. Accordingly, these thin ISEs render an energy density of ~ 400 Wh $kg^{-1}$ in LMBs using an NCM811 cathode. Therefore, it is of vital importance to develop techniques for preparing thin SE membranes [247]. Currently, the dry method still dominates as it avoids the influences of solvents. Taking advantage of the malleable and thermoset properties of several self-healing polymers (as shown in Fig. 15d), Lee and Zhang's group developed a new method for preparing solid electrolyte in-polymer matrix (SEPM) [248]. With about 20 wt% (wt% means the weight percentage) polymers filling between the sulfide electrolyte particles, the SEPM showed enhanced ionic conductivity and relative density; impressively, the thickness of the electrolyte membrane decreased from 1 mm to 64 μm, which is beneficial for the energy density enhancement of the SSBs.

PTFE is the most widely used binder in active carbon electrode (for supercapacitors) fabrication. It forms elastic fibrous structure networks, which makes it show little side effect on electron transport. Recently, it was used as a binder for multiple ISEs in Yao's [249] and Sun's [246] work as it can interweave the ISE particles to form flexible membranes with reduced thicknesses of about 15–30 μm. It is noteworthy that the PTFE doses are quite low in these reports, only 0.2% and 0.5%, respectively, which makes the mixing process quite important.

The wet method was also used in thin ISE membrane fabrications. Zhang's group prepared a 60-μm freestanding argyrodite membrane using a cellulose (CEL) skeleton [250]. LPSCl was coated onto the CEL with silicone rubber as the binder and chloroform as the dispersant. Because the strong action between the CEL and SSE particles, LPSCl prefers to interact with the CEL fiber rather than themselves. Thus, the thickness of the SSE film shows a special self-limited phenomenon. Considering the incompatible polarity of the binders, solvents, and sulfide electrolytes, Choi's group proposed a novel binder concept of "protection-deprotection chemistry" and its function mechanism was illustrated in Fig. 15e [251]. Poly(*tert*-butyl acrylate) (TBA) and its block copolymer poly(*tert*-butyl acrylate)-*b*-poly(1,4-butadiene) (TBA-*b*-BR) with nonpolar *tert*-butyl (*t*-butyl) groups can protect the polar groups from side reactions with the sulfide ISE and LPSCl in the slurry mixing process. Then the binders could be deprotected by heat treatment during the drying process to cleave the *t*-butyl groups to ensure their high adhesion. It can be noted in Fig. 15f that the deprotected films show enhanced ionic conductivity when compared to the protected counterparts or the one with butadiene rubber as the binder. However, the thickness of the film still needs to be reduced.

In summary, as the core component of SSBs, SE films should not only have enough ionic conductivity ($> 10^{-4}$ S $cm^{-1}$ at room temperature), high lithium-ion transference numbers and wide electrochemical stability windows to fulfill the electrochemical requirements of a battery [252], but also be thin (< 30 μm) and flexible so that the high energy density LMB is possible. Currently, some inert binders could support the thin ISE film preparation. However, the process is still a bit complicated and inevitably reduces the ionic conductivity. As discussed in the former part, some intrinsic ionic conductive polymer binders may provide new chances here, as they can potentially reduce the space charge layer between ISE particles and diminish the electrode/electrolyte interfacial resistance. However, it is noteworthy that different SEs have different requirements for the binder/solvent and their percentage. Proper optimization of the system is still challenging. Meanwhile, new processing techniques should also be developed so that large scale production is possible.

### 4.2 Binders for Insertion-Type Cathodes of SSBs

Different to LIB electrodes where the ions can be conducted by the liquid electrolytes infiltrated in the electrode pores, the ion passages in SSBs are constructed by AM particles and SEs (or the binders). Most SOA cathodes prepared by either hot or cold press usually include 20%–40% SE. Although demonstrating satisfying electrochemical performance, the energy density is very limited even on the electrode level [253–257]. Therefore, the electrode design is of vital importance for the development of high-energy–density SSBs. Considering that lithium metal is usually adopted as anodes, the challenge mainly lies on the porous cathodes. Slurry casting is no doubt the most mature and convenient method for the preparation of electrodes. Adding a certain amount of polymer binders can not only promote the uniform dispersion of the particles [258] thus reducing the dose of SSE, but also adjust the slurry rheology and make the higher AM loadings possible [232]. The relevant works on binders for SEs can certainly afford us lessons that the additional issues such as the electron transport and AM particle volume change should also be considered. Different to the cases in

SEs, some special binders with extra properties, such as the PAALi [259] that is able to stabilize the CEI, reduce the interfacial resistance and enhance the battery kinetics, are being trialed in electrode designs for SSBs. Here, we classify them according to the functional groups, including PEO and its derivatives, carboxyl-rich polymers, other ionic conductive binders, and the none-conductive ones.

#### 4.2.1 PEO and Its Derivatives

As the earliest and most widely studied polymer host, PEO can not only transport the $Li^+$ by chain motions but also show certain adhesion ability by physical interlocking the AM particles, which makes it a promising binder candidate in SSBs [260–264]. Zhang et al. added 2% LiFSI into a composite of SIC, lithium poly[(4-styrenesulfonyl)(trifluoromethanesulfonyl) imide] (LiPSTFSI) and PEO (where the EO:Li ratio was set to 20:1), and used it as both the binder and the electrolyte for solid-state LFP cells [265]. Although its ionic conductivity is lower than that of the PEO:LiTFSI counterpart with the same EO:Li ratio, the cell showed enhanced cycle stability due to the enhanced dendrite suppression. Note that the lithium salt (e.g., LiTFSI and LiFSI) is inevitable even in the binder while the EO:Li ratio is relatively higher (typically, 16:1 or 20:1) than that in SPEs, the major consideration may lie on ensuring the stiffness and thus the electrode structure integrity. However, the PEO-based binders confront with two challenges. Firstly, the low ionic conductivity PEO (~ $10^{-5}$ S $cm^{-1}$)-based binders may bring about large bulk resistance to the cell and thus influence the kinetics. In fact, most SSBs adopting PEO-based binders can only work under relatively high-temperature environments. Secondly, PEO is generally believed to easily fail when the potential is higher than 4.0 V (vs. $Li/Li^+$) (the underlying mechanism is still controversial [266–269]). It is hard to be used in those 4.0-V class cathodes such as LCO and NCM without any additional treatment.

Some derivatives and composites of PEO are prepared to conquer these issues. Abraham et al. systematically studied the mixture of LiTFSI, oligomeric poly(ethylene glycol) dimethyl ether (PEGDME) [a low molecular weight ($M_n$) analog of PEO, the $M_n$ ranges in 250–500] and PVDF-HFP, and tries to use the composite as both the electrolyte and binder for a $LiMn_2O_4$ battery working within 3.0–4.5 V [270]. The authors believed that the PEGDME provides ion carriers and transport sites, acts as a plasticizer for PVDF-HFP. The PVDF-HFP not only strengthened the composite but also somewhat cross-linked with PEGDME via the lithium bond, O–Li–F. The resultant composites showed high ionic conductivity > $10^{-4}$ S $cm^{-1}$ and wide electrochemical stability windows up to 4.5 V. A semi-interpenetrating solid polymer (semi-IPN) was prepared in Kang's work via the polymerization of bisphenol A ethoxylate diacrylate in the mixture of LiTFSI and PEGDME ($M_n \approx 500$) with an EO:Li ratio of 20:1 [271]. The LCO cathode with the semi-IPN binder showed stable cycle performance within the voltage range of 3.0–4.3 V, which demonstrated its enhanced electrochemical stability compared to that of PEO. However, no direct comparison was given in this work. Latterly, Sun's group studied the influence of the terminal group on PEO, although the study was carried out on SPE rather than binder [269]. They found that replacing the terminal –OH group with the stabler $–OCH_3$ (such as PEGDME) group could broaden the electrochemical stability window of SPE from 4.05 to 4.30 V, and the SPE could support the long-term work of NCM523 SSBs. Recently, Kim's group grafted poly(ethylene glycol) (PEG) ($M_w$ = 2 000 or 4 000 g $mol^{-1}$, –OH as terminal group) onto poly(arylene ether sulfone) (PAES) and obtained a PAES-g-PEG copolymer. They further blended it with LiTFSI or an electrolyte of 0.5 M LiTFSI in 1-butyl-1-methylpyrrollidum bis(fluoromethane sulfonyl) (Pyr14TFSI) ionic liquid (IL) to enhance the ionic transportation [272]. These composites were used as binders (with salt) for NCM622, LCO and sulfur cathodes, and solid electrolytes (with the electrolyte), respectively. It proves that the composites not only show enough adhesive force and high ionic conductivity (> $10^{-4}$ S $cm^{-1}$) that could support the room temperature work of SSBs, but also largely suppress the oxidation of PEG with the PAES backbone. Recently, Jeong and coworkers found that although neither Pyr14TFSI nor PEO is miscible in xylene, the mixture of Pyr14TFSI, LiTFSI and PEO could form a glue-like solution (namely, LCBIM) [273]. They used the LCBIM as the binder for both LGPS SE and NCM electrodes and compared the SSB performance to that of NBR binder. It was found that the LCBIM ensured close contact between particles, where higher ionic conductivity (0.54 vs. 0.46 mS $dcm^{-1}$) and reversible capacity (166 mAh $g^{-1}$) were obtained for the SE film and the SSB, respectively.

By far, the studies on PEO and its derivatives are relatively limited. However, all these works came to a similar conclusion that it may not be the EO group that is vulnerable to be oxidized. It means that there is still a large space for exploration, such as that whether they can be used in more electrode systems, what on earth leads to the PEO-based SSBs' failure, and so forth.

#### 4.2.2 Carbonate or Carboxyl-Rich Polymer Binders

In-situ polymerization is a facile way to reduce the interfacial resistance and is currently widely studied in semi-solid-state batteries [33, 274–276]. Cui and coworkers further implemented this strategy into electrode preparation [277]. A poly(vinyl carbonate)-based binder, PVCA, was synthesized by a free radical polymerization of 1 M LiDFOB/vinyl carbonate electrolyte, and it was utilized in an LCO

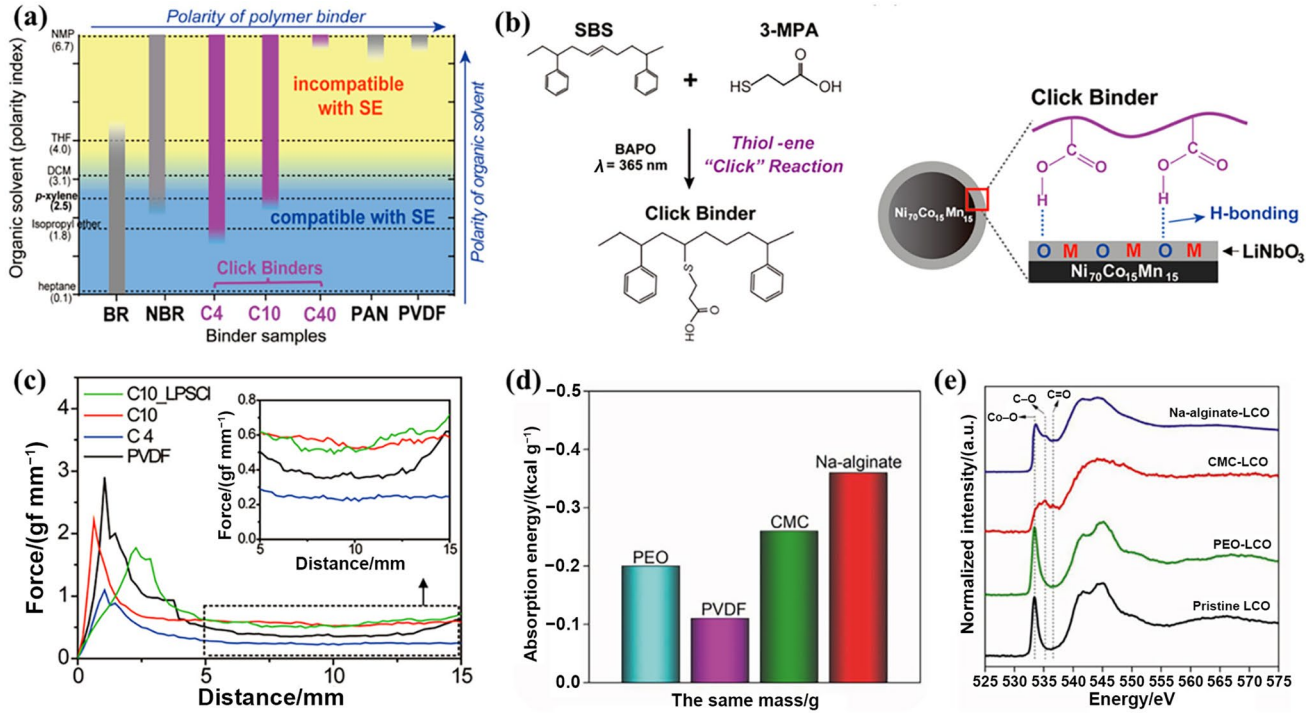


**Fig. 16** **a** Solubility of various binders in solvents with different polarity. **b** Synthesis of the click binder using the click (thiol-ene) reaction between SBS and mercaptocarboxylic acid, and its working mechanism in the electrode. **c** The 180° peeling tests for the electrodes using the click binders and PVDF. *P*-xylene and NMP were used as the solvents for the dissolution of the click binders and PVDF, respectively. Reproduced with permission from Ref. [285]. Copyright © 2019, American Chemical Society. **d** Absorption energy of various binders on LCO. **e** O K-edge XAS at TEY mode for LCO samples with different binders. Reproduced with permission from Ref. [286]. Copyright © 2020, Wiley-VCH

electrode. The same electrolyte was injected into the cell and in-situ polymerized to form the SSB. It was found that LiDFOB can be dissociated in PVAC and $Li^+$ interacts with the oxygen on carbonate group, thus providing a comparable room temperature ionic conductivity ($2.23 \times 10^{-5}$ S cm$^{-1}$) to that of PEO. The resultant SSB demonstrated a high reversible capacity of 146 mAh g$^{-1}$ at 50 °C and a 0.1 C rate, and a high capacity retention of 84.2% after 150 cycles between 3.0 and 4.3 V.

Compared to PEO and its derivatives, carboxyl-rich polymers such as PAA and PAALi have saturated polyolefine main chains, which endow them with wider electrochemical windows, better thermal stability, higher adhesive force [278], higher glass transition temperatures and melting points. PAA and PAALi were widely used in Si anodes [279–282], LIB cathodes [101, 114, 283], separators [222, 284], and cathodes for SSBs [259]. Lu et al. used PAALi as the binder for both the LNMO cathode and $RuO_2$ anode [259]. Comparing with the counterpart using the PVDF binder that delivered no capacity under room temperature (23.8 °C), the SSB using the PAALi binder showed a low reversible capacity in the initial cycles; however, the reversible capacity gradually increased to about 87.5 mAh g$^{-1}$ after 80 cycles at a 0.2 C rate, which was attributed to the $Li^+$ conductive nature of PAALi.

Just like the case in sulfide SEs, there is a trade-off among the three parameters in SSB cathode preparation, chemical compatibility with SEs, slurry dispersion and the adhesion of electrodes, as illustrated in Fig. 16a [285]. The compatibility of the SEs with solvents is indicated in blue (compatible) and yellow (incompatible) regions. Those binders with low polarity, such as butadiene rubber (BR), SBR and NBR that could disperse in heptane and *p*-xylene, usually suffer from low adhesive forces, which may in turn result in the loss of contact during the charge/discharge cycles thus increasing the cell resistance. Choi and coworkers developed a series of graft polymer binders through the reaction between polystyrene-block-polybutadiene-block-polystyrene (SBS) rubber and 3-mercaptocarboxylic acid (3-MPA) via a photolysis reaction with the aid of phenylbis (2,4,6-trimethylbenzoyl)-phosphine oxide (BAPO) initiator, as shown in Fig. 16b. The as-prepared binders were named after the molar ratios between SBS and 3-MPA (C4 for 100:4, C10 for 100:10, and C40 for 100:40). Although the carboxyl group on 3-MPA leads to better adhesion, too much 3-MPA results in higher reactivity toward the LPSCl SE. C10 was chosen as the optimal, which not only showed

comparable adhesion to that of PVDF (Fig. 16c) but also satisfied the ionic conductivity (1.9 mS $cm^{-1}$) when used as a binder for the SE. The SSB demonstrated better cycle stability than that with the BR binder.

As discussed above, binders with more carboxyl groups could provide better adhesion due to the H-bonding with the AM particles [285]. Sun's group further studied this phenomenon by utilizing four different binders (PEO, PVDF, CMC and Alg) in LCO electrodes [286]. They calculated the adsorption energy between these binders with LCO, as shown in Fig. 16d. Obviously, the CRP ones have stronger interactions. O K-edge XAS test was further carried out (Fig. 16e). It can be noted that the PEO brought about some changes to the spectrum. The authors attributed this to that the PEO flew down to the bottom of the electrode, and thus could not effectively cover the AM particles. By contrast, the CMC and Alg could cover the LCO surfaces effectively and render better adhesion and longer cycle life to the SSBs. It is noteworthy that no SE was used in the electrode, although the authors did not mention the areal capacity while it should be limited. It is important to study the underneath fundamental mechanisms. In addition, more attention should be paid on those ways toward practical applications.

#### 4.2.3 None-Conductive Binders

None-conductive binders such as PVDF were also used in many SSB works. Considering their poor lithium salt dissociation power and thus the low conductivity, none-conductive binders may be only suitable for those electrodes with low areal capacity or the ones work under high temperatures [287]. Jung's group developed a novel infiltration method, where the solution of SSEs (e.g., the LPSCl in ethanol, and 0.4LiI-0.6$Li_4SnS_4$ in methanol) was infiltrated into the porous LCO (with PVDF binder) or the graphite electrode by the dip-coating process followed by cold-pressing [288]. With an area capacity of 1.4 mAh $cm^{-2}$, both electrodes showed satisfying rates and wide temperature working ability (30–100 °C). Moreover, the work also highlighted the importance of percolated ion and electron passages via the variation of CA and binder quantities. The insulating nature of PVDF would affect the charge transfer in electrodes and thus the battery rate capability. They found that the LCO electrode with less (1%) PVDF and enough (2%) SP demonstrated the highest reversible capacity under all studied current densities, as the graphite with 5% binders.

Some insulating polymers with high thermal stability were also used in SSB electrodes prepared by thermal-pressing to ensure the structure integrity and flexibility. Poly(ethylene-*co*-propylene-*co*-5-methylene-2-norbornene) (PEP-MNB) was adopted as the binder for NCM622 electrodes due to its heptane solubility, good electrochemical stability toward cathodes, lithium metal anodes and the LPSCl SSEs [289]. Most importantly, it has a high melting point up to 350 °C, which could endure the post-annealing treatment after the slurry casting process. Ha's work proved that the annealing process enhanced the ionic transport in the electrode, and thus lower resistance and better rate capability could be achieved. Similarly, taking advantage of the high thermal stability of PTFE (softening point 320–330 °C), Hippauf et al. adopted a dry film approach to prepare a free-standing NCM electrode with a high areal loading of 6.5 mAh $cm^{-2}$ [232]. Although it has been widely accepted that the binders may block the conduction passways, a reduced charge transfer impedance was found for the electrodes using 0.1% and 0.3% binders compared to the one without binders. The authors attributed this to the reduced cathode surface area due to the binder coverage, which leads to less parasitic reactions between the LPSCl SE and NCM.

Polymer binder has a significant influence on the slurry rheology and thus the dispersion of SE among AM particles. Uchimoto et al. [258] prepared NCM111 electrodes with different binders [SBR dissolved in anisole, and styrene-ethylene-butylene-styrene (SEBS) in heptane] and then analyzed the SE [$75Li_2S{\cdot}25P_2S_5$ (LPS)] dispersion using the 2D-imaging X-ray absorption spectroscopy. It was found that the SBR led to a uniform distribution of SE in the electrode and reduced the local SOC difference.

### 4.3 Binders for Solid-State Lithium-Sulfur Batteries

Compared to those insertion-type cathodes, conversion-type cathodes, such as sulfur (S), have higher theoretical capacity (1 675 mAh $g^{-1}$) but lower electronic conductivity and larger volume changes (~ 80%) on lithiation, which makes the binder design more challenging as it needs to ensure the electrode integrity just like in the Si electrodes. The binder for S is the second most widely studied object after that for Si [109, 250, 274, 283, 290–324]. These binders demonstrated different functions such as self-healing, conducting, reducing the shuttle effect, and unquestionably, greatly enhancing the cycle stability and areal loading of Li-S batteries. Considering the multiple high-quality review papers published in the past few years [60, 325–330], here we simply focus on the binders for solid-state Li-S cells.

The shuttle phenomenon is the most prominent challenge for Li-S batteries, even though a little $Li_2S$ is in favor for stable lithium deposition [331]. Compared with those Li-S cells with liquid electrolytes, SEs could largely decrease the shuttle due to the limited solubility of PS species. It was proved that the shuttle phenomenon still exists when PEO or its derivatives are used [22, 332]. Wen and coworkers prepared solid-state Li-S batteries (SSLSBs) with PVDF (dissolved in NMP) as the cathode binder and 60% [PEO-LiTFSI] (EO:Li = 20:1) + 40% LLZTO as the composite electrolyte [22]. Via the real-time optical microscope and

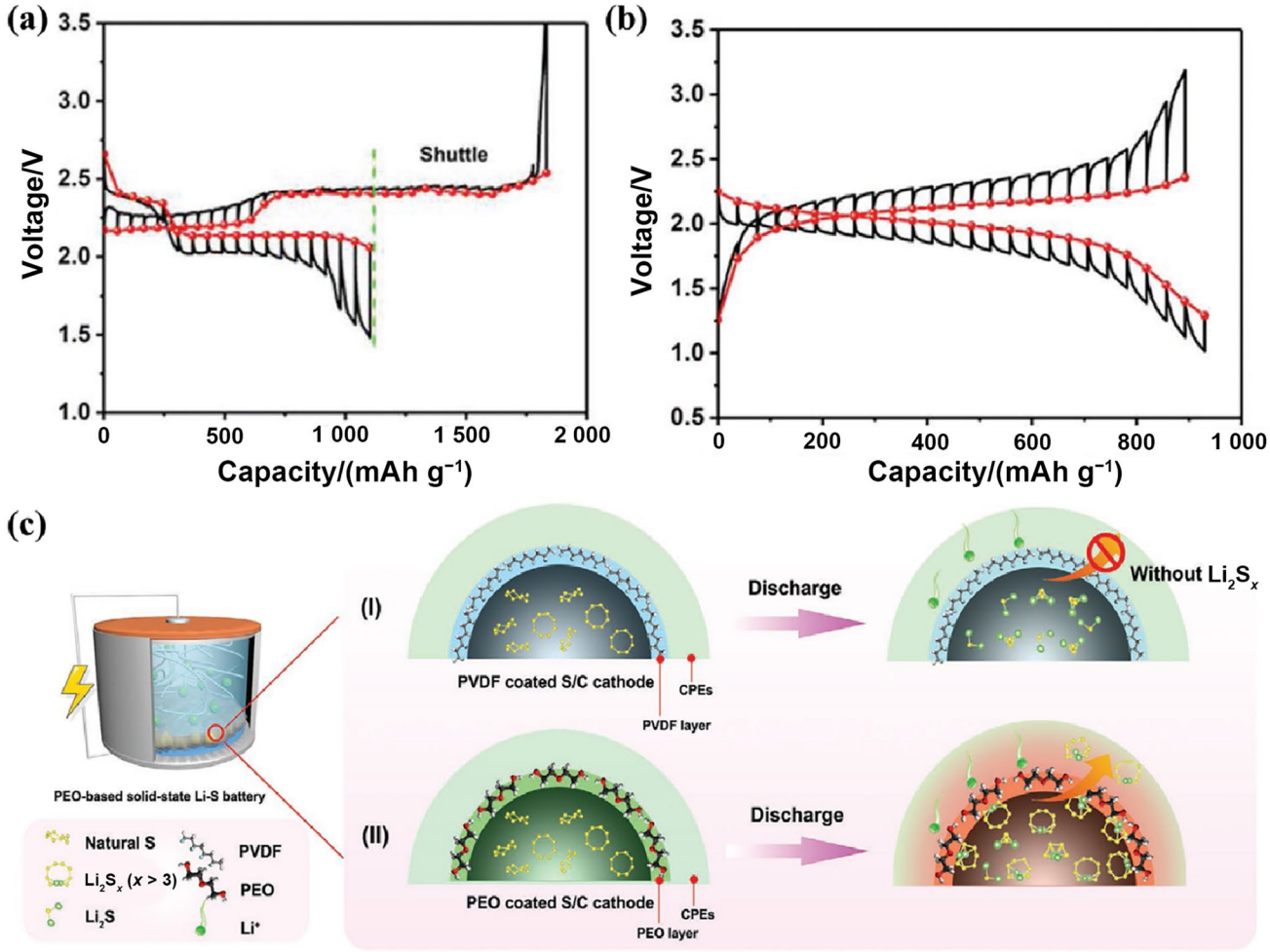


**Fig. 17** Typical GITT profiles of SSLSBs using different binders and their possible working mechanism at 55 °C. **a** PEO-LiTFSI; **b** PVDF-LiTFSI; and **c** schematic diagram for the proposed mechanism. Reproduced with permission from Ref. [332]. Copyright © 2020, Wiley-VCH

ex-situ XPS and Raman observation, they found that the reaction mechanism under high temperatures ($\geqslant T_m$ of PEO) in this SSLSB is similar to that of Li-S cells with liquid electrolytes. That is, a solid–liquid–solid process where the soluble $Li_2S_x$ ($x = 4$–8) could shuttle to the anode and forms $Li_2S$, was proved by the XRD patterns. It is noteworthy that, as proved by Nan's group [333], PVDF suffers from partial HF loss on contact with LLZTO in Lewis bases, which might also be the reason responsible for the poor cycle performance of the SSLSB under high temperatures.

Goodenough's work also came to the similar conclusion that the shuttle effect happens in SSLSBs [332]. The complex of PEO/PVDF with LiTFSI (3:2 by weight) was adopted as the binder for S composite cathodes, and a PEO-LiTFSI + 15% $Al_2O_3$ (EO:Li = 10:1) composite electrolyte was used in their work. Figure 17a, b shows the typical GITT curves of SSLSBs using different binders. Obviously, the one using the PEO binder showed higher discharge capacity, however, with prominent shuttle phenomenon. As to the PVDF case, although it did not show high-voltage plateaux (~ 2.4 V) and the specific capacity is low, limited shuttle effect was demonstrated. The authors attributed this to the low solubility of PVDF to the long chain polysulfides, which changed the reaction to a solid–solid mechanism as shown in Fig. 17c.

Ionic conductivity is another essential feature of binders for SSLSBs, as they could work as the supplement of SE, thus potentially, reduce the SE quantity demand for percolating ion passage formation. This is also an important reason why the PEO-LiTFSI binder was used in the up-mentioned work [332]. Kim et al. prepared a poly[diallyldimethylammonium bis(trifluoromethylsulfonyl) imide] (PDATFSI)-ionic liquid (IL) composite binder and used it in quasi-solid-state Li-S batteries [334]. It showed not only a high $Li^+$ conductivity of 0.45 mS $cm^{-1}$ and good thermal stability but also sustainable nonflammability and desirable flexibility. Besides, the rich anions enhanced the Li deposition stability. Compared with the counterpart PVDF,

the PDATFSI binder greatly enhanced the rate and cycle stability of the battery. After 200 cycles at 0.2 C, it still showed a reversible capacity of more than 1 000 mAh $g^{-1}$, almost 2 times that of PVDF. Note that a large quantity of IL was used in both binders and electrolytes in this work, which makes the battery a quasi-solid-state one. However, it is still inspiring considering the limited reports on SSLSB electrode designs.

Besides, other binders applicable to sulfide SEs, such as PTFE [335–337] and silicone rubber [338], are also being adopted in SSLSBs, since sulfides were usually used for their high ionic conductivity. As most of the relevant materials such as sulfur, carbon, and sulfide SEs are vulnerable to stress, more studies chose a binder free approach. Ball milling and hot/cold press are enough to form free-standing electrodes with satisfying areal loadings. Moreover, the addition of binders sometimes leads to higher tortuosity, which is harmful to the ion and electron transportation [339]. However, considering the high specific area of S-based AMs (usually tens to hundred times that of LIBs), more SEs (up to 40%–50% [339–341]) are needed to form percolated ion passages in the electrode, which seriously affects the battery energy density. Proper binders may greatly reduce the SE requirement thus promoting the advance of SSBs. Furthermore, it is worth noting that some sulfides are not stable within the potential range where the cell works [342]. Special attention should be paid on this kind of systems in data analysis.

To summarize, SSLSB is a fast-developing direction and its exploration is just beginning [343]. Similar to those using liquid electrolytes, the sulfur species also suffer from volume changes, low ion/electron conductivity and even shuttle effect. The challenge is even huger for the construction of practical SSLSBs. Many fundamental issues, such as the construction of percolating ion/electron passages, self-adaption of electrode/electrolyte interfaces on charge/discharge, and the volume changes on the cell level, are yet to be studied. Although binder only takes a quite small share in SSLSBs, it may play more vital roles in the future applications.

### 4.4 Binders for Anode Electrodes of SSBs and LMBs

The research on binders for anodes of SSBs is rare, since most SSBs adopted Li foil, Li–In alloy or 3D Li anodes prepared by a fused method as the anodes. For the development of SSBs, it was found that they usually need to work under certain pressure because of the volume changes of both electrodes during the charge/discharge processes, where it is hard for the cathode and the anode to compensate each other. In this consideration, anode structures with certain porosity might be necessary, where binders are needed.

Similar to that in SEs, compatibility is the first factor to be considered in the binder choice for anodes. Jung and coworkers prepared all-solid-state NCM622||sulfide SE||graphite (Gra.) LIBs using a single step wet method. NBR and PVC were used as the binders with THF as the solvent [344]. They found that PVC might be reduced by the sulfide SE, for C=C bonds were found in the Raman spectrum of the mixture. Moreover, the SE-PVC composite also showed the lowest ionic conductivity. On the contrary, NBR can be used in both NCM622 and Gra. electrodes. The as-prepared electrodes showed satisfying rate performance, especially that the anode delivered a high capacity of 265 mAh $g^{-1}$ even under a 1 C rate and 30 °C. The full cell can even work under a high rate of 50 C at 100 °C, which is beyond most of the SOA LIBs. Considering the low theoretical capacity of Gra., Lee's group studied the possibility of Sn to be used in SSBs [345]. Polyacrylonitrile (PAN) was used as the binder due to its strong adhesive force and the special pyrolytic characters: an ion and electron mixed conducting polymer was formed when it was heat treated between 250 and 350 °C, which is of vital importance in electrodes. The authors prepared Sn electrodes with different binder contents and treated them under 270 °C for 3 h. An optimal binder content of 5% was found, with which the electrode demonstrated not only the highest ICE of 87.5% but also the best specific capacity and cycle stability. Via an ideal spherical model, the authors calculated the PAN thickness on the Sn particles to be ~ 5.9 nm. They supposed that less binder could not provide enough toughness to ensure the electrode integrity, while a higher binder content may influence the ion/electron transportation. It is noteworthy that no CA and SE were used in this electrode and the AM areal loading is ~ 2.55 mg (corresponding to the areal capacity of ~ 2 mAh $cm^{-2}$), which makes it a promising method.

In respect of the high electronic conductivity, satisfying $Li^+$ diffusion coefficient, and the mechanically deformable nature of Gra., Kim and coworkers proposed a more convenient method to prepare electrodes for SSBs [346]. It was found that the lithiation of the Gra. electrode is a diffusion-dependent process, and $Li^+$ could hop between adjacent Gra. particles when they were close enough, as illustrated in Fig. 18a. Using 2 wt% PVDF binders, wet coating and the following 550 MPa compress, seamless interfaces could be formed in the electrode, which makes the SE free thick electrode possible. Although the diffusion-dependent electrode showed inferior rate performance to that of composite electrode (with SBR binders and a ratio between Gra. and LPS of 6:4) with similar areal capacity, much better volume energy density was achieved as no SE was used. Moreover, as illustrated in Fig. 18b, it delivered high capacity close to the theoretical value when the areal loading is less than 7.5 mg $cm^{-2}$ under a constant current (CC) mode. When a CC/CV (constant voltage) mode was used, this value is as much

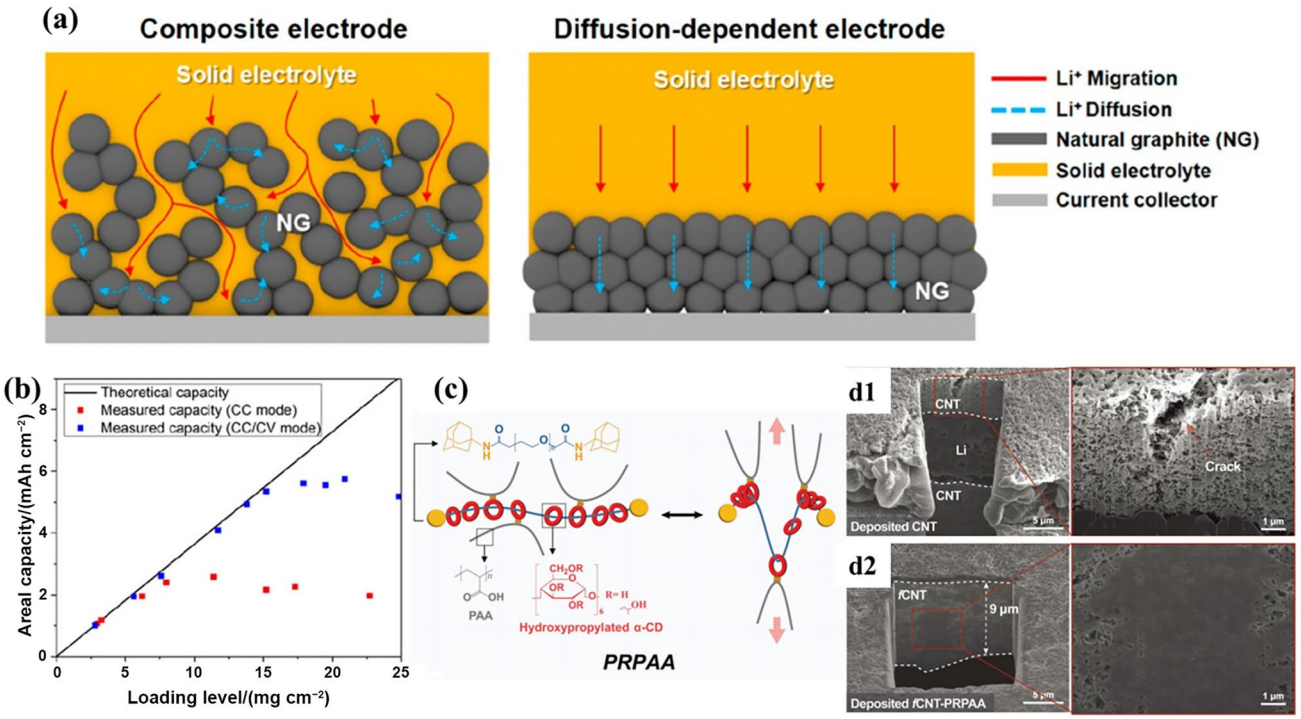


**Fig. 18** **a** Schematic comparison of the all-solid-state composite electrode and the diffusion-dependent natural graphite (NG) electrode. **b** Summarized areal capacity of the all-solid-state diffusion-dependent electrode depending on the loading level and the charge–discharge mode under a 0.1 C rate. Reproduced with permission from Ref. [346]. Copyright © 2020, American Chemical Society. **c** Schematic illustration of the structure and stress dissipation mechanism of the polyrotaxane-linked polyacrylic acid (PRPAA) binder. Cross-sectional SEM images of the bare CNT network (d1) and fCNT–PRPAA network (d2) after first Li plating. Reproduced with permission from Ref. [347]. Copyright © 2019, Wiley-VCH

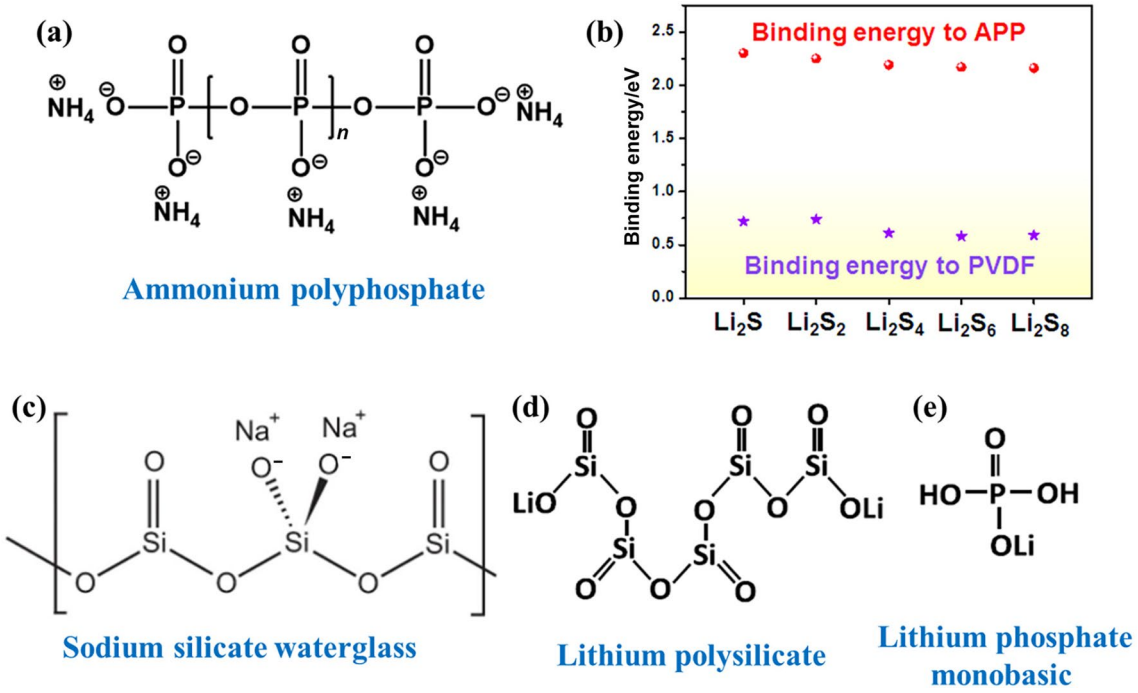


**Fig. 19** **a** Molecular structure of APP; **b** the binding energy between APP and PVDF with different $Li_2S_x$ [351]. Copyright © 2018, American Chemical Society. **c–e** Molecular structures of waterglass, lithium polysilicate and lithium phosphate. Reproduced with permission from Ref. [352]. Copyright © 2021, Elsevier

as 15.2 mg $cm^{-2}$ (> 5 mAh $cm^{-2}$), which is even higher than that of SOA LIBs.

In pursuit of high-energy–density SSBs, metal Li anodes are indispensable. PRPAA (as shown in Fig. 18c) was prepared by Choi and coworkers to integrate with carboxylic acid functionalized CNT (fCNT) networks to regulate the Li deposition process [347]. After the first Li deposition process of 1 mAh $cm^{-2}$, it can be seen that the CNT networks were still loosely packed and some cracks occurred on the surface due to the stress generated during Li deposition (Fig. 18d1). The 5% PRPAA meditated fCNT (fCNT-PRPAA) shows a compact cross-section with no cracks (Fig. 18d2), demonstrating the stress dissipation and keeping the network interconnected effect of PRPAA. They proved that the fCNT-PRPAA network could withstand a large amount of Li deposition of 6 Ah $g^{-1}$ at current densities up to 6 mA $cm^{-2}$ (18 A $g^{-1}$ CNT), which could effectively support the quick charge of LMBs. Although the authors did not use this concept in SSBs, it is a common sense that the EO groups on PR and PAA are $Li^+$ conductive. Meanwhile, the CNT endows the system with high electronic conduction. Therefore, the fCNT-PRPAA network may also be suitable for the solid configuration.

To summarize, after a decade of fast development, some high-quality SE materials are readily produced currently, which lets us see the dawn of SSBs. However, issues also come, e.g., the designs of thin SE films and high-loading electrodes, their interfacial stability, the compatibility with SOA LIB equipment, the volume/thickness changes on the cell level, etc. Although binders only take a very small share in cells, they can link the particles, endow the electrode/separator with certain flexibility, and sometimes, suppress the parasitic reactions and even buffer the volume changes on lithiation/delithiation. This makes the relevant research meaningful and important for the SSBs, both in science and technology.

## 5 Inorganic Binders

All aforementioned binders are organic polymers. They realize their adhesive function by physical interlocking or chemical binding, and in most cases, by both of them. Some inorganics could also work as binders, e.g., the MgO, $Al_2O_3$ and $SiO_2$ in thermal battery electrolytes [348, 349], waterglass in high-temperature refractory adhesives [350], etc. Compared with organics, inorganics usually have better thermal stability and higher ionic conductivity due to the delocalized ion cloud, which, however, may also bring about more parasitic reactions especially in the electric field. Therefore, the research on inorganic binders only started few years ago along with the increasing requirements on battery safety [350–352]. In fact, many relevant patents have been granted in this field. Their applications can be tracked back to more than a decade ago, and the assignees include large companies such as Dow, Samsung, CATL and LG Chem., [353–356].

Ammonium polyphosphate (APP, as shown in Fig. 19a) was adopted as a binder for sulfur cathodes in Cui's work due to its moderate binding strength, flame retardant and water-soluble properties. Moreover, it can also promote the transport of $Li^+$ thus enhancing the battery kinetics as evidenced by the improved rate performance [351]. Compared to PVDF, APP has stronger affinity to $Li_2S_x$ via the interaction between Li and the multiple O atoms on the molecular chains (Fig. 19b); thus, the shuttle effect was suppressed. Meanwhile, the cell with the APP binder showed little self-discharge within a month, while the open circuit voltage (OCV) of the cell with the PVDF binder dropped from 2.42 to 2.29 V. In a long-term cycling test, APP also demonstrated its feasibility with 640 mAh $g^{-1}$ retained after 400 cycles at 0.5 C. As a contrast, it was 329 mAh $g^{-1}$ for the one with PVDF.

Waterglass (sodium silicate as the main component, as shown in Fig. 19c) is a water-soluble earth-abundant inorganic compound that binds to a diverse range of materials with high-adhesion strength and exhibits extreme chemical and thermal stability. Structural ceramic batteries (SCBs) are capable of acting as an electrochemical energy storage system (i.e., batteries) while possessing mechanical integrity [357], thus having higher requirements on electrode modulus, which is usually beyond the capability of polymer binders. Ransil and Belcher trailed the waterglass in SCBs as the binders for LFP electrodes [350]. Impressively, it showed high Young's moduli of 75–85 GPa under both dry and wet (by electrolyte) conditions. XRD tests proved that the mixture of LFP and waterglass is stable even when heated to 600 °C, which greatly enhances the battery safety in use. Paring with a mesoporous carbon microbead (MCMB) anode and a silica modified separator (high-density ultra-thin fiberglass) using the same binder, a full cell was prepared. It demonstrated a satisfying tensile modulus of 1.4 GPa and a much higher energy density of 93.9 Wh $kg^{-1}$ than that in previous works on SCBs.

Both APP and waterglass are polymers, thus it is reasonable for them to show high adhesive ability toward other materials either by physical interlocking or chemical bonding (such as H-bond and Li-bond). Recently, Obrovac and Wei used three kinds of salts [the sodium polyphosphate (SPP), lithium polysilicate ($Li_2Si_5O_{11}$, Fig. 19d) and lithium phosphate monobasic ($LiH_2PO_4$, Fig. 19e)] for Si and Gra. anodes [352]. Surprisingly, all these binders could form good coating layers on Si alloys when the dosage is 10% and show good cycle stability similar to that with PAALi binders. The authors proposed that there might be a hydrolysis-polymerization process between $Li_2Si_5O_{11}$/

$LiH_2PO_4$ and –OH groups on the Si particles. As a contrast, the binders (10%) form poor coating layers when being used in graphite due to the lacking of functional groups. Increasing the binder content to 20% could also improve the coating quality, although no reason was given in the paper. The cross-sectional SEM images and EDS mapping illustrated that $Li_2Si_5O_{11}$ takes a larger volume fraction of ~ 30% in the graphite electrode, 3 times the theoretical value or that of other binders, for which the authors inferred that its hydrate process may form an open structure like sol–gel. Considering the areal capacity of the Si-alloy anode (2.4 mAh $cm^{-2}$), which is close to the commercial level, these inorganic binders especially the small molecular ones (e.g., $Li_2Si_5O_{11}$ and $LiH_2PO_4$) may be good choices in the future applications.

Unlike the organic binders' adhesion that usually resulted from direct chemical reactions, hydrogen bonding or mechanical interlocking [43], the adhesion theory between inorganics in batteries is still lacking of intensive study and far from mature. Although organic binders can fulfill most of the requirements of SOA LIBs, in some special applications such as the ultra-low/-high-temperature operations, structural batteries and space explorations where the irradiation may influence the organic stability, inorganic binders may provide good chances.

## 6 Conclusion and Prospective

As a small but indispensable part in cells (usually < 3% in SOA battery industry), binders not only influence the slurry rheology on the coating process and quality, but also keep the electrode integrity during the whole battery life. Most binders in LIB industry form a coating layer on the AM particles and thus influence the SEI components. For the development of conversion-type electrode materials and SSBs, binders with more functions such as self-healing, ionic/electronic conductive, and forming special shapes (e.g., fibrous PTFE), are required. Although so many binders have been developed and showed enhanced performance within specific systems in the past years, as the binders are difficult to be distinguished from the CA in the CBD, their detailed working mechanisms are yet to be clarified. Therefore, future works should emphasize on the following points.

(1) The development of high-energy LIBs calls for systematic and standardized research on binders. Binder and conductive agent fractions as well as the areal capacity of electrodes have significant influences on the cell energy density. Although some binders demonstrated outstanding cycle stability and rate performance, 10% or even 20% binders and relatively low-loading active materials are typically used, which in fact results in quite limited energy density even at the electrode level. Therefore, it is of vital importance to test the binders' performance under restricted fractions and areal AM loadings, so that their feasibility in mass production could be exhibited. Besides, most anode materials including graphite, silicon [181] and their composites have enough electronic conductivity, which could support the CA free design especially when conductive binders are used. In fact, 5% conductive binders could support the batteries working as reported in several papers. Systematic studies on these binders may promote the applications of high-capacity anode materials. Meanwhile, the environmental influences of binders should be considered along with the fast development of battery industry and the relevant recycle process. Although the binder can be removed by simply washing or sintering the coating layer, the bio-derived and water-soluble binders might be better choices.

(2) Novel binders are essential for SSBs. As previously discussed, SSBs are coming to the dawn before applications, and intensive efforts are now being devoted on electrode (particularly, the cathode) and electrode/electrolyte interface design and optimization. Functional binders can not only form percolating ion and electron passages and targeted porous structures in the electrodes thus reducing the cell volume changes, but also potentially construct integrated interfaces (e.g., using the PEO-based binder when PEO SE is adopted) thus diminishing the space charge layer and enhancing the interfacial stability, which is quite important as the inner resistance of SSBs is usually much larger than that in LIBs. Considering the trade-off between ionic conductivity, electrochemical stability and mechanical processability, organic/inorganic composite binders with higher degrees of freedom might be good choices. Besides, special techniques such as dip coating might be useful here.

(3) Multiscale and in-situ research on the interactions among binders, CAs, AMs, and electrolytes, especially when they work under the electric field (during the charge/discharge process), is urgently required. Most binders are polymers composed of C, H, O, F, and sometimes, some alkalis such as Li and Na. They usually mix with CA and form the CBD in the electrode and are difficult to be differentiated. Most binders were considered to be inert even in the battery working processes. Along with the development of high-voltage LIBs and functional binders such as the self-healing ones and the conductive ones, more and more works proved that some binders are reactive, either participating in the formation of SEI/CEI or changing their conduction with voltage variations. Therefore, more attention is deserved for the advanced characterization

methods of monitoring this small but essential part, so that better battery techniques could be achieved.

In conclusion, we have good reasons to believe that binders could work much more than being adhesive. As predicted in Schmidt's work, LIBs will be the most cost-effective electricity storage technology as of 2030 [358]. Furthermore, the exploration of higher energy density would bring lithium batteries to wider markets beyond electric vehicles, such as drones and electric airplanes [359]. Thus, we have good reasons to believe that novel binders may provide new choices to the battery industry.

**Acknowledgements** This work is financially supported by National Key Research and Development Program of China (No. 2021YFB2500100), National Natural Science Foundation of China (No. 21878308), Science Fund for Creative Research Groups of the National Natural Science Foundation of China (No. 21921005).

**Conflict of Interest** All authors declare that there are no competing interests.



## References

1. Duffner, F., Kronemeyer, N., Tübke, J., et al.: Post-lithium-ion battery cell production and its compatibility with lithium-ion cell production infrastructure. Nat. Energy **6**, 123–134 (2021). https://doi.org/10.1038/s41560-020-00748-8
2. Jaumann, T., Balach, J., Langklotz, U., et al.: Lifetime vs. rate capability: understanding the role of FEC and VC in high-energy Li-ion batteries with nano-silicon anodes. Energy Storage Mater. **6**, 26–35 (2017). https://doi.org/10.1016/j.ensm.2016.08.002
3. Jin, Y., Li, S., Kushima, A., et al.: Self-healing SEI enables full-cell cycling of a silicon-majority anode with a coulombic efficiency exceeding 99.9%. Energy Environ. Sci. **10**, 580–592 (2017). https://doi.org/10.1039/C6EE02685K
4. Stoddart, A.: Lithium-ion batteries: stress relief for silicon. Nat. Rev. Mater. **2**, 1 (2017). https://doi.org/10.1038/natrevmats.2017.57
5. Yamaguchi, K., Domi, Y., Usui, H., et al.: Influence of the structure of the anion in an ionic liquid electrolyte on the electrochemical performance of a silicon negative electrode for a lithium-ion battery. J. Power Sour. **338**, 103–107 (2017). https://doi.org/10.1016/j.jpowsour.2016.10.111
6. Yoon, T., Milien, M.S., Parimalam, B.S., et al.: Thermal decomposition of the solid electrolyte interphase (SEI) on silicon electrodes for lithium ion batteries. Chem. Mater. **29**, 3237–3245 (2017). https://doi.org/10.1021/acs.chemmater.7b00454
7. Huang, Q.Q., Song, J.X., Gao, Y., et al.: Supremely elastic gel polymer electrolyte enables a reliable electrode structure for silicon-based anodes. Nat. Commun. **10**, 1–7 (2019). https://doi.org/10.1038/s41467-019-13434-5
8. Chae, S., Choi, S.H., Kim, N., et al.: Integration of graphite and silicon anodes for the commercialization of high-energy lithium-ion batteries. Angew. Chem. Int. Ed. **59**, 110–135 (2020). https://doi.org/10.1002/anie.201902085
9. Fang, Z., Ma, Q., Liu, P., et al.: Novel concentrated Li[($FSO_2$)($n$-$C_4F_9SO_2$)N]-based ether electrolyte for superior stability of metallic lithium anode. ACS Appl. Mater. Interfaces **9**, 4282–4289 (2017). https://doi.org/10.1021/acsami.6b03857
10. Diederichsen, K.M., McShane, E.J., McCloskey, B.D.: Promising routes to a high $Li^+$ transference number electrolyte for lithium ion batteries. ACS Energy Lett. **2**, 2563–2575 (2017). https://doi.org/10.1021/acsenergylett.7b00792
11. Cui, X.M., Chu, Y., Qin, L.M., et al.: Stabilizing Li metal anodes through a novel self-healing strategy. ACS Sustain. Chem. Eng. **6**, 11097–11104 (2018). https://doi.org/10.1021/acssuschemeng.8b02564
12. Li, J.C., Ma, C., Chi, M.F., et al.: Solid electrolyte: the key for high-voltage lithium batteries. Adv. Energy Mater. **5**, 1401408 (2015). https://doi.org/10.1002/aenm.201401408
13. Ma, Q., Zhang, H., Zhou, C.W., et al.: Single lithium-ion conducting polymer electrolytes based on a super-delocalized polyanion. Angew. Chem. Int. Ed. **55**, 2521–2525 (2016). https://doi.org/10.1002/anie.201509299
14. Fan, X.L., Chen, L., Ji, X., et al.: Highly fluorinated interphases enable high-voltage Li-metal batteries. Chem **4**, 174–185 (2018). https://doi.org/10.1016/j.chempr.2017.10.017
15. Liu, Q., Cresce, A., Schroeder, M., et al.: Insight on lithium metal anode interphasial chemistry: reduction mechanism of cyclic ether solvent and SEI film formation. Energy Storage Mater. **17**, 366–373 (2019). https://doi.org/10.1016/j.ensm.2018.09.024
16. Ma, L., Fu, C.Y., Li, L.J., et al.: Nanoporous polymer films with a high cation transference number stabilize lithium metal anodes in light-weight batteries for electrified transportation. Nano Lett. **19**, 1387–1394 (2019). https://doi.org/10.1021/acs.nanolett.8b05101
17. Kim, S., Huang, H.Y.S.: Mechanical stresses at the cathode-electrolyte interface in lithium-ion batteries. J. Mater. Res. **31**, 3506–3512 (2016). https://doi.org/10.1557/jmr.2016.373
18. Zeng, X.Q., Xu, G.L., Li, Y., et al.: Kinetic study of parasitic reactions in lithium-ion batteries: a case study on $LiNi_{0.6}Mn_{0.2}Co_{0.2}O_2$. ACS Appl. Mater. Interfaces **8**, 3446–3451 (2016). https://doi.org/10.1021/acsami.5b11800
19. Kim, J., Lee, H., Cha, H., et al.: Prospect and reality of Ni-rich cathode for commercialization. Adv. Energy Mater. **8**, 1702028 (2018). https://doi.org/10.1002/aenm.201702028
20. Kim, J., Lee, J., Ma, H., et al.: Controllable solid electrolyte interphase in nickel-rich cathodes by an electrochemical rearrangement for stable lithium-ion batteries. Adv. Mater. **30**, 1704309 (2018). https://doi.org/10.1002/adma.201704309
21. Li, W.D., Dolocan, A., Li, J.Y., et al.: Ethylene carbonate-free electrolytes for high-nickel layered oxide cathodes in lithium-ion batteries. Adv. Energy Mater. **9**, 1901152 (2019). https://doi.org/10.1002/aenm.201901152
22. Song, Y.X., Shi, Y., Wan, J., et al.: Direct tracking of the polysulfide shuttling and interfacial evolution in all-solid-state lithium-sulfur batteries: a degradation mechanism study. Energy Environ. Sci. **12**, 2496–2506 (2019). https://doi.org/10.1039/C9EE00578A
23. Barghamadi, M., Best, A.S., Bhatt, A.I., et al.: Lithium-sulfur batteries: the solution is in the electrolyte, but is the electrolyte

a solution? Energy Environ. Sci. **7**, 3902–3920 (2014). https://doi.org/10.1039/C4EE02192D
24. Chen, L., Fan, L.Z.: Dendrite-free Li metal deposition in all-solid-state lithium sulfur batteries with polymer-in-salt polysiloxane electrolyte. Energy Storage Mater. **15**, 37–45 (2018). https://doi.org/10.1016/j.ensm.2018.03.015
25. Li, Z., Pan, M.S., Su, L., et al.: Air-breathing aqueous sulfur flow battery for ultralow-cost long-duration electrical storage. Joule **1**, 306–327 (2017). https://doi.org/10.1016/j.joule.2017.08.007
26. Fan, F.Y., Pan, M.S., Lau, K.C., et al.: Solvent effects on polysulfide redox kinetics and ionic conductivity in lithium-sulfur batteries. J. Electrochem. Soc. **163**, A3111–A3116 (2016). https://doi.org/10.1149/2.1181614jes
27. Magasinski, A., Zdyrko, B., Kovalenko, I., et al.: Toward efficient binders for Li-ion battery Si-based anodes: polyacrylic acid. ACS Appl. Mater. Interfaces **2**, 3004–3010 (2010). https://doi.org/10.1021/am100871y
28. Kovalenko, I., Zdyrko, B., Magasinski, A., et al.: A major constituent of brown algae for use in high-capacity Li-ion batteries. Science **334**, 75–79 (2011). https://doi.org/10.1126/science.1209150
29. Koo, B., Kim, H., Cho, Y., et al.: A highly cross-linked polymeric binder for high-performance silicon negative electrodes in lithium ion batteries. Angew. Chem. **124**, 8892–8897 (2012). https://doi.org/10.1002/ange.201201568
30. Liu, G., Zheng, H., Song, X., et al.: Particles and polymer binder interaction: a controlling factor in lithium-ion electrode performance. J. Electrochem. Soc. **159**, A214–A221 (2012). https://doi.org/10.1149/2.024203jes
31. Ryou, M.H., Kim, J., Lee, I., et al.: Mussel-inspired adhesive binders for high-performance silicon nanoparticle anodes in lithium-ion batteries. Adv. Mater. **25**, 1571–1576 (2013). https://doi.org/10.1002/adma.201203981
32. Wang, C., Wu, H., Chen, Z., et al.: Self-healing chemistry enables the stable operation of silicon microparticle anodes for high-energy lithium-ion batteries. Nat. Chem. **5**, 1042–1048 (2013). https://doi.org/10.1038/nchem.1802
33. Wu, H., Yu, G.H., Pan, L.J., et al.: Stable Li-ion battery anodes by in situ polymerization of conducting hydrogel to conformally coat silicon nanoparticles. Nat. Commun. **4**, 1–6 (2013). https://doi.org/10.1038/ncomms2941
34. Kwon, T.W., Jeong, Y.K., Lee, I., et al.: Systematic molecular-level design of binders incorporating meldrum's acid for silicon anodes in lithium rechargeable batteries. Adv. Mater. **26**, 7979–7985 (2014). https://doi.org/10.1002/adma.201402950
35. Song, J.X., Zhou, M.J., Yi, R., et al.: Interpenetrated gel polymer binder for high-performance silicon anodes in lithium-ion batteries. Adv. Funct. Mater. **24**, 5904–5910 (2014). https://doi.org/10.1002/adfm.201401269
36. Chen, Z., Wang, C., Lopez, J., et al.: High-areal-capacity silicon electrodes with low-cost silicon particles based on spatial control of self-healing binder. Adv. Energy Mater. **5**, 1401826 (2015). https://doi.org/10.1002/aenm.201401826
37. Lu, H.R., Cornell, A., Alvarado, F., et al.: Lignin as a binder material for eco-friendly Li-ion batteries. Materials **9**, 127 (2016). https://doi.org/10.3390/ma9030127
38. Choi, S., Kwon, T.W., Coskun, A., et al.: Highly elastic binders integrating polyrotaxanes for silicon microparticle anodes in lithium ion batteries. Science **357**, 279–283 (2017). https://doi.org/10.1126/science.aal4373
39. Chen, W., Lei, T.Y., Qian, T., et al.: A new hydrophilic binder enabling strongly anchoring polysulfides for high-performance sulfur electrodes in lithium-sulfur battery. Adv. Energy Mater. **8**, 1702889 (2018). https://doi.org/10.1002/aenm.201702889
40. Xu, Z.X., Yang, J., Zhang, T., et al.: Silicon microparticle anodes with self-healing multiple network binder. Joule **2**, 950–961 (2018). https://doi.org/10.1016/j.joule.2018.02.012
41. Lee, Y.: The effect of active material, conductive additives, and binder in a cathode composite electrode on battery performance. Energies **12**, 658 (2019). https://doi.org/10.3390/en12040658
42. Pan, Y.Y., Gao, S.L., Sun, F.Y., et al.: Polymer binders constructed through dynamic noncovalent bonds for high-capacity silicon-based anodes. Chem. Eur. J. **25**, 10976–10994 (2019). https://doi.org/10.1002/chem.201900988
43. Licari, J.J., Swanson, D.W.: Functions and theory of adhesives. In: Licari, J.J., Swanson, D.W. (eds.) Adhesives Technology for Electronic Applications, pp. 35–74. Elsevier, Amsterdam (2011)
44. Lee, H., Scherer, N.F., Messersmith, P.B.: Single-molecule mechanics of mussel adhesion. Proc. Natl. Acad. Sci. U.S.A. **103**, 12999–13003 (2006). https://doi.org/10.1073/pnas.0605552103
45. Lee, H., Dellatore, S.M., Miller, W.M., et al.: Mussel-inspired surface chemistry for multifunctional coatings. Science **318**, 426–430 (2007). https://doi.org/10.1126/science.1147241
46. Lee, H., Lee, B.P., Messersmith, P.B.: A reversible wet/dry adhesive inspired by mussels and geckos. Nature **448**, 338–341 (2007). https://doi.org/10.1038/nature05968
47. Zhao, H., Wei, Y., Wang, C., et al.: Mussel-inspired conductive polymer binder for Si-alloy anode in lithium-ion batteries. ACS Appl. Mater. Interfaces **10**, 5440–5446 (2018). https://doi.org/10.1021/acsami.7b14645
48. Han, L., Lu, X., Wang, M.H., et al.: A mussel-inspired conductive, self-adhesive, and self-healable tough hydrogel as cell stimulators and implantable bioelectronics. Small **13**, 1601916 (2017). https://doi.org/10.1002/smll.201601916
49. Kwon, T.W., Choi, J.W., Coskun, A.: The emerging era of supramolecular polymeric binders in silicon anodes. Chem. Soc. Rev. **47**, 2145–2164 (2018). https://doi.org/10.1039/c7cs00858a
50. Hochgatterer, N.S., Schweiger, M.R., Koller, S., et al.: Silicon/graphite composite electrodes for high-capacity anodes: influence of binder chemistry on cycling stability. Electrochem. Solid-State Lett. **11**, A76 (2008). https://doi.org/10.1149/1.2888173
51. Dyatkin, B., Presser, V., Heon, M., et al.: Development of a green supercapacitor composed entirely of environmentally friendly materials. Chemsuschem **6**, 2269–2280 (2013). https://doi.org/10.1002/cssc.201300852
52. Birkl, C.R., Roberts, M.R., McTurk, E., et al.: Degradation diagnostics for lithium ion cells. J. Power Sour. **341**, 373–386 (2017). https://doi.org/10.1016/j.jpowsour.2016.12.011
53. Lu, Y., Zhao, C.Z., Yuan, H., et al.: Dry electrode technology, the rising star in solid-state battery industrialization. Matter **5**, 876–898 (2022). https://doi.org/10.1016/j.matt.2022.01.011
54. Choi, N.S., Ha, S.Y., Lee, Y., et al.: Recent progress on polymeric binders for silicon anodes in lithium-ion batteries. J. Electrochem. Sci. Technol. **6**, 35–49 (2015). https://doi.org/10.5229/jecst.2015.6.2.35
55. Jeong, Y.K., Park, S.H., Choi, J.W.: Mussel-inspired coating and adhesion for rechargeable batteries: a review. ACS Appl. Mater. Interfaces **10**, 7562–7573 (2018). https://doi.org/10.1021/acsami.7b08495
56. Shi, Y., Zhou, X.Y., Yu, G.H.: Material and structural design of novel binder systems for high-energy, high-power lithium-ion batteries. Acc. Chem. Res. **50**, 2642–2652 (2017). https://doi.org/10.1021/acs.accounts.7b00402
57. Chen, H., Ling, M., Hencz, L., et al.: Exploring chemical, mechanical, and electrical functionalities of binders for advanced energy-storage devices. Chem. Rev. **118**, 8936–8982 (2018). https://doi.org/10.1021/acs.chemrev.8b00241

58. Bresser, D., Buchholz, D., Moretti, A., et al.: Alternative binders for sustainable electrochemical energy storage: the transition to aqueous electrode processing and bio-derived polymers. Energy Environ. Sci. **11**, 3096–3127 (2018). https://doi.org/10.1039/C8EE00640G
59. Li, J.T., Wu, Z.Y., Lu, Y.Q., et al.: Water soluble binder, an electrochemical performance booster for electrode materials with high energy density. Adv. Energy Mater. **7**, 1701185 (2017). https://doi.org/10.1002/aenm.201701185
60. Yuan, H., Huang, J.Q., Peng, H.J., et al.: A review of functional binders in lithium-sulfur batteries. Adv. Energy Mater. **8**, 1802107 (2018). https://doi.org/10.1002/aenm.201802107
61. Liu, J., Zhang, Q., Sun, Y.K.: Recent progress of advanced binders for Li-S batteries. J. Power Sour. **396**, 19–32 (2018). https://doi.org/10.1016/j.jpowsour.2018.05.096
62. Wang, H.W., Fu, J.Z., Wang, C., et al.: A universal aqueous conductive binder for flexible electrodes. Adv. Funct. Mater. **31**, 2102284 (2021). https://doi.org/10.1002/adfm.202102284
63. Madec, L., Coquil, G., Ledeuil, J.B., et al.: How the binder/solvent formulation impacts the electrolyte reactivity/solid electrolyte interphase formation and cycling stability of conversion type electrodes. J. Electrochem. Soc. **167**, 060533 (2020). https://doi.org/10.1149/1945-7111/ab861f
64. Patnaik, S.G., Vedarajan, R., Matsumi, N.: BIAN based functional diimine polymer binder for high performance Li ion batteries. J. Mater. Chem. A **5**, 17909–17919 (2017). https://doi.org/10.1039/C7TA03843G
65. Duduta, M., Ho, B., Wood, V.C., et al.: Semi-solid lithium rechargeable flow battery. Adv. Energy Mater. **1**, 511–516 (2011). https://doi.org/10.1002/aenm.201100152
66. Koos, E., Willenbacher, N.: Capillary forces in suspension rheology. Science **331**, 897–900 (2011). https://doi.org/10.1126/science.1199243
67. Li, C.C., Lin, Y.S.: Interactions between organic additives and active powders in water-based lithium iron phosphate electrode slurries. J. Power Sour. **220**, 413–421 (2012). https://doi.org/10.1016/j.jpowsour.2012.07.125
68. Lim, S., Kim, S., Ahn, K.H., et al.: The effect of binders on the rheological properties and the microstructure formation of lithium-ion battery anode slurries. J. Power Sour. **299**, 221–230 (2015). https://doi.org/10.1016/j.jpowsour.2015.09.009
69. Sung, S.H., Kim, S., Park, J.H., et al.: Role of PVDF in rheology and microstructure of NCM cathode slurries for lithium-ion battery. Materials **13**, 4544 (2020). https://doi.org/10.3390/ma13204544
70. Haarmann, M., Haselrieder, W., Kwade, A.: Extrusion-based processing of cathodes: influence of solid content on suspension and electrode properties. Energy Technol. **8**, 1801169 (2020). https://doi.org/10.1002/ente.201801169
71. Kim, K.M., Jeon, W.S., Chung, I.J., et al.: Effect of mixing sequences on the electrode characteristics of lithium-ion rechargeable batteries. J. Power Sour. **83**, 108–113 (1999). https://doi.org/10.1016/S0378-7753(99)00281-5
72. Wang, M., Dang, D.Y., Meyer, A., et al.: Effects of the mixing sequence on making lithium ion battery electrodes. J. Electrochem. Soc. **167**, 100518 (2020). https://doi.org/10.1149/1945-7111/ab95c6
73. Hagiwara, H., Suszynski, W.J., Francis, L.F.: A Raman spectroscopic method to find binder distribution in electrodes during drying. J. Coat. Technol. Res. **11**, 11–17 (2014). https://doi.org/10.1007/s11998-013-9509-z
74. Lim, S., Ahn, K.H., Yamamura, M.: Latex migration in battery slurries during drying. Langmuir **29**, 8233–8244 (2013). https://doi.org/10.1021/la4013685
75. Zang, Y.H., Du, J., Du, Y.F., et al.: The migration of styrene butadiene latex during the drying of coating suspensions: when and how does migration of colloidal particles occur? Langmuir **26**, 18331–18339 (2010). https://doi.org/10.1021/la103675f
76. Baunach, M., Jaiser, S., Schmelzle, S., et al.: Delamination behavior of lithium-ion battery anodes: influence of drying temperature during electrode processing. Dry. Technol. **34**, 462–473 (2016). https://doi.org/10.1080/07373937.2015.1060497
77. Westphal, B.G., Kwade, A.: Critical electrode properties and drying conditions causing component segregation in graphitic anodes for lithium-ion batteries. J. Energy Storage **18**, 509–517 (2018). https://doi.org/10.1016/j.est.2018.06.009
78. Li, C.C., Wang, Y.W.: Binder distributions in water-based and organic-based $LiCoO_2$ electrode sheets and their effects on cell performance. J. Electrochem. Soc. **158**, A1361 (2011). https://doi.org/10.1149/2.107112jes
79. Lim, S., Kim, S., Ahn, K.H., et al.: Stress development of Li-ion battery anode slurries during the drying process. Ind. Eng. Chem. Res. **54**, 6146–6155 (2015). https://doi.org/10.1021/acs.iecr.5b00878
80. Ma, Y., Ma, J., Cui, G.L.: Small things make big deal: powerful binders of lithium batteries and post-lithium batteries. Energy Storage Mater. **20**, 146–175 (2019). https://doi.org/10.1016/j.ensm.2018.11.013
81. Komini Babu, S., Mohamed, A.I., Whitacre, J.F., et al.: Multiple imaging mode X-ray computed tomography for distinguishing active and inactive phases in lithium-ion battery cathodes. J. Power Sour. **283**, 314–319 (2015). https://doi.org/10.1016/j.jpowsour.2015.02.086
82. Liu, H.S., Foster, J.M., Gully, A., et al.: Three-dimensional investigation of cycling-induced microstructural changes in lithium-ion battery cathodes using focused ion beam/scanning electron microscopy. J. Power Sour. **306**, 300–308 (2016). https://doi.org/10.1016/j.jpowsour.2015.11.108
83. Song, K.F., Zhang, C., Hu, N.F., et al.: High performance thick cathodes enabled by gradient porosity. Electrochim. Acta **377**, 138105 (2021). https://doi.org/10.1016/j.electacta.2021.138105
84. Miranda, D., Gören, A., Costa, C.M., et al.: Theoretical simulation of the optimal relation between active material, binder and conductive additive for lithium-ion battery cathodes. Energy **172**, 68–78 (2019). https://doi.org/10.1016/j.energy.2019.01.122
85. Zielke, L., Hutzenlaub, T., Wheeler, D.R., et al.: A combination of X-ray tomography and carbon binder modeling: reconstructing the three phases of $LiCoO_2$ Li-ion battery cathodes. Adv. Energy Mater. **4**, 1301617 (2014). https://doi.org/10.1002/aenm.201301617
86. Vogel, J.E., Forouzan, M.M., Hardy, E.E., et al.: Electrode microstructure controls localized electronic impedance in Li-ion batteries. Electrochim. Acta **297**, 820–825 (2019). https://doi.org/10.1016/j.electacta.2018.11.204
87. Chouchane, M., Rucci, A., Lombardo, T., et al.: Lithium ion battery electrodes predicted from manufacturing simulations: assessing the impact of the carbon-binder spatial location on the electrochemical performance. J. Power Sour. **444**, 227285 (2019). https://doi.org/10.1016/j.jpowsour.2019.227285
88. Lee, J.T., Jo, C., De Volder, M.: Bicontinuous phase separation of lithium-ion battery electrodes for ultrahigh areal loading. Proc. Natl. Acad. Sci. U.S.A. **117**, 21155–21161 (2020). https://doi.org/10.1073/pnas.2007250117
89. Rago, D.N., Bareño, J., Li, J.L., et al.: Effect of overcharge on $Li(Ni_{0.5}Mn_{0.3}Co_{0.2})O_2$/graphite lithium ion cells with poly(vinylidene fluoride) binder. I. Microstructural changes in the anode. J. Power Sour. **385**, 148–155 (2018). https://doi.org/10.1016/j.jpowsour.2018.01.009
90. Dietz Rago, N., Graczyk, D.G., Tsai, Y., et al.: Effect of overcharge on $Li(Ni_{0.5}Mn_{0.3}Co_{0.2})O_2$/graphite cells: effect of binder. J. Power Sour. **448**, 227414 (2020). https://doi.org/10.1016/j.jpowsour.2019.227414

91. Shim, J., Kostecki, R., Richardson, T., et al.: Electrochemical analysis for cycle performance and capacity fading of a lithium-ion battery cycled at elevated temperature. J. Power Sour. **112**, 222–230 (2002). https://doi.org/10.1016/s0378-7753(02)00363-4
92. Brilloni, A., Poli, F., Spina, G.E., et al.: Easy recovery of Li-ion cathode powders by the use of water-processable binders. Electrochim. Acta **418**, 140376 (2022). https://doi.org/10.1016/j.electacta.2022.140376
93. Chou, W.Y., Jin, Y.C., Duh, J.G., et al.: A facile approach to derive binder protective film on high voltage spinel cathode materials against high temperature degradation. Appl. Surf. Sci. **355**, 1272–1278 (2015). https://doi.org/10.1016/j.apsusc.2015.08.046
94. Li, G.J., Liao, Y.H., He, Z.Y., et al.: A new strategy to improve the cyclic stability of high voltage lithium nickel manganese oxide cathode by poly(butyl methacrylate-acrylonitrile-styrene) terpolymer as co-binder in lithium ion batteries. Electrochim. Acta **319**, 527–540 (2019). https://doi.org/10.1016/j.electacta.2019.07.011
95. Zhang, T., Li, J.T., Liu, J., et al.: Suppressing the voltage-fading of layered lithium-rich cathode materials via an aqueous binder for Li-ion batteries. Chem. Commun. **52**, 4683–4686 (2016). https://doi.org/10.1039/C5CC10534J
96. Pham, H.Q., Kim, G., Jung, H.M., et al.: Fluorinated polyimide as a novel high-voltage binder for high-capacity cathode of lithium-ion batteries. Adv. Funct. Mater. **28**, 1704690 (2018). https://doi.org/10.1002/adfm.201704690
97. Yang, J.S., Li, P., Zhong, F.P., et al.: Suppressing voltage fading of Li-rich oxide cathode via building a well-protected and partially-protonated surface by polyacrylic acid binder for cycle-stable Li-ion batteries. Adv. Energy Mater. **10**, 1904264 (2020). https://doi.org/10.1002/aenm.201904264
98. Zhao, T.L., Meng, Y., Ji, R.X., et al.: Maintaining structure and voltage stability of Li-rich cathode materials by green water-soluble binders containing $Na^+$ ions. J. Alloy. Compd. **811**, 152060 (2019). https://doi.org/10.1016/j.jallcom.2019.152060
99. Tang, Y.X., Deng, J.Y., Li, W.L., et al.: Water-soluble sericin protein enabling stable solid-electrolyte interphase for fast charging high voltage battery electrode. Adv. Mater. **29**, 1701828 (2017). https://doi.org/10.1002/adma.201701828
100. Liu, Q., Liu, Y.Y., Jiao, X.X., et al.: Enhanced ionic conductivity and interface stability of hybrid solid-state polymer electrolyte for rechargeable lithium metal batteries. Energy Storage Mater. **23**, 105–111 (2019). https://doi.org/10.1016/j.ensm.2019.05.023
101. Pieczonka, N.P.W., Borgel, V., Ziv, B., et al.: Lithium polyacrylate (LiPAA) as an advanced binder and a passivating agent for high-voltage Li-ion batteries. Adv. Energy Mater. **5**, 1501008 (2015). https://doi.org/10.1002/aenm.201501008
102. Dong, T.T., Zhang, H.R., Ma, Y., et al.: A well-designed water-soluble binder enlightening the 5 V-class $LiNi_{0.5}Mn_{1.5}O_4$ cathodes. J. Mater. Chem. A **7**, 24594–24601 (2019). https://doi.org/10.1039/C9TA08299A
103. Zhang, G.H., Qiu, B., Xia, Y.G., et al.: Double-helix-superstructure aqueous binder to boost excellent electrochemical performance in Li-rich layered oxide cathode. J. Power Sour. **420**, 29–37 (2019). https://doi.org/10.1016/j.jpowsour.2019.02.086
104. Li, R., Bai, C.J., Liu, H., et al.: New insights into the mechanism of enhanced performance of $Li[Ni_{0.8}Co_{0.1}Mn_{0.1}]O_2$ with a polyacrylic acid-modified binder. ACS Appl. Mater. Interfaces **13**, 10064–10070 (2021). https://doi.org/10.1021/acsami.0c22052
105. Chang, B., Kim, J., Cho, Y., et al.: Highly elastic binder for improved cyclability of nickel-rich layered cathode materials in lithium-ion batteries. Adv. Energy Mater. **10**, 2001069 (2020). https://doi.org/10.1002/aenm.202001069
106. Borodin, O., Self, J., Persson, K.A., et al.: Uncharted waters: super-concentrated electrolytes. Joule **4**, 69–100 (2020). https://doi.org/10.1016/j.joule.2019.12.007
107. Wan, Z.P., Lei, D.N., Yang, W., et al.: Low resistance-integrated all-solid-state battery achieved by $Li_7La_3Zr_2O_{12}$ nanowire upgrading polyethylene oxide (PEO) composite electrolyte and PEO cathode binder. Adv. Funct. Mater. **29**, 1805301 (2019). https://doi.org/10.1002/adfm.201805301
108. Tsao, C.H., Hsu, C.H., Kuo, P.L.: Ionic conducting and surface active binder of poly (ethylene oxide)-block-poly(acrylonitrile) for high power lithium-ion battery. Electrochim. Acta **196**, 41–47 (2016). https://doi.org/10.1016/j.electacta.2016.02.154
109. Zhang, H., Hu, X.H., Zhang, Y., et al.: 3D-crosslinked tannic acid/poly(ethylene oxide) complex as a three-in-one multifunctional binder for high-sulfur-loading and high-stability cathodes in lithium-sulfur batteries. Energy Storage Mater. **17**, 293–299 (2019). https://doi.org/10.1016/j.ensm.2018.07.006
110. Aldalur, I., Zhang, H., Piszcz, M., et al.: Jeffamine® based polymers as highly conductive polymer electrolytes and cathode binder materials for battery application. J. Power Sour. **347**, 37–46 (2017). https://doi.org/10.1016/j.jpowsour.2017.02.047
111. Jia, M.M., Guo, Y.W., Bian, H.Y., et al.: An ultra-stable lithium plating process enabled by the nanoscale interphase of a macromolecular additive. J. Mater. Chem. A **8**, 23844–23850 (2020). https://doi.org/10.1039/d0ta08492a
112. Bouchet, R., Maria, S., Meziane, R., et al.: Single-ion BAB triblock copolymers as highly efficient electrolytes for lithium-metal batteries. Nat. Mater. **12**, 452–457 (2013). https://doi.org/10.1038/nmat3602
113. Oh, J.M., Geiculescu, O., DesMarteau, D., et al.: Ionomer binders can improve discharge rate capability in lithium-ion battery cathodes. J. Electrochem. Soc. **158**, A207 (2011). https://doi.org/10.1149/1.3526598
114. He, J.R., Zhong, H.X., Zhang, L.Z.: Water-soluble binder PAALi with terpene resin emulsion as tackifier for $LiFePO_4$ cathode. J. Appl. Polym. Sci. **135**, 46132 (2018). https://doi.org/10.1002/app.46132
115. Huang, S., Ren, J.G., Liu, R., et al.: Enhanced electrochemical properties of $LiFePO_4$ cathode using waterborne lithiated ionomer binder in Li-ion batteries with low amount. ACS Sustain. Chem. Eng. **6**, 12650–12657 (2018). https://doi.org/10.1021/acssuschemeng.8b01532
116. Ma, X.G., Zou, S.L., Tang, A.J., et al.: Three-dimensional hierarchical walnut kernel shape conducting polymer as water soluble binder for lithium-ion battery. Electrochim. Acta **269**, 571–579 (2018). https://doi.org/10.1016/j.electacta.2018.03.031
117. Shi, Q.R., Xue, L.X., Wei, Z.B., et al.: Improvement in $LiFePO_4$-Li battery performance via poly(perfluoroalkylsulfonyl) imide (PFSI) based ionene composite binder. J. Mater. Chem. A **1**, 15016–15021 (2013). https://doi.org/10.1039/C3TA13364H
118. Huang, S., Chen, H., Chen, M., et al.: Design of conductive binders for $LiFePO_4$ cathodes with long-term cycle life. ACS Sustain. Chem. Eng. **9**, 13277–13286 (2021). https://doi.org/10.1021/acssuschemeng.1c04552
119. Wei, Z.B., Xue, L.X., Nie, F., et al.: Study of sulfonated polyether ether ketone with pendant lithiated fluorinated sulfonic groups as ion conductive binder in lithium-ion batteries. J. Power Sour. **256**, 28–31 (2014). https://doi.org/10.1016/j.jpowsour.2014.01.018
120. Liu, G., Xun, S.D., Vukmirovic, N., et al.: Polymers with tailored electronic structure for high capacity lithium battery electrodes. Adv. Mater. **23**, 4679–4683 (2011). https://doi.org/10.1002/adma.201102421
121. Xun, S.D., Song, X.Y., Battaglia, V., et al.: Conductive polymer binder-enabled cycling of pure tin nanoparticle composite anode

electrodes for a lithium-ion battery. J. Electrochem. Soc. **160**, A849–A855 (2013). https://doi.org/10.1149/2.087306jes
122. Shao, D., Zhong, H.X., Zhang, L.Z.: Water-soluble conductive composite binder containing PEDOT: PSS as conduction promoting agent for Si anode of lithium-ion batteries. ChemElectroChem **1**, 1679–1687 (2014). https://doi.org/10.1002/celc.201402210
123. Zhao, H., Wang, Z.H., Lu, P., et al.: Toward practical application of functional conductive polymer binder for a high-energy lithium-ion battery design. Nano Lett. **14**, 6704–6710 (2014). https://doi.org/10.1021/nl503490h
124. Kim, S.M., Kim, M.H., Choi, S.Y., et al.: Poly(phenanthrenequinone) as a conductive binder for nano-sized silicon negative electrodes. Energy Environ. Sci. **8**, 1538–1543 (2015). https://doi.org/10.1039/C5EE00472A
125. Park, M., Zhang, X.C., Chung, M., et al.: A review of conduction phenomena in Li-ion batteries. J. Power Sour. **195**, 7904–7929 (2010). https://doi.org/10.1016/j.jpowsour.2010.06.060
126. Eliseeva, S.N., Apraksin, R.V., Tolstopjatova, E.G., et al.: Electrochemical impedance spectroscopy characterization of $LiFePO_4$ cathode material with carboxymethylcellulose and poly-3,4-ethylendioxythiophene/polystyrene sulfonate. Electrochim. Acta **227**, 357–366 (2017). https://doi.org/10.1016/j.electacta.2016.12.157
127. Apraksin, R.V., Eliseeva, S.N., Tolstopjatova, E.G., et al.: High-rate performance of $LiFe_{0.4}Mn_{0.6}PO_4$ cathode materials with poly(3,4-ethylenedioxythiopene): poly(styrene sulfonate)/carboxymethylcellulose. Mater. Lett. **176**, 248–252 (2016). https://doi.org/10.1016/j.matlet.2016.04.106
128. Du Pasquier, A., Orsini, F., Gozdz, A.S., et al.: Electrochemical behaviour of $LiMn_2O_4$PPy composite cathodes in the 4-V region. J. Power Sour. **81**(82), 607–611 (1999). https://doi.org/10.1016/S0378-7753(99)00230-X
129. Vorobeva, K.A., Eliseeva, S.N., Apraksin, R.V., et al.: Improved electrochemical properties of cathode material $LiMn_2O_4$ with conducting polymer binder. J. Alloys Compd. **766**, 33–44 (2018). https://doi.org/10.1016/j.jallcom.2018.06.324
130. Rivnay, J., Inal, S., Collins, B.A., et al.: Structural control of mixed ionic and electronic transport in conducting polymers. Nat. Commun. **7**, 11287 (2016). https://doi.org/10.1038/ncomms11287
131. Zhong, H.X., He, A.Q., Lu, J.D., et al.: Carboxymethyl chitosan/conducting polymer as water-soluble composite binder for $LiFePO_4$ cathode in lithium ion batteries. J. Power Sour. **336**, 107–114 (2016). https://doi.org/10.1016/j.jpowsour.2016.10.041
132. Lai, C.H., Ashby, D.S., Lin, T.C., et al.: Application of poly(3-hexylthiophene-2,5-diyl) as a protective coating for high rate cathode materials. Chem. Mater. **30**, 2589–2599 (2018). https://doi.org/10.1021/acs.chemmater.7b05116
133. Das, P., Zayat, B., Wei, Q.L., et al.: Dihexyl-substituted poly(3,4-propylenedioxythiophene) as a dual ionic and electronic conductive cathode binder for lithium-ion batteries. Chem. Mater. **32**, 9176–9189 (2020). https://doi.org/10.1021/acs.chemmater.0c02601
134. Ryou, M.H., Hong, S., Winter, M., et al.: Improved cycle lives of $LiMn_2O_4$ cathodes in lithium ion batteries by an alginate biopolymer from seaweed. J. Mater. Chem. A **1**, 15224–15229 (2013). https://doi.org/10.1039/C3TA13514D
135. Wright, D.R., Garcia-Araez, N., Owen, J.R.: Review on high temperature secondary Li-ion batteries. Energy Proc. **151**, 174–181 (2018). https://doi.org/10.1016/j.egypro.2018.09.044
136. Jin, X.T., Sun, G.Q., Zhang, G.F., et al.: A cross-linked polyacrylamide electrolyte with high ionic conductivity for compressible supercapacitors with wide temperature tolerance. Nano Res. **12**, 1199–1206 (2019). https://doi.org/10.1007/s12274-019-2382-z
137. Yoon, T., Park, S., Mun, J., et al.: Failure mechanisms of $LiNi_{0.5}Mn_{1.5}O_4$ electrode at elevated temperature. J. Power Sour. **215**, 312–316 (2012). https://doi.org/10.1016/j.jpowsour.2012.04.103
138. Hu, Q.C., Osswald, S., Daniel, R., et al.: Graft copolymer-based lithium-ion battery for high-temperature operation. J. Power Sour. **196**, 5604–5610 (2011). https://doi.org/10.1016/j.jpowsour.2011.03.001
139. Jin, M.H., Li, B., Hu, L.L., et al.: Functional copolymer binder for nickel-rich cathode with exceptional cycling stability at high temperature through coordination interaction. J. Energy Chem. **60**, 156–161 (2021). https://doi.org/10.1016/j.jechem.2020.12.028
140. Mindemark, J., Lacey, M.J., Bowden, T., et al.: Beyond PEO: alternative host materials for $Li^+$-conducting solid polymer electrolytes. Prog. Polym. Sci. **81**, 114–143 (2018). https://doi.org/10.1016/j.progpolymsci.2017.12.004
141. Drofenik, J., Gaberscek, M., Dominko, R., et al.: Cellulose as a binding material in graphitic anodes for Li ion batteries: a performance and degradation study. Electrochim. Acta **48**, 883–889 (2003). https://doi.org/10.1016/S0013-4686(02)00784-3
142. Luo, L., Xu, Y.L., Zhang, H., et al.: Comprehensive understanding of high polar polyacrylonitrile as an effective binder for Li-ion battery nano-Si anodes. ACS Appl. Mater. Interfaces **8**, 8154–8161 (2016). https://doi.org/10.1021/acsami.6b03046
143. Lee, J.H., Lee, S., Paik, U., et al.: Aqueous processing of natural graphite particulates for lithium-ion battery anodes and their electrochemical performance. J. Power Sour. **147**, 249–255 (2005). https://doi.org/10.1016/j.jpowsour.2005.01.022
144. Chong, J., Xun, S.D., Zheng, H.H., et al.: A comparative study of polyacrylic acid and poly(vinylidene difluoride) binders for spherical natural graphite/$LiFePO_4$ electrodes and cells. J. Power Sour. **196**, 7707–7714 (2011). https://doi.org/10.1016/j.jpowsour.2011.04.043
145. Cuesta, N., Ramos, A., Cameán, I., et al.: Hydrocolloids as binders for graphite anodes of lithium-ion batteries. Electrochim. Acta **155**, 140–147 (2015). https://doi.org/10.1016/j.electacta.2014.12.122
146. Nowak, A.P., Trzciński, K., Zarach, Z., et al.: Poly(hydroxybutyrate-*co*-hydroxyvalerate) as a biodegradable binder in a negative electrode material for lithium-ion batteries. Appl. Surf. Sci. **606**, 154933 (2022). https://doi.org/10.1016/j.apsusc.2022.154933
147. Tran, B., Oladeji, I.O., Wang, Z.D., et al.: Adhesive PEG-based binder for aqueous fabrication of thick $Li_4Ti_5O_{12}$ electrode. Electrochim. Acta **88**, 536–542 (2013). https://doi.org/10.1016/j.electacta.2012.10.139
148. Lee, B.R., Oh, E.S.: Effect of molecular weight and degree of substitution of a sodium-carboxymethyl cellulose binder on $Li_4Ti_5O_{12}$ anodic performance. J. Phys. Chem. C **117**, 4404–4409 (2013). https://doi.org/10.1021/jp311678p
149. Lee, B.R., Kim, S.J., Oh, E.S.: Bio-derivative galactomannan gum binders for $Li_4Ti_5O_{12}$ negative electrodes in lithium-ion batteries. J. Electrochem. Soc. **161**, A2128–A2132 (2014). https://doi.org/10.1149/2.0641414jes
150. Léonard, A.F., Job, N.: Safe and green Li-ion batteries based on $LiFePO_4$ and $Li_4Ti_5O_{12}$ sprayed as aqueous slurries with xanthan gum as common binder. Mater. Today Energy **12**, 168–178 (2019). https://doi.org/10.1016/j.mtener.2019.01.008
151. Fan, X.Y., Han, J.X., Ding, Y.L., et al.: 3D nanowire arrayed Cu current collector toward homogeneous alloying anode deposition for enhanced sodium storage. Adv. Energy Mater. **9**, 1900673 (2019). https://doi.org/10.1002/aenm.201900673

152. Zhou, L., Cao, Z., Wahyudi, W., et al.: Electrolyte engineering enables high stability and capacity alloying anodes for sodium and potassium ion batteries. ACS Energy Lett. **5**, 766–776 (2020). https://doi.org/10.1021/acsenergylett.0c00148
153. Gao, Y., Yi, R., Li, Y.C., et al.: General method of manipulating formation, composition, and morphology of solid-electrolyte interphases for stable Li-alloy anodes. J. Am. Chem. Soc. **139**, 17359–17367 (2017). https://doi.org/10.1021/jacs.7b07584
154. Tian, M., Chen, X., Sun, S.T., et al.: A bioinspired high-modulus mineral hydrogel binder for improving the cycling stability of microsized silicon particle-based lithium-ion battery. Nano Res. **12**, 1121–1127 (2019)
155. Han, L., Liu, T.F., Sheng, O.W., et al.: Undervalued roles of binder in modulating solid electrolyte interphase formation of silicon-based anode materials. ACS Appl. Mater. Interfaces **13**, 45139–45148 (2021). https://doi.org/10.1021/acsami.1c13971
156. Li, L.Y., Li, T., Sha, Y.F., et al.: A web-like three-dimensional binder for silicon anode in lithium-ion batteries. Energy Environ. Mater. (2023). https://doi.org/10.1002/eem2.12482
157. Yang, L.Y., Wei, D.X., Xu, M., et al.: Transferring lithium ions in nanochannels: a PEO/$Li^+$ solid polymer electrolyte design. Angew. Chem. Int. Ed. **53**, 3631–3635 (2014). https://doi.org/10.1002/anie.201307423
158. Jeong, Y.K., Kwon, T.W., Lee, I., et al.: Millipede-inspired structural design principle for high performance polysaccharide binders in silicon anodes. Energy Environ. Sci. **8**, 1224–1230 (2015). https://doi.org/10.1039/C5EE00239G
159. Maier, G.P., Rapp, M.V., Waite, J.H., et al.: Adaptive synergy between catechol and lysine promotes wet adhesion by surface salt displacement. Science **349**, 628–632 (2015). https://doi.org/10.1126/science.aab0556
160. Li, C.H., Wang, C., Keplinger, C., et al.: A highly stretchable autonomous self-healing elastomer. Nat. Chem. **8**, 618–624 (2016). https://doi.org/10.1038/nchem.2492
161. Guo, S.T., Li, H., Li, Y.Q., et al.: $SiO_2$-enhanced structural stability and strong adhesion with a new binder of konjac glucomannan enables stable cycling of silicon anodes for lithium-ion batteries. Adv. Energy Mater. **8**, 1800434 (2018). https://doi.org/10.1002/aenm.201800434
162. Kim, S., Jeong, Y.K., Wang, Y., et al.: A "sticky" mucin-inspired DNA-polysaccharide binder for silicon and silicon-graphite blended anodes in lithium-ion batteries. Adv. Mater. **30**, 1707594 (2018). https://doi.org/10.1002/adma.201707594
163. Jiang, S.S., Hu, B., Shi, Z.X., et al.: Re-engineering poly(acrylic acid) binder toward optimized electrochemical performance for silicon lithium-ion batteries: branching architecture leads to balanced properties of polymeric binders. Adv. Funct. Mater. **30**, 1908558 (2020). https://doi.org/10.1002/adfm.201908558
164. Tomaszewska, A., Chu, Z.Y., Feng, X.N., et al.: Lithium-ion battery fast charging: a review. eTransportation **1**, 100011 (2019). https://doi.org/10.1016/j.etran.2019.100011
165. Jiao, X.X., Yin, J.Q., Xu, X.Y., et al.: Highly energy-dissipative, fast self-healing binder for stable Si anode in lithium-ion batteries. Adv. Funct. Mater. **31**, 2005699 (2021). https://doi.org/10.1002/adfm.202005699
166. Li, Z.H., Zhang, Y.P., Liu, T.F., et al.: Silicon anode with high initial coulombic efficiency by modulated trifunctional binder for high-areal-capacity lithium-ion batteries. Adv. Energy Mater. **10**, 1903110 (2020). https://doi.org/10.1002/aenm.201903110
167. Zhang, Q.Y., Zhang, C.F., Luo, W.W., et al.: Sequence-defined peptoids with –OH and –COOH groups as binders to reduce cracks of Si nanoparticles of lithium-ion batteries. Adv. Sci. **7**, 2000749 (2020). https://doi.org/10.1002/advs.202000749
168. Lee, H.A., Shin, M., Kim, J., et al.: Designing adaptive binders for microenvironment settings of silicon anode particles. Adv. Mater. **33**, 2007460 (2021). https://doi.org/10.1002/adma.202007460
169. Nguyen, V.A., Kuss, C.: Review: conducting polymer-based binders for lithium-ion batteries and beyond. J. Electrochem. Soc. **167**, 065501 (2020). https://doi.org/10.1149/1945-7111/ab856b
170. Zou, F., Manthiram, A.: A review of the design of advanced binders for high-performance batteries. Adv. Energy Mater. **10**, 2002508 (2020). https://doi.org/10.1002/aenm.202002508
171. Taskin, O.S., Hubble, D., Zhu, T.Y., et al.: Biomass-derived polymeric binders in silicon anodes for battery energy storage applications. Green Chem. **23**, 7890–7901 (2021). https://doi.org/10.1039/d1gc01814k
172. Zhao, Y.M., Yue, F.S., Li, S.C., et al.: Advances of polymer binders for silicon-based anodes in high energy density lithium-ion batteries. InfoMat **3**, 460–501 (2021). https://doi.org/10.1002/inf2.12185
173. Liu, X.H., Zhong, L., Huang, S., et al.: Size-dependent fracture of silicon nanoparticles during lithiation. ACS Nano **6**, 1522–1531 (2012). https://doi.org/10.1021/nn204476h
174. Lee, S.W., McDowell, M.T., Berla, L.A., et al.: Fracture of crystalline silicon nanopillars during electrochemical lithium insertion. Proc. Natl. Acad. Sci. U.S.A. **109**, 4080–4085 (2012). https://doi.org/10.1073/pnas.1201088109
175. Baasner, A., Reuter, F., Seidel, M., et al.: The role of balancing nanostructured silicon anodes and NMC cathodes in lithium-ion full-cells with high volumetric energy density. J. Electrochem. Soc. **167**, 020516 (2020). https://doi.org/10.1149/1945-7111/ab68d7
176. Sung, J., Kim, N., Ma, J., et al.: Subnano-sized silicon anode via crystal growth inhibition mechanism and its application in a prototype battery pack. Nat. Energy **6**, 1164–1175 (2021). https://doi.org/10.1038/s41560-021-00945-z
177. Chen, Z., Zhang, L., Wu, X.K., et al.: Effect of N/P ratios on the performance of $LiNi_{0.8}Co_{0.15}Al_{0.05}O_2$||SiO/graphite lithium-ion batteries. J. Power Sour. **439**, 227056 (2019)
178. Lopez, J., Chen, Z., Wang, C., et al.: The effects of cross-linking in a supramolecular binder on cycle life in silicon microparticle anodes. ACS Appl. Mater. Interfaces **8**, 2318–2324 (2016). https://doi.org/10.1021/acsami.5b11363
179. Kim, D., Hyun, S., Han, S.M.: Freestanding silicon microparticle and self-healing polymer composite design for effective lithiation stress relaxation. J. Mater. Chem. A **6**, 11353–11361 (2018). https://doi.org/10.1039/C7TA11269F
180. Munaoka, T., Yan, X.Z., Lopez, J., et al.: Ionically conductive self-healing binder for low cost Si microparticles anodes in Li-ion batteries. Adv. Energy Mater. **8**, 1703138 (2018). https://doi.org/10.1002/aenm.201703138
181. Tan, D.H.S., Chen, Y.T., Yang, H.D., et al.: Carbon-free high-loading silicon anodes enabled by sulfide solid electrolytes. Science **373**, 1494–1499 (2021). https://doi.org/10.1126/science.abg7217
182. Döhler, D., Michael, P., Binder, W.: Principles of self-healing polymers. In: Binder, W.H. (ed.) Self-Healing Polymers, pp. 5–60. Wiley-VCH Verlag GmbH, Weinheim (2013). https://doi.org/10.1002/9783527670185.ch1
183. Wang, K.L., Chen, K.T., Yi, Y.H., et al.: High-performance lithium ion batteries combining submicron silicon and thiophene-terephthalic acid-conjugated polymer binders. ACS Sustain. Chem. Eng. **8**, 1043–1049 (2020). https://doi.org/10.1021/acssuschemeng.9b05800
184. Wen, Y.F., Zhang, H.W.: Highly stretchable polymer binder engineered with polysaccharides for silicon microparticles as high-performance anodes. Chemsuschem **13**, 3887–3892 (2020). https://doi.org/10.1002/cssc.202000911
185. Ryu, J., Park, S.: Sliding chains keep particles together. Science **357**, 250–251 (2017). https://doi.org/10.1126/science.aan6685

186. Kim, H.J., Choi, S., Lee, S.J., et al.: Controlled prelithiation of silicon monoxide for high performance lithium-ion rechargeable full cells. Nano Lett. **16**, 282–288 (2016). https://doi.org/10.1021/acs.nanolett.5b03776
187. Pan, Q.R., Zuo, P.J., Mu, T.S., et al.: Improved electrochemical performance of micro-sized SiO-based composite anode by prelithiation of stabilized lithium metal powder. J. Power Sour. **347**, 170–177 (2017). https://doi.org/10.1016/j.jpowsour.2017.02.061
188. Zhao, J., Sun, J., Pei, A., et al.: A general prelithiation approach for group IV elements and corresponding oxides. Energy Storage Mater. **10**, 275–281 (2018). https://doi.org/10.1016/j.ensm.2017.06.013
189. Liu, X.X., Liu, T.C., Wang, R., et al.: Prelithiated Li-enriched gradient interphase toward practical high-energy NMC-silicon full cell. ACS Energy Lett. **6**, 320–328 (2021). https://doi.org/10.1021/acsenergylett.0c02487
190. Pan, J., Peng, H.L., Yan, Y.H., et al.: Solid-state batteries designed with high ion conductive composite polymer electrolyte and silicon anode. Energy Storage Mater. **43**, 165–171 (2021). https://doi.org/10.1016/j.ensm.2021.09.001
191. Delattre, B., Amin, R., Sander, J., et al.: Impact of pore tortuosity on electrode kinetics in lithium battery electrodes: study in directionally freeze-cast $LiNi_{0.8}Co_{0.15}Al_{0.05}O_2$ (NCA). J. Electrochem. Soc. **165**, A388–A395 (2018). https://doi.org/10.1149/2.1321802jes
192. Yang, K., Yang, L.Y., Wang, Z.J., et al.: Constructing a highly efficient aligned conductive network to facilitate depolarized high-areal-capacity electrodes in Li-ion batteries. Adv. Energy Mater. **11**, 2100601 (2021). https://doi.org/10.1002/aenm.202100601
193. Singh, K.B., Tirumkudulu, M.S.: Cracking in drying colloidal films. Phys. Rev. Lett. **98**, 218302 (2007). https://doi.org/10.1103/physrevlett.98.218302
194. Rollag, K., Juarez-Robles, D., Du, Z.J., et al.: Drying temperature and capillarity-driven crack formation in aqueous processing of Li-ion battery electrodes. ACS Appl. Energy Mater. **2**, 4464–4476 (2019). https://doi.org/10.1021/acsaem.9b00704
195. Lu, L.L., Lu, Y.Y., Xiao, Z.J., et al.: Wood-inspired high-performance ultrathick bulk battery electrodes. Adv. Mater. **30**, 1706745 (2018). https://doi.org/10.1002/adma.201706745
196. Li, L.S., Erb, R.M., Wang, J.J., et al.: Fabrication of low-tortuosity ultrahigh-area-capacity battery electrodes through magnetic alignment of emulsion-based slurries. Adv. Energy Mater. **9**, 1802472 (2019). https://doi.org/10.1002/aenm.201802472
197. Huang, C., Grant, P.S.: Coral-like directional porosity lithium ion battery cathodes by ice templating. J. Mater. Chem. A **6**, 14689–14699 (2018). https://doi.org/10.1039/C8TA05049J
198. Amin, R., Delattre, B., Tomsia, A.P., et al.: Electrochemical characterization of high energy density graphite electrodes made by freeze-casting. ACS Appl. Energy Mater. **1**, 4976–4981 (2018). https://doi.org/10.1021/acsaem.8b00962
199. Ghadkolai, M.A., Creager, S., Nanda, J., et al.: Freeze tape cast thick Mo doped $Li_4Ti_5O_{12}$ electrodes for lithium-ion batteries. J. Electrochem. Soc. **164**, A2603–A2610 (2017). https://doi.org/10.1149/2.1311712jes
200. Yang, X.F., Sun, Q., Zhao, C.T., et al.: High-areal-capacity all-solid-state lithium batteries enabled by rational design of fast ion transport channels in vertically-aligned composite polymer electrodes. Nano Energy **61**, 567–575 (2019). https://doi.org/10.1016/j.nanoen.2019.05.002
201. Wang, N.N., Zhang, X., Ju, Z.Y., et al.: Thickness-independent scalable high-performance Li-S batteries with high areal sulfur loading via electron-enriched carbon framework. Nat. Commun. **12**, 1–10 (2021). https://doi.org/10.1038/s41467-021-24873-4
202. Sander, J.S., Erb, R.M., Li, L., et al.: High-performance battery electrodes via magnetic templating. Nat. Energy **1**, 1–7 (2016). https://doi.org/10.1038/nenergy.2016.99
203. Park, S.H., King, P.J., Tian, R.Y., et al.: High areal capacity battery electrodes enabled by segregated nanotube networks. Nat. Energy **4**, 560–567 (2019). https://doi.org/10.1038/s41560-019-0398-y
204. Ibing, L., Gallasch, T., Schneider, P., et al.: Towards water based ultra-thick Li ion battery electrodes: a binder approach. J. Power Sour. **423**, 183–191 (2019). https://doi.org/10.1016/j.jpowsour.2019.03.020
205. Li, W., Zhu, J.E., Xia, Y., et al.: Data-driven safety envelope of lithium-ion batteries for electric vehicles. Joule **3**, 2703–2715 (2019). https://doi.org/10.1016/j.joule.2019.07.026
206. Duan, J., Tang, X., Dai, H.F., et al.: Building safe lithium-ion batteries for electric vehicles: a review. Electrochem. Energy Rev. **3**, 1–42 (2020). https://doi.org/10.1007/s41918-019-00060-4
207. Chen, Y.Q., Kang, Y.Q., Zhao, Y., et al.: A review of lithium-ion battery safety concerns: the issues, strategies, and testing standards. J. Energy Chem. **59**, 83–99 (2021). https://doi.org/10.1016/j.jechem.2020.10.017
208. Wu, X.K., Song, K.F., Zhang, X.Y., et al.: Safety issues in lithium ion batteries: materials and cell design. Front. Energy Res. **7**, 65 (2019). https://doi.org/10.3389/fenrg.2019.00065
209. Deimede, V., Elmasides, C.: Separators for lithium-ion batteries: a review on the production processes and recent developments. Energy Technol. **3**, 453–468 (2015). https://doi.org/10.1002/ente.201402215
210. Lee, H., Yanilmaz, M., Toprakci, O., et al.: A review of recent developments in membrane separators for rechargeable lithium-ion batteries. Energy Environ. Sci. **7**, 3857–3886 (2014). https://doi.org/10.1039/C4EE01432D
211. Lagadec, M.F., Zahn, R., Wood, V.: Characterization and performance evaluation of lithium-ion battery separators. Nat. Energy **4**, 16–25 (2019). https://doi.org/10.1038/s41560-018-0295-9
212. Shi, C., Zhang, P., Huang, S.H., et al.: Functional separator consisted of polyimide nonwoven fabrics and polyethylene coating layer for lithium-ion batteries. J. Power Sour. **298**, 158–165 (2015). https://doi.org/10.1016/j.jpowsour.2015.08.008
213. Dai, J.H., Shi, C., Li, C., et al.: A rational design of separator with substantially enhanced thermal features for lithium-ion batteries by the polydopamine-ceramic composite modification of polyolefin membranes. Energy Environ. Sci. **9**, 3252–3261 (2016). https://doi.org/10.1039/C6EE01219A
214. Shi, C., Dai, J.H., Shen, X., et al.: A high-temperature stable ceramic-coated separator prepared with polyimide binder/$Al_2O_3$ particles for lithium-ion batteries. J. Membr. Sci. **517**, 91–99 (2016). https://doi.org/10.1016/j.memsci.2016.06.035
215. Wang, Z., Pang, P.P., Ma, Z., et al.: A four-layers hamburger-structure PVDF-HFP/$Al_2O_3$/PE/PVDF-HFP composite separator for pouch lithium-ion batteries with enhanced safety and reliability. J. Electrochem. Soc. **167**, 090507 (2020). https://doi.org/10.1149/1945-7111/ab7f88
216. Lee, J., Lee, C.L., Park, K., et al.: Synthesis of an $Al_2O_3$-coated polyimide nanofiber mat and its electrochemical characteristics as a separator for lithium ion batteries. J. Power Sour. **248**, 1211–1217 (2014). https://doi.org/10.1016/j.jpowsour.2013.10.056
217. Deng, Y.M., Song, X.N., Ma, Z., et al.: $Al_2O_3$/PVdF-HFP-CMC/PE separator prepared using aqueous slurry and post-hot-pressing method for polymer lithium-ion batteries with enhanced safety. Electrochim. Acta **212**, 416–425 (2016). https://doi.org/10.1016/j.electacta.2016.07.016
218. Song, Y.H., Wu, K.J., Zhang, T.W., et al.: A nacre-inspired separator coating for impact-tolerant lithium batteries. Adv. Mater. **31**, 1905711 (2019). https://doi.org/10.1002/adma.201905711

219. Ahn, J.H., Kim, H.M., Lee, Y.J., et al.: Nanostructured reactive alumina particles coated with water-soluble binder on the polyethylene separator for highly safe lithium-ion batteries. J. Power Sour. **506**, 230119 (2021). https://doi.org/10.1016/j.jpowsour.2021.230119
220. Kang, S.M., Ryou, M.H., Choi, J.W., et al.: Mussel- and diatom-inspired silica coating on separators yields improved power and safety in Li-ion batteries. Chem. Mater. **24**, 3481–3485 (2012). https://doi.org/10.1021/cm301967f
221. Zhang, K.Y., Xiao, W., Li, X.R., et al.: Highly thermostable expanded polytetrafluoroethylene separator with mussel-inspired silica coating for advanced Li-ion batteries. J. Power Sour. **468**, 228403 (2020). https://doi.org/10.1016/j.jpowsour.2020.228403
222. Xu, R., Sheng, L., Gong, H., et al.: High-performance $Al_2O_3$/PAALi composite separator prepared by water-based slurry for high-power density lithium-based battery. Adv. Eng. Mater. **23**, 2001009 (2021). https://doi.org/10.1002/adem.202001009
223. Ko, Y., Yoo, H., Kim, J.: Curable polymeric binder-ceramic composite-coated superior heat-resistant polyethylene separator for lithium ion batteries. RSC Adv. **4**, 19229–19233 (2014). https://doi.org/10.1039/C4RA01309C
224. Zhang, Y.C., Wang, Z.H., Xiang, H.F., et al.: A thin inorganic composite separator for lithium-ion batteries. J. Membr. Sci. **509**, 19–26 (2016). https://doi.org/10.1016/j.memsci.2016.02.047
225. Manthiram, A., Yu, X.W., Wang, S.F.: Lithium battery chemistries enabled by solid-state electrolytes. Nat. Rev. Mater. **2**, 1–16 (2017). https://doi.org/10.1038/natrevmats.2016.103
226. Miao, X.G., Wang, H.Y., Sun, R., et al.: Interface engineering of inorganic solid-state electrolytes for high-performance lithium metal batteries. Energy Environ. Sci. **13**, 3780–3822 (2020). https://doi.org/10.1039/D0EE01435D
227. He, F., Tang, W.J., Zhang, X.Y., et al.: High energy density solid state lithium metal batteries enabled by sub-5 μm solid polymer electrolytes. Adv. Mater. **33**, 2105329 (2021). https://doi.org/10.1002/adma.202105329
228. Wang, Z.Y., Shen, L., Deng, S.G., et al.: 10 μm-thick high-strength solid polymer electrolytes with excellent interface compatibility for flexible all-solid-state lithium-metal batteries. Adv. Mater. **33**, 2100353 (2021). https://doi.org/10.1002/adma.202100353
229. Tan, D.H.S., Banerjee, A., Chen, Z., et al.: From nanoscale interface characterization to sustainable energy storage using all-solid-state batteries. Nat. Nanotechnol. **15**, 170–180 (2020). https://doi.org/10.1038/s41565-020-0657-x
230. Schnell, J., Günther, T., Knoche, T., et al.: All-solid-state lithium-ion and lithium metal batteries: paving the way to large-scale production. J. Power Sour. **382**, 160–175 (2018). https://doi.org/10.1016/j.jpowsour.2018.02.062
231. Bielefeld, A., Weber, D.A., Janek, J.: Modeling effective ionic conductivity and binder influence in composite cathodes for all-solid-state batteries. ACS Appl. Mater. Interfaces **12**, 12821–12833 (2020). https://doi.org/10.1021/acsami.9b22788
232. Hippauf, F., Schumm, B., Doerfler, S., et al.: Overcoming binder limitations of sheet-type solid-state cathodes using a solvent-free dry-film approach. Energy Storage Mater. **21**, 390–398 (2019). https://doi.org/10.1016/j.ensm.2019.05.033
233. Zhao, Q., Stalin, S., Zhao, C.Z., et al.: Designing solid-state electrolytes for safe, energy-dense batteries. Nat. Rev. Mater. **5**, 229–252 (2020). https://doi.org/10.1038/s41578-019-0165-5
234. Zhang, Z.Z., Shao, Y.J., Lotsch, B., et al.: New horizons for inorganic solid state ion conductors. Energy Environ. Sci. **11**, 1945–1976 (2018). https://doi.org/10.1039/C8EE01053F
235. Zhang, Y.B., Chen, R.J., Wang, S., et al.: Free-standing sulfide/polymer composite solid electrolyte membranes with high conductance for all-solid-state lithium batteries. Energy Storage Mater. **25**, 145–153 (2020). https://doi.org/10.1016/j.ensm.2019.10.020
236. Tan, D.H.S., Banerjee, A., Deng, Z., et al.: Enabling thin and flexible solid-state composite electrolytes by the scalable solution process. ACS Appl. Energy Mater. **2**, 6542–6550 (2019). https://doi.org/10.1021/acsaem.9b01111
237. Miura, A., Rosero-Navarro, N.C., Sakuda, A., et al.: Liquid-phase syntheses of sulfide electrolytes for all-solid-state lithium battery. Nat. Rev. Chem. **3**, 189–198 (2019). https://doi.org/10.1038/s41570-019-0078-2
238. Oh, D.Y., Nam, Y.J., Park, K.H., et al.: Excellent compatibility of solvate ionic liquids with sulfide solid electrolytes: toward favorable ionic contacts in bulk-type all-solid-state lithium-ion batteries. Adv. Energy Mater. **5**, 1500865 (2015). https://doi.org/10.1002/aenm.201500865
239. Lee, K., Kim, S., Park, J., et al.: Selection of binder and solvent for solution-processed all-solid-state battery. J. Electrochem. Soc. **164**, A2075–A2081 (2017). https://doi.org/10.1149/2.1341709jes
240. Riphaus, N., Strobl, P., Stiaszny, B., et al.: Slurry-based processing of solid electrolytes: a comparative binder study. J. Electrochem. Soc. **165**, A3993–A3999 (2018). https://doi.org/10.1149/2.0961816jes
241. Oh, D.Y., Nam, Y.J., Park, K.H., et al.: Slurry-fabricable $Li^+$-conductive polymeric binders for practical all-solid-state lithium-ion batteries enabled by solvate ionic liquids. Adv. Energy Mater. **9**, 1802927 (2019). https://doi.org/10.1002/aenm.201802927
242. Kim, K.T., Oh, D.Y., Jun, S., et al.: Tailoring slurries using cosolvents and Li salt targeting practical all-solid-state batteries employing sulfide solid electrolytes. Adv. Energy Mater. **11**, 2003766 (2021). https://doi.org/10.1002/aenm.202003766
243. Oh, D.Y., Kim, K.T., Jung, S.H., et al.: Tactical hybrids of $Li^+$-conductive dry polymer electrolytes with sulfide solid electrolytes: toward practical all-solid-state batteries with wider temperature operability. Mater. Today **53**, 7–15 (2022). https://doi.org/10.1016/j.mattod.2021.01.006
244. Inada, T., Takada, K., Kajiyama, A., et al.: Fabrications and properties of composite solid-state electrolytes. Solid State Ion. **158**, 275–280 (2003). https://doi.org/10.1016/S0167-2738(02)00889-5
245. Inada, T., Takada, K., Kajiyama, A., et al.: Silicone as a binder in composite electrolytes. J. Power Sour. **119**(120/121), 948–950 (2003). https://doi.org/10.1016/S0378-7753(03)00293-3
246. Wang, C.H., Yu, R.Z., Duan, H., et al.: Solvent-free approach for interweaving freestanding and ultrathin inorganic solid electrolyte membranes. ACS Energy Lett. **7**, 410–416 (2022). https://doi.org/10.1021/acsenergylett.1c02261
247. Balaish, M., Gonzalez-Rosillo, J.C., Kim, K.J., et al.: Processing thin but robust electrolytes for solid-state batteries. Nat. Energy **6**, 227–239 (2021). https://doi.org/10.1038/s41560-020-00759-5
248. Whiteley, J.M., Taynton, P., Zhang, W., et al.: Ultra-thin solid-state Li-ion electrolyte membrane facilitated by a self-healing polymer matrix. Adv. Mater. **27**, 6922–6927 (2015). https://doi.org/10.1002/adma.201502636
249. Zhang, Z.H., Wu, L.P., Zhou, D., et al.: Flexible sulfide electrolyte thin membrane with ultrahigh ionic conductivity for all-solid-state lithium batteries. Nano Lett. **21**, 5233–5239 (2021). https://doi.org/10.1021/acs.nanolett.1c01344
250. Zhu, G.L., Zhao, C.Z., Peng, H.J., et al.: A self-limited free-standing sulfide electrolyte thin film for all-solid-state lithium metal batteries. Adv. Funct. Mater. **31**, 2101985 (2021). https://doi.org/10.1002/adfm.202101985
251. Lee, J., Lee, K., Lee, T., et al.: In situ deprotection of polymeric binders for solution-processible sulfide-based all-solid-state

batteries. Adv. Mater. **32**, 2001702 (2020). https://doi.org/10.1002/adma.202001702
252. Zheng, F., Kotobuki, M., Song, S.F., et al.: Review on solid electrolytes for all-solid-state lithium-ion batteries. J. Power Sour. **389**, 198–213 (2018). https://doi.org/10.1016/j.jpowsour.2018.04.022
253. Kamaya, N., Homma, K., Yamakawa, Y., et al.: A lithium superionic conductor. Nat. Mater. **10**, 682–686 (2011). https://doi.org/10.1038/nmat3066
254. Choi, J.W., Aurbach, D.: Promise and reality of post-lithium-ion batteries with high energy densities. Nat. Rev. Mater. **1**, 1–16 (2016). https://doi.org/10.1038/natrevmats.2016.13
255. Kato, Y., Hori, S., Saito, T., et al.: High-power all-solid-state batteries using sulfide superionic conductors. Nat. Energy **1**, 1–7 (2016). https://doi.org/10.1038/nenergy.2016.30
256. Yamamoto, M., Terauchi, Y., Sakuda, A., et al.: Binder-free sheet-type all-solid-state batteries with enhanced rate capabilities and high energy densities. Sci. Rep. **8**, 1–10 (2018). https://doi.org/10.1038/s41598-018-19398-8
257. Hao, F., Han, F.D., Liang, Y.L., et al.: Architectural design and fabrication approaches for solid-state batteries. MRS Bull. **43**, 775–781 (2018). https://doi.org/10.1557/mrs.2018.211
258. Chen, K.Z., Shinjo, S., Sakuda, A., et al.: Morphological effect on reaction distribution influenced by binder materials in composite electrodes for sheet-type all-solid-state lithium-ion batteries with the sulfide-based solid electrolyte. J. Phys. Chem. C **123**, 3292–3298 (2019). https://doi.org/10.1021/acs.jpcc.8b09569
259. He, L.C., Chen, C., Kotobuki, M., et al.: A new approach for synthesizing bulk-type all-solid-state lithium-ion batteries. J. Mater. Chem. A **7**, 9748–9760 (2019). https://doi.org/10.1039/c8ta12375f
260. Zhang, H., Liu, C.Y., Zheng, L.P., et al.: Lithium bis(fluorosulfonyl)imide/poly(ethylene oxide) polymer electrolyte. Electrochim. Acta **133**, 529–538 (2014). https://doi.org/10.1016/j.electacta.2014.04.099
261. Wan, J.Y., Xie, J., Kong, X., et al.: Ultrathin, flexible, solid polymer composite electrolyte enabled with aligned nanoporous host for lithium batteries. Nat. Nanotechnol. **14**, 705–711 (2019). https://doi.org/10.1038/s41565-019-0465-3
262. Cao, X., Ren, X.D., Zou, L.F., et al.: Monolithic solid-electrolyte interphases formed in fluorinated orthoformate-based electrolytes minimize Li depletion and pulverization. Nat. Energy **4**, 796–805 (2019). https://doi.org/10.1038/s41560-019-0464-5
263. Chen, Y.M., Wang, Z.Q., Li, X.Y., et al.: Li metal deposition and stripping in a solid-state battery via Coble creep. Nature **578**, 251–255 (2020). https://doi.org/10.1038/s41586-020-1972-y
264. Yang, Z.L., Yuan, H.Y., Zhou, C.J., et al.: Facile interfacial adhesion enabled LATP-based solid-state lithium metal battery. Chem. Eng. J. **392**, 123650 (2020). https://doi.org/10.1016/j.cej.2019.123650
265. Martinez-Ibañez, M., Sanchez-Diez, E., Qiao, L.X., et al.: Unprecedented improvement of single Li-ion conductive solid polymer electrolyte through salt additive. Adv. Funct. Mater. **30**, 2000455 (2020). https://doi.org/10.1002/adfm.202000455
266. Homann, G., Stolz, L., Nair, J., et al.: Poly(ethylene oxide)-based electrolyte for solid-state-lithium-batteries with high voltage positive electrodes: evaluating the role of electrolyte oxidation in rapid cell failure. Sci. Rep. **10**, 4390 (2020). https://doi.org/10.1038/s41598-020-61373-9
267. Homann, G., Stolz, L., Winter, M., et al.: Elimination of "voltage noise" of poly(ethylene oxide)-based solid electrolytes in high-voltage lithium batteries: linear versus network polymers. iScience **23**, 101225 (2020). https://doi.org/10.1016/j.isci.2020.101225
268. Nie, K.H., Wang, X.L., Qiu, J.L., et al.: Increasing poly(ethylene oxide) stability to 4.5 V by surface coating of the cathode. ACS Energy Lett. **5**, 826–832 (2020). https://doi.org/10.1021/acsenergylett.9b02739
269. Yang, X.F., Jiang, M., Gao, X.J., et al.: Determining the limiting factor of the electrochemical stability window for PEO-based solid polymer electrolytes: main chain or terminal –OH group? Energy Environ. Sci. **13**, 1318–1325 (2020). https://doi.org/10.1039/D0EE00342E
270. Abraham, K.M., Jiang, Z., Carroll, B.: Highly conductive PEO-like polymer electrolytes. Chem. Mater. **9**, 1978–1988 (1997). https://doi.org/10.1021/cm970075a
271. Nguyen, T., Suk, J., Kang, Y.K.: Semi-interpenetrating solid polymer electrolyte for $LiCoO_2$-based lithium polymer batteries operated at room temperature. J. Electrochem. Sci. Technol. **10**, 250–255 (2019). https://doi.org/10.5229/JECST.2019.10.2.250
272. Hoang, H.A., Le Mong, A., Kim, D.: A straightforward fabrication of solid-state lithium secondary batteries based on multifunctional poly(arylene ether sulfone)-g-poly(ethylene glycol) material. J. Power Sour. **507**, 230288 (2021). https://doi.org/10.1016/j.jpowsour.2021.230288
273. Cho, W., Park, J., Kim, K., et al.: Sulfide-compatible conductive and adhesive glue-like interphase engineering for sheet-type all-solid-state battery. Small **17**, 1902138 (2021). https://doi.org/10.1002/smll.201902138
274. Yuan, J.J., Huang, Z., Song, Y.Z., et al.: In-situ crosslinked binder for high-stability S cathodes with greatly enhanced conduction and polysulfides anchoring. Chem. Eng. J. **426**, 128705 (2021). https://doi.org/10.1016/j.cej.2021.128705
275. Yang, C.G., Du, Q.K., Li, Z.H., et al.: In-situ covalent bonding of polysulfides with electrode binders in operando for lithium-sulfur batteries. J. Power Sour. **402**, 1–6 (2018). https://doi.org/10.1016/j.jpowsour.2018.09.008
276. Li, L., Zuo, Z.C., Shang, H., et al.: In-situ constructing 3D graphdiyne as all-carbon binder for high-performance silicon anode. Nano Energy **53**, 135–143 (2018). https://doi.org/10.1016/j.nanoen.2018.08.039
277. Chai, J.C., Liu, Z.H., Ma, J., et al.: In situ generation of poly(vinylene carbonate) based solid electrolyte with interfacial stability for $LiCoO_2$ lithium batteries. Adv. Sci. **4**, 1600377 (2017). https://doi.org/10.1002/advs.201600377
278. Graham, J.: The influence of capitation and tuition on the decline in dental school applicants. New Dent. **10**, 12–13 (1980)
279. Porcher, W., Chazelle, S., Boulineau, A., et al.: Understanding polyacrylic acid and lithium polyacrylate binder behavior in silicon based electrodes for Li-ion batteries. J. Electrochem. Soc. **164**, A3633–A3640 (2017). https://doi.org/10.1149/2.0821714jes
280. Bie, Y.T., Yang, J., Liu, X.L., et al.: Polydopamine wrapping silicon cross-linked with polyacrylic acid as high-performance anode for lithium-ion batteries. ACS Appl. Mater. Interfaces **8**, 2899–2904 (2016). https://doi.org/10.1021/acsami.5b10616
281. Urbanski, A., Omar, A., Guo, J., et al.: An efficient two-polymer binder for high-performance silicon nanoparticle-based lithium-ion batteries: a systematic case study with commercial polyacrylic acid and polyvinyl butyral polymers. J. Electrochem. Soc. **166**, A5275–A5286 (2019). https://doi.org/10.1149/2.0371903jes
282. Tsai, M.H., Hong, J.L.: Dual crosslinked binders based on poly(2-hydroxyethyl methacrylate) and polyacrylic acid for silicon anode in lithium-ion battery. Electrochim. Acta **359**, 136967 (2020). https://doi.org/10.1016/j.electacta.2020.136967
283. Xu, G.Y., Yan, Q.B., Kushima, A., et al.: Conductive graphene oxide-polyacrylic acid (GOPAA) binder for lithium-sulfur battery. Nano Energy **31**, 568–574 (2017). https://doi.org/10.1016/j.nanoen.2016.12.002

284. Li, M.L., Sheng, L., Xu, R., et al.: Enhanced the mechanical strength of polyimide (PI) nanofiber separator via PAALi binder for lithium ion battery. Compos. Commun. **24**, 100607 (2021). https://doi.org/10.1016/j.coco.2020.100607
285. Lee, K., Lee, J., Choi, S., et al.: Thiol-ene click reaction for fine polarity tuning of polymeric binders in solution-processed all-solid-state batteries. ACS Energy Lett. **4**, 94–101 (2019). https://doi.org/10.1021/acsenergylett.8b01726
286. Liang, J.N., Chen, D.C., Adair, K., et al.: Insight into prolonged cycling life of 4 V all-solid-state polymer batteries by a high-voltage stable binder. Adv. Energy Mater. **11**, 2002455 (2021). https://doi.org/10.1002/aenm.202002455
287. Zhang, Q.P., Pan, K.C., Jia, M.M., et al.: Ionic liquid additive stabilized cathode/electrolyte interface in $LiCoO_2$ based solid-state lithium metal batteries. Electrochim. Acta **368**, 137593 (2021). https://doi.org/10.1016/j.electacta.2020.137593
288. Kim, D.H., Oh, D.Y., Park, K.H., et al.: Infiltration of solution-processable solid electrolytes into conventional Li-ion-battery electrodes for all-solid-state Li-ion batteries. Nano Lett. **17**, 3013–3020 (2017). https://doi.org/10.1021/acs.nanolett.7b00330
289. Choi, S.J., Choi, S.H., Bui, A.D., et al.: LiI-doped sulfide solid electrolyte: enabling a high-capacity slurry-cast electrode by low-temperature post-sintering for practical all-solid-state lithium batteries. ACS Appl. Mater. Interfaces **10**, 31404–31412 (2018). https://doi.org/10.1021/acsami.8b11244
290. Zhang, S.S.: Binder based on polyelectrolyte for high capacity density lithium/sulfur battery. J. Electrochem. Soc. **159**, A1226–A1229 (2012). https://doi.org/10.1149/2.039208jes
291. Bao, W.Z., Zhang, Z.A., Gan, Y.Q., et al.: Enhanced cyclability of sulfur cathodes in lithium-sulfur batteries with Na-alginate as a binder. J. Energy Chem. **22**, 790–794 (2013). https://doi.org/10.1016/S2095-4956(13)60105-9
292. Seh, Z.W., Zhang, Q.F., Li, W.Y., et al.: Stable cycling of lithium sulfide cathodes through strong affinity with a bifunctional binder. Chem. Sci. **4**, 3673–3677 (2013). https://doi.org/10.1039/C3SC51476E
293. Lacey, M.J., Jeschull, F., Edström, K., et al.: Functional, water-soluble binders for improved capacity and stability of lithium-sulfur batteries. J. Power Sour. **264**, 8–14 (2014). https://doi.org/10.1016/j.jpowsour.2014.04.090
294. Ai, G., Dai, Y.L., Ye, Y.F., et al.: Investigation of surface effects through the application of the functional binders in lithium sulfur batteries. Nano Energy **16**, 28–37 (2015). https://doi.org/10.1016/j.nanoen.2015.05.036
295. Li, G.R., Cai, W.L., Liu, B.H., et al.: A multi functional binder with lithium ion conductive polymer and polysulfide absorbents to improve cycleability of lithium-sulfur batteries. J. Power Sour. **294**, 187–192 (2015). https://doi.org/10.1016/j.jpowsour.2015.06.083
296. Li, G.R., Ling, M., Ye, Y.F., et al.: Acacia Senegal-inspired bifunctional binder for longevity of lithium-sulfur batteries. Adv. Energy Mater. **5**, 1500878 (2015). https://doi.org/10.1002/aenm.201500878
297. Bhattacharya, P., Nandasiri, M.I., Lv, D.P., et al.: Polyamidoamine dendrimer-based binders for high-loading lithium-sulfur battery cathodes. Nano Energy **19**, 176–186 (2016). https://doi.org/10.1016/j.nanoen.2015.11.012
298. Frischmann, P.D., Hwa, Y., Cairns, E.J., et al.: Redox-active supramolecular polymer binders for lithium-sulfur batteries that adapt their transport properties in operando. Chem. Mater. **28**, 7414–7421 (2016). https://doi.org/10.1021/acs.chemmater.6b03013
299. Milroy, C., Manthiram, A.: An elastic, conductive, electroactive nanocomposite binder for flexible sulfur cathodes in lithium-sulfur batteries. Adv. Mater. **28**, 9744–9751 (2016). https://doi.org/10.1002/adma.201601665
300. Chen, W., Qian, T., Xiong, J., et al.: A new type of multifunctional polar binder: toward practical application of high energy lithium sulfur batteries. Adv. Mater. **29**, 1605160 (2017). https://doi.org/10.1002/adma.201605160
301. Li, L.J., Pascal, T.A., Connell, J.G., et al.: Molecular understanding of polyelectrolyte binders that actively regulate ion transport in sulfur cathodes. Nat. Commun. **8**, 1–10 (2017). https://doi.org/10.1038/s41467-017-02410-6
302. Ling, M., Zhang, L., Zheng, T.Y., et al.: Nucleophilic substitution between polysulfides and binders unexpectedly stabilizing lithium sulfur battery. Nano Energy **38**, 82–90 (2017). https://doi.org/10.1016/j.nanoen.2017.05.020
303. Liu, J., Galpaya, D.G.D., Yan, L.J., et al.: Exploiting a robust biopolymer network binder for an ultrahigh-areal-capacity Li-S battery. Energy Environ. Sci. **10**, 750–755 (2017). https://doi.org/10.1039/C6EE03033E
304. Su, H.P., Fu, C.Y., Zhao, Y.F., et al.: Polycation binders: an effective approach toward lithium polysulfide sequestration in Li-S batteries. ACS Energy Lett. **2**, 2591–2597 (2017). https://doi.org/10.1021/acsenergylett.7b00779
305. Wu, F., Ye, Y.S., Chen, R.J., et al.: Gluing carbon black and sulfur at nanoscale: a polydopamine-based "nano-binder" for double-shelled sulfur cathodes. Adv. Energy Mater. **7**, 1601591 (2017). https://doi.org/10.1002/aenm.201601591
306. Zhang, L., Ling, M., Feng, J., et al.: Effective electrostatic confinement of polysulfides in lithium/sulfur batteries by a functional binder. Nano Energy **40**, 559–565 (2017). https://doi.org/10.1016/j.nanoen.2017.09.003
307. Yang, Z.X., Li, R.G., Deng, Z.H.: Polyelectrolyte binder for sulfur cathode to improve the cycle performance and discharge property of lithium-sulfur battery. ACS Appl. Mater. Interfaces **10**, 13519–13527 (2018). https://doi.org/10.1021/acsami.8b01163
308. Zhu, X.Y., Zhang, F., Zhang, L., et al.: A highly stretchable cross-linked polyacrylamide hydrogel as an effective binder for silicon and sulfur electrodes toward durable lithium-ion storage. Adv. Funct. Mater. **28**, 1705015 (2018). https://doi.org/10.1002/adfm.201705015
309. Eom, J.Y., Kim, S.I., Ri, V., et al.: The effect of polymeric binders in the sulfur cathode on the cycling performance for lithium-sulfur batteries. Chem. Commun. **55**, 14609–14612 (2019). https://doi.org/10.1039/c9cc07061c
310. Jin, B.Y., Yang, L.F., Zhang, J.W., et al.: Bioinspired binders actively controlling ion migration and accommodating volume change in high sulfur loading lithium-sulfur batteries. Adv. Energy Mater. **9**, 1902938 (2019). https://doi.org/10.1002/aenm.201902938
311. Fan, X.X., Yuan, R.M., Lei, J., et al.: Turning soluble polysulfide intermediates back into solid state by a molecule binder in Li-S batteries. ACS Nano **14**, 15884–15893 (2020). https://doi.org/10.1021/acsnano.0c07240
312. Kim, S., Cho, M., Lee, Y.: Multifunctional chitosan-rGO network binder for enhancing the cycle stability of Li-S batteries. Adv. Funct. Mater. **30**, 1907680 (2020). https://doi.org/10.1002/adfm.201907680
313. Kim, S., Kim, D.H., Cho, M., et al.: Fast-charging lithium-sulfur batteries enabled via lean binder content. Small **16**, 2004372 (2020). https://doi.org/10.1002/smll.202004372
314. Liu, Z.M., He, X., Fang, C., et al.: Reversible crosslinked polymer binder for recyclable lithium sulfur batteries with high performance. Adv. Funct. Mater. **30**, 2003605 (2020). https://doi.org/10.1002/adfm.202003605
315. Mo, Y.X., Wu, Y.J., Yin, Z.W., et al.: High cycling performance Li-S battery via fenugreek gum binder through chemical bonding of the binder with polysulfides in nanosulfur@CNFs cathode.

ChemistrySelect **5**, 8969–8979 (2020). https://doi.org/10.1002/slct.202002471
316. Niu, C.Q., Liu, J., Qian, T., et al.: Single lithium-ion channel polymer binder for stabilizing sulfur cathodes. Natl. Sci. Rev. **7**, 315–323 (2020). https://doi.org/10.1093/nsr/nwz149
317. Wang, H., Zheng, P.T., Yi, H., et al.: Low-cost and environmentally friendly biopolymer binders for Li-S batteries. Macromolecules **53**, 8539–8547 (2020). https://doi.org/10.1021/acs.macromol.0c01576
318. Yang, H.J., Chen, J.H., Yang, J., et al.: Dense and high loading sulfurized pyrolyzed poly(acrylonitrile) (S@pPAN) cathode for rechargeable lithium batteries. Energy Storage Mater. **31**, 187–194 (2020). https://doi.org/10.1016/j.ensm.2020.06.003
319. Yi, H., Yang, Y., Lan, T., et al.: Water-based dual-cross-linked polymer binders for high-energy-density lithium–sulfur batteries. ACS Appl. Mater. Interfaces **12**(26), 29316–29323 (2020). https://doi.org/10.1021/acsami.0c05910
320. Chen, W.P., Duan, H., Shi, J.L., et al.: Bridging interparticle $Li^+$ conduction in a soft ceramic oxide electrolyte. J. Am. Chem. Soc. **143**, 5717–5726 (2021). https://doi.org/10.1021/jacs.0c12965
321. Sun, R.M., Hu, J., Shi, X.X., et al.: Water-soluble cross-linking functional binder for low-cost and high-performance lithium-sulfur batteries. Adv. Funct. Mater. **31**, 2104858 (2021). https://doi.org/10.1002/adfm.202104858
322. Wang, H., Wang, Y.Y., Zhang, G.Z., et al.: Water-based dual-network conductive polymer binders for high-performance Li-S batteries. Electrochim. Acta **371**, 137822 (2021). https://doi.org/10.1016/j.electacta.2021.137822
323. Yang, Y.J., Qiu, J.C., Cai, L., et al.: Water-soluble trifunctional binder for sulfur cathodes for lithium-sulfur battery. ACS Appl. Mater. Interfaces **13**, 33066–33074 (2021). https://doi.org/10.1021/acsami.1c07901
324. Yuan, H.H., Guo, C., Chen, J.H., et al.: A crosslinking hydrogel binder for high-sulfur content S@pPAN cathode in rechargeable lithium batteries. J. Energy Chem. **60**, 360–367 (2021). https://doi.org/10.1016/j.jechem.2021.01.045
325. Zhang, Q., Huang, Q.H., Hao, S.M., et al.: Polymers in lithium-sulfur batteries. Adv. Sci. **9**, 2103798 (2022). https://doi.org/10.1002/advs.202103798
326. Jo, C.H., Voronina, N., Sun, Y.K., et al.: Gifts from nature: bio-inspired materials for rechargeable secondary batteries. Adv. Mater. **33**, 2006019 (2021). https://doi.org/10.1002/adma.202006019
327. Chen, Y., Wang, T.Y., Tian, H.J., et al.: Advances in lithium-sulfur batteries: from academic research to commercial viability. Adv. Mater. **33**, 2003666 (2021). https://doi.org/10.1002/adma.202003666
328. Guo, Q.Y., Zheng, Z.J.: Rational design of binders for stable Li-S and Na-S batteries. Adv. Funct. Mater. **30**, 1907931 (2020). https://doi.org/10.1002/adfm.201907931
329. Qi, Q., Lv, X.H., Lv, W., et al.: Multifunctional binder designs for lithium-sulfur batteries. J. Energy Chem. **39**, 88–100 (2019). https://doi.org/10.1016/j.jechem.2019.02.001
330. Pan, H., Cheng, Z., He, P., et al.: A review of solid-state lithium-sulfur battery: ion transport and polysulfide chemistry. Energy Fuels **34**, 11942–11961 (2020). https://doi.org/10.1021/acs.energyfuels.0c02647
331. Xu, S., Cheng, Y.Y., Zhang, L., et al.: An effective polysulfides bridgebuilder to enable long-life lithium-sulfur flow batteries. Nano Energy **51**, 113–121 (2018). https://doi.org/10.1016/j.nanoen.2018.06.044
332. Fang, R.Y., Xu, H.H., Xu, B.Y., et al.: Reaction mechanism optimization of solid-state Li-S batteries with a PEO-based electrolyte. Adv. Funct. Mater. **31**, 2001812 (2021). https://doi.org/10.1002/adfm.202001812
333. Zhang, X., Liu, T., Zhang, S.F., et al.: Synergistic coupling between $Li_{6.75}La_3Zr_{1.75}Ta_{0.25}O_{12}$ and poly(vinylidene fluoride) induces high ionic conductivity, mechanical strength, and thermal stability of solid composite electrolytes. J. Am. Chem. Soc. **139**, 13779–13785 (2017). https://doi.org/10.1021/jacs.7b06364
334. Hoang, H.A., Kim, D.: High performance solid-state lithium-sulfur battery enabled by multi-functional cathode and flexible hybrid solid electrolyte. Small **18**, 2202963 (2022). https://doi.org/10.1002/smll.202202963
335. Xu, R.C., Yue, J., Liu, S.F., et al.: Cathode-supported all-solid-state lithium-sulfur batteries with high cell-level energy density. ACS Energy Lett. **4**, 1073–1079 (2019). https://doi.org/10.1021/acsenergylett.9b00430
336. Hu, J.K., Yuan, H., Yang, S.J., et al.: Dry electrode technology for scalable and flexible high-energy sulfur cathodes in all-solid-state lithium-sulfur batteries. J. Energy Chem. **71**, 612–618 (2022). https://doi.org/10.1016/j.jechem.2022.04.048
337. Jiang, Z., Peng, H.L., Li, J.R., et al.: A facile path from fast synthesis of Li-argyrodite conductor to dry forming ultrathin electrolyte membrane for high-energy-density all-solid-state lithium batteries. J. Energy Chem. **74**, 309–316 (2022). https://doi.org/10.1016/j.jechem.2022.07.029
338. Yuan, H., Nan, H.X., Zhao, C.Z., et al.: Slurry-coated sulfur/sulfide cathode with Li metal anode for all-solid-state lithium-sulfur pouch cells. Batter. Supercaps **3**, 596–603 (2020). https://doi.org/10.1002/batt.202000051
339. Dewald, G.F., Ohno, S., Hering, J.G.C., et al.: Analysis of charge carrier transport toward optimized cathode composites for all-solid-state Li-S batteries. Batter. Supercaps **4**, 183–194 (2021). https://doi.org/10.1002/batt.202000194
340. Liu, G.Z., Shi, J.M., Zhu, M.T., et al.: Ultra-thin free-standing sulfide solid electrolyte film for cell-level high energy density all-solid-state lithium batteries. Energy Storage Mater. **38**, 249–254 (2021). https://doi.org/10.1016/j.ensm.2021.03.017
341. Xu, S.Q., Kwok, C.Y., Zhou, L.D., et al.: A high capacity all solid-state Li-sulfur battery enabled by conversion-intercalation hybrid cathode architecture. Adv. Funct. Mater. **31**, 2004239 (2021). https://doi.org/10.1002/adfm.202004239
342. Ohno, S., Rosenbach, C., Dewald, G.F., et al.: Linking solid electrolyte degradation to charge carrier transport in the thiophosphate-based composite cathode toward solid-state lithium-sulfur batteries. Adv. Funct. Mater. **31**, 2010620 (2021). https://doi.org/10.1002/adfm.202010620
343. Ohno, S., Zeier, W.G.: Toward practical solid-state lithium-sulfur batteries: challenges and perspectives. Acc. Mater. Res. **2**, 869–880 (2021). https://doi.org/10.1021/accountsmr.1c00116
344. Oh, D.Y., Kim, D.H., Jung, S.H., et al.: Single-step wet-chemical fabrication of sheet-type electrodes from solid-electrolyte precursors for all-solid-state lithium-ion batteries. J. Mater. Chem. A **5**, 20771–20779 (2017). https://doi.org/10.1039/C7TA06873E
345. Dunlap, N.A., Kim, J., Oh, K.H., et al.: Slurry-coated sheet-style Sn-PAN anodes for all-solid-state Li-ion batteries. J. Electrochem. Soc. **166**, A915–A922 (2019). https://doi.org/10.1149/2.0151906jes
346. Kim, J.Y., Park, J., Lee, M.J., et al.: Diffusion-dependent graphite electrode for all-solid-state batteries with extremely high energy density. ACS Energy Lett. **5**, 2995–3004 (2020). https://doi.org/10.1021/acsenergylett.0c01628
347. Yoo, D.J., Elabd, A., Choi, S., et al.: Highly elastic polyrotaxane binders for mechanically stable lithium hosts in lithium-metal batteries. Adv. Mater. **31**, 1901645 (2019). https://doi.org/10.1002/adma.201901645
348. Masset, P., Guidotti, R.A.: Thermal activated (thermal) battery technology. J. Power Sour. **164**, 397–414 (2007). https://doi.org/10.1016/j.jpowsour.2006.10.080

349. Zhao, J.X., Liu, J.S., Li, H.Q., et al.: Porous MgO pompons as a binder for the molten electrolyte applied in thermal batteries. Ionics **27**, 1271–1278 (2021). https://doi.org/10.1007/s11581-020-03885-y
350. Ransil, A., Belcher, A.M.: Structural ceramic batteries using an earth-abundant inorganic waterglass binder. Nat. Commun. **12**, 1–8 (2021). https://doi.org/10.1038/s41467-021-26801-y
351. Zhou, G.M., Liu, K., Fan, Y.C., et al.: An aqueous inorganic polymer binder for high performance lithium-sulfur batteries with flame-retardant properties. ACS Cent. Sci. **4**, 260–267 (2018). https://doi.org/10.1021/acscentsci.7b00569
352. Wei, C.X., Obrovac, M.N.: Inorganic compounds as binders for Si-alloy anodes. J. Electrochem. Soc. **168**, 020505 (2021). https://doi.org/10.1149/1945-7111/abdc74
353. Kay, A.: Inorganic binders for battery electrodes and aqueous processing thereof. US Patent 20,110,117,432, 19 May 2011
354. Chang, C.C., Chang, T. Y.: Methods and systems for making an electrode free from a polymer binder. US Patent 10,923,709, 16 Feb 2021
355. Lee, H.D., Park, Y.C., Song, M.R., et al.: Positive electrode, method of manufacturing the same, and lithium battery comprising the positive electrode, US Patent 20,130,196,227, 1 Aug 2013
356. Yu, Z.X., Li, K.X., Mo, M.L., et al.: Anode Piece of Lithium Ion Battery and Preparation Method of Anode Piece. Ningde Amperex Technology Ltd Dongguan Amperex Technology Ltd Amperex Technology Ltd, China (2011)
357. Johannisson, W., Ihrner, N., Zenkert, D., et al.: Multifunctional performance of a carbon fiber UD lamina electrode for structural batteries. Compos. Sci. Technol. **168**, 81–87 (2018). https://doi.org/10.1016/j.compscitech.2018.08.044
358. Schmidt, O., Melchior, S., Hawkes, A., et al.: Projecting the future levelized cost of electricity storage technologies. Joule **3**, 81–100 (2019). https://doi.org/10.1016/j.joule.2018.12.008
359. Viswanathan, V., Epstein, A.H., Chiang, Y.M., et al.: The challenges and opportunities of battery-powered flight. Nature **601**, 519–525 (2022). https://doi.org/10.1038/s41586-021-04139-1


**Lan Zhang** is currently an associate Professor of Institute of Process Engineering, CAS. Her research interest focuses on advance electrolytes (including liquid and solid), binders, cathode materials, and electrode structure optimization for lithium batteries.

**Xiangkun Wu** is currently an Associate Professor of Electrochemical Engineering at Institute of Process Engineering, CAS. His research interest is structure design and process optimization for lithium-ion batteries.

**Weiwei Qian** is currently an Assistant Professor of Institute of Process Engineering, CAS. Her research interest focuses on Li-S batteries and flow batteries.

**Suojiang Zhang** is a Member of CAS. He is currently Director-General of the Institute of Process Engineering (IPE), CAS; Dean of College of Chemical Engineering, University of CAS; and Vice-Chairman of the Chemical Industry and Engineering Society of China. He is mainly engaged in the research of green energy, materials, and chemical processes and has breaking through major technological and engineering challenges in molecular conformational design, dynamic regulation of nanoprocesses, process innovation and system integration, and realizing the industrial application of a number of green complete technologies.